

March 1996

EUROPEAN ORGANIZATION FOR EXPERIMENTAL
PHOTOGRAMMETRIC RESEARCH

EXPERIMENTAL TEST
ON
DIGITAL AERIAL TRIANGULATION

Report by J. Jaakola and T. Sarjakoski
Finnish Geodetic Institute



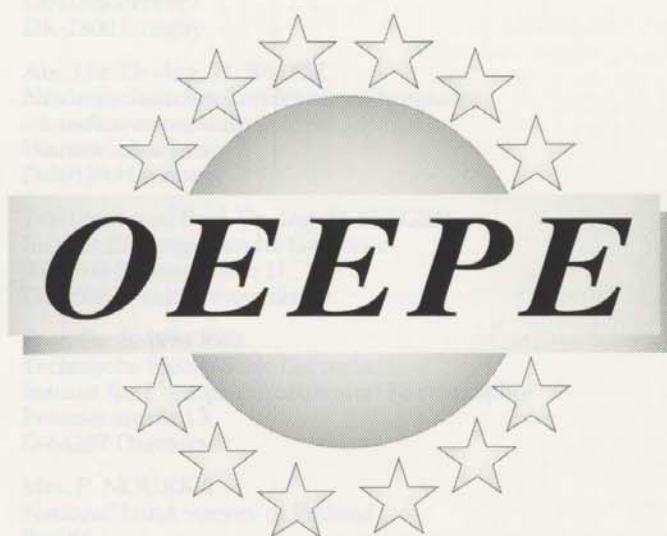
Official Publication No 31

March 1996

EUROPEAN ORGANIZATION FOR EXPERIMENTAL PHOTOGRAMMETRIC RESEARCH

EXPERIMENTAL TEST ON DIGITAL AERIAL TRIANGULATION

Report by J. Jaakola and T. Sarjakoski
Finnish Geodetic Institute



Official Publication No 31

ISSN 0257-0505

The present publication is the exclusive property of the
European Organization for Experimental Photogrammetric Research

All rights of translation and reproduction are reserved on behalf of the OEEPE.
Printed and published by the Institut für Angewandte Geodäsie, Frankfurt am Main

EUROPEAN ORGANIZATION
for
EXPERIMENTAL PHOTOGRAMMETRIC RESEARCH

STEERING COMMITTEE

(composed of Representatives of the Governments of the Member Countries)

<i>President:</i>	Dipl.-Ing. R. KILGA Bundesamt für Eich- und Vermessungswesen Krotenthallergasse 3 A-1080 Wien	Austria
<i>Members:</i>	Administrateur-Général J. DE SMET Institut Géographique National 13, Abbaye de la Cambre B-1050 Bruxelles	Belgium
	Mr. J. VANOMMES LAEGHE Dept. of Photogrammetry Institut Géographique National 13, Abbaye de la Cambre B-1050 Bruxelles	
	Mr. O. JACOBI Institut for Surveying and Photogrammetry Technical University of Denmark Landmaalervej 7 DK-2800 Lyngby	Denmark
	Abt. Dir. Dr.-Ing. H. BAUER Niedersächsisches Landesverwaltungsamt - Landesvermessung - Warmbüchenkamp 2 D-30159 Hannover	Federal Republic of Germany
	Präsident und Prof. Dr.-Ing. H. SEEGER Institut für Angewandte Geodäsie Richard-Strauss-Allee 11 D-60598 Frankfurt am Main	
	Prof. Dr. B. WROBEL Technische Hochschule Darmstadt Institut für Photogrammetrie und Kartographie Petersenstraße 13 D-64287 Darmstadt	
	Mrs. P. NOUKKA National Land Survey of Finland Box 84 SF-00521 Helsinki 52	Finland
	Prof. Dr. R. KUITTINEN Department of Photogrammetry and Remote Sensing Finnish Geodetic Institut Geodeetinrinne 2 SF-02430 Masala	

Mr. P. DENIS Ecole Nationale des Sciences Geographiques 2, Avenue Pasteur F-94160 Saint-Mande	France
Mr. A. BAUDOIN Centre National d'Etudes Spatiales 2, Place Maurice-Quentin F-75039 Paris Cedex 01	
Dr. Eng. L. SURACE Geographical Military Institute Via Cesare Battista 8-10 I-50100 Firenze	Italy
Prof. R. GALETTO University of Pavia Dept. di Ingegneria del Territorio Via Abbiategrasso 209 I-27100 Pavia	
Prof. Dr. M. G. VOSSelman Delft University of Technology Thijssseweg 11 NL-2629 JA Delft	Netherlands
Ir. P. VAN DER MOLEN Dienst Kadaster en de Openbare Registers Waltersingel 1 NL-7314 NK Apeldoorn	
Mr. I. INDSET Statens Kartverk N-3500 Hønefoss	Norway
Prof. Ø. ANDERSEN Norges Landbrukshøgskole Institutt for Landmåling P. O. Box 5034 N-1432 Ås	
Prof. J. TALTS National Land Survey of Sweden S-80112 Gävle	Sweden
Prof. K. TORLEGÅRD Royal Institute of Technology Dept. of Photogrammetry S-10044 Stockholm 70	
Prof. Dr. O. KÖLBL Institut de Photogrammétrie, EPFL GR-Ecublens CH-1015 Lausanne	Switzerland
Mr. F. JEANRICHARD Bundesamt für Landestopographie Seftigenstrasse 264 CH-3084 Wabern	
Lt. Col. M. ÖNDER Ministry of National Defence General Command of Mapping TR-06100 Ankara	Turkey

Col. S. FOÇALIGIL
Ministry of National Defence
General Command of Mapping
TR-06100 Ankara

Turkey

MR. N. S. SMITH
Ordnance Survey
Romsey Road
Maybush
Southampton SO16 4GU

United Kingdom

Prof. Dr. I. J. DOWMAN
Dept. of Photogrammetry and Surveying
University College London
Gower Street 6
London WC 1E 6BT

SCIENCE COMMITTEE

Prof. Dr. I. J. DOWMAN
Dept. of Photogrammetry and Surveying
University College London
Gower Street 6
London WC 1E 6BT

United Kingdom

EXECUTIVE BUREAU

Mr. C. PARESI
Secretary General of the OEEPE
International Institute for Aerospace Survey
and Earth Sciences
350 Boulevard 1945, P. O. Box 6
NL-7500 AA Enschede (Netherlands)

Ir. J. TIMMERMAN
Smaragdstraat 20
NL-7314 HG Apeldoorn

SCIENTIFIC COMMISSIONS

Commission A – Aerotriangulation

President: Prof. Dr. T. SARJAKOSKI
Finnish Geodetic Institute
Geodeetinrinne 2
SF-02430 Masala

Commission B – Digital Elevation Models

President: Dr. G. ROBINSON
NUTIS
University of Reading
White Knights
GB-Reading

Commission C – Large Scale Restitution

President: Prof. Eng. S. DEQUAL
Dipartimento Georisorse e Territorio
Polytecnico di Torino
Corso Duca Degli Abruzzi 24
I-10129 Torino

Commission D – Photogrammetry and Cartography

President: see Commission I

Commission E – Topographic Interpretation

President: Prof. Dr. B.-S. SCHULZ
Institut für Angewandte Geodäsie
Richard-Strauss-Allee 11
D-60598 Frankfurt am Main

Commission F – Fundamental Problems of Photogrammetry

President: Prof. Dr. W. FÖRSTNER
Institut für Photogrammetrie
Universität Bonn
Nußallee 15
D-53115 Bonn

APPLICATION COMMISSIONS

Commission I – Topographic Mapping

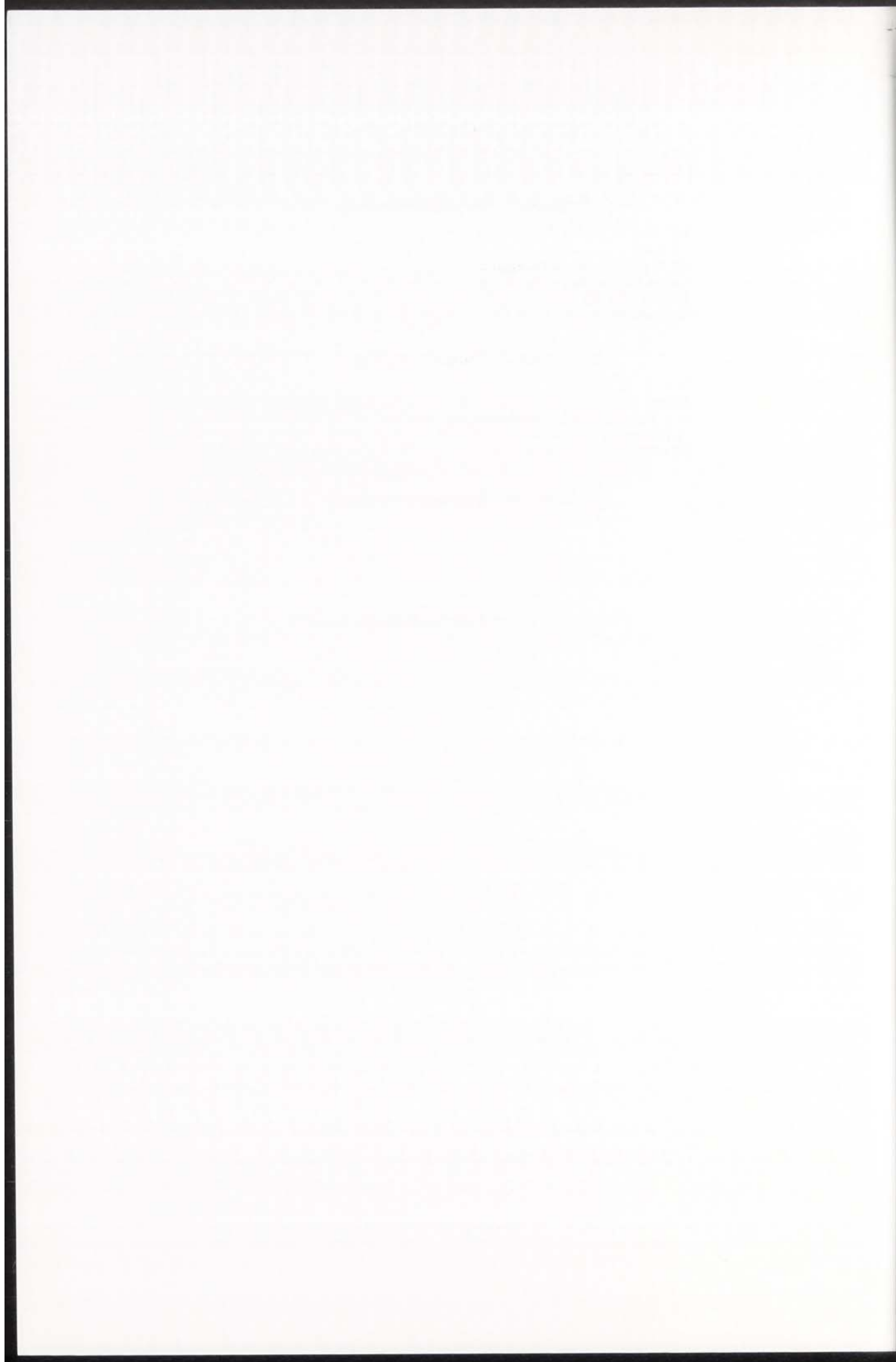
President: Mr. M. J. D. BRAND
Director
Ordnance Survey of N. Ireland
Colby House, Stranmillis Court
Belfast BT 9 5BJ
United Kingdom

Commission II – Cadastral Mapping

President: Ir. L. A. KOEN
Dienst
v. h. Kadaster en de Openbare Registers
Waltersingel 1
NL-7314 GH Apeldoorn

Commission III – Engineering Surveys

Commission V – Land Information Systems



EXPERIMENTAL TEST
ON
DIGITAL AERIAL TRIANGULATION

(with 24 Figures, 7 Tables and 2 Appendices)

Report by J. Jaakola and T. Sarjakoski

THE UNIVERSITY OF CHICAGO
LIBRARY
1100 EAST 58TH STREET
CHICAGO, ILL. 60637

THE UNIVERSITY OF CHICAGO
LIBRARY
1100 EAST 58TH STREET
CHICAGO, ILL. 60637

THE UNIVERSITY OF CHICAGO
LIBRARY
1100 EAST 58TH STREET
CHICAGO, ILL. 60637

THE UNIVERSITY OF CHICAGO
LIBRARY
1100 EAST 58TH STREET
CHICAGO, ILL. 60637

THE UNIVERSITY OF CHICAGO
LIBRARY
1100 EAST 58TH STREET
CHICAGO, ILL. 60637

Table of Contents

	page
1 Summary.....	13
2 Introduction.....	13
3 State of the Art of Digital Aerial Triangulation in 1992.....	16
3.1 Hardware and software prerequisites.....	16
3.2 Early studies on image correlation.....	16
3.3 Digital point transfer for aerial triangulation.....	17
3.4 Towards automatic digital aerial triangulation.....	17
4 Set-up and goal of the project.....	18
5 Test Area.....	19
5.1 Image material.....	21
5.2 Signalised ground points.....	22
5.2.1 Control points.....	22
5.2.2 Check points.....	23
5.2.3 Checking of individual points.....	24
5.2.4 Selection of check points.....	25
6 Task of the Participants.....	26
7 Method for Analysis.....	27
7.1 Ground coordinates.....	27
7.2 Known distances.....	27
7.3 Parameters of exterior orientation.....	28
8 Measurements of the participants.....	28
8.1 Measurements of individual participants.....	30
8.2 Additional measurements for comparative purposes.....	33
9 Analysis and Results.....	33
9.1 Comparative Triangulations.....	35
9.2 Triangulation using 15 μm images.....	36
9.2.1 Coordinate accuracy from check points.....	36
9.2.2 Plane coordinate accuracy from distances.....	39
9.3 Triangulation using 30 μm images.....	39
9.3.1 Coordinate accuracy from check points.....	41
9.3.2 Plane coordinate accuracy from distances.....	42
9.4 Effect of pixel size.....	43
9.5 Effect of measuring resolution.....	46
9.6 Effect of tie point quality.....	47
9.7 Effect of control point density.....	48
9.8 Effect of bad imaging of signals.....	50
9.9 Theoretical accuracy estimates.....	51
9.9.1 Elements of exterior orientation.....	51
9.9.2 Ground points.....	53
10 Conclusions.....	56

	page
11 Acknowledgements	57
12 References.....	57

APPENDICES

APPENDIX A	63
APPENDIX B	79

1 Summary

The accuracy potential of aerotriangulation using digitized images has been investigated from 1 : 4000 large scale photography. The block consisted of 28 images in 4 strips, 7 images in each. The measurements were made on digital images of 15 and 30 μm pixel size. The original analogue images were also measured using conventional methods to give a reference to contemporary systems. The accuracy of the block was mainly investigated calculating root mean square errors on check points.

In all, 13 participants delivered 155 different adjustments, which represented different levels of automation in selecting tie points, and measuring points and parallaxes. Usually the measurements were made using visual interactive selection and measurements of the points, but using digital methods for point transfer. Some systems were completely visual, in one case an advanced automation had been used in the selection, transfer and measurement of tie points.

The results show that the best systems using digital imagery and non-signalized tie points reach the same accuracy level as the most accurate analytical triangulation methods with analogue imagery obtain with signalized points. There is experimental indication and theoretical expectation that digital systems can be even more accurate.

In the most accurate cases, the pixel size has a relatively small effect on the accuracy of determined ground points. In some semiautomatic cases, the height accuracy was even better on 30 μm imagery than on 15 μm imagery. Also systems with low measuring resolution (1/2 pixel) produced good results with 15 μm pixel size. The investigation has also shown that, in digital systems with digital image matching of homologous points, natural points as tie points are as good as signals.

The achieved results are based on systems, which have been developed during the last years. Future research and development work will lead to new systems, which will improve the accuracy and operational features of digital systems.

2 Introduction

Photogrammetric practice is currently entering and has already partly entered the digital era. For aerial photogrammetry and mapping applications this means currently that analogue images will be scanned into digital form and that all the subsequent process phases will utilise only the digital images. What is the role aerial triangulation in this process? Quoting *Helava* (1991): "digital photogrammetry can establish an accurate and everlasting mathematical relationship between sensor pixels and the ground". The numerical parameters of this relationship are established in aerial triangulation and will be its primary outcome in most of the cases – the coordinates of triangulation points are usually of secondary importance.

Regarding aerial triangulation in isolation, digital photogrammetry can be seen as a technique for improved degree of automation, improved accuracy and better economy only for this process phase. Although all these aspects would come into realisation – as is already proven to a great extent – this kind of process view will last only for a very limited time period. Emphasis has to be put on the idea that digital image files are a new medium to facilitate utilisation of computerised technology in its full extent and flexibility. This means that the photogrammetric production line has to be made fully digital up to the end-user of the imagery, to benefit from digital aerial triangulation in its full capacity.

The decision to start a research project on digital aerial triangulation was taken in the OEEPE Brussels meeting in October 1992. It was recognised at that time that there were enough theoretical and experimental studies about digital aerial triangulation for organising a multi-site experimental work. The setup for the test project was a rather traditional one as has been common in research on aerial triangulation: the same block was to be measured by several participants using different methods, and the quality of the results would be evaluated using ground check points.

The objective of the project was to get experimental results of photogrammetric aerial triangulation when using high quality digital imagery. The main concern was accuracy. Also the operational aspects were of interest although most programs were not yet operational. Some specific questions were raised in the discussions preceding the project set up, like:

- What is the effect of pixel size?
- Can we reach the same or a better accuracy level by digital methods as by using analytical plotters or photogrammetric comparators?
- Can we meet practical needs in a more economical way?
- How to evaluate the accuracy of digitally computed blocks, especially the accuracy of orientation elements?
- What degree of automation is foreseeable?
- Can we reach high-accuracy by using visual on-screen measurement techniques?
- Is the currently used size of the signalised targets sufficient for accurate digital measurement process?
- Can the signalised targets be measured automatically?
- Can high accuracy results be obtained without signalized points (except for control points)?
- How to deal with the large data volumes?
- What is the operational status of currently available commercial software packages for digital aerial triangulation?

For most of the questions no direct answer could be expected, the whole development being at its beginning only. The actual experiments were to concentrate on the execution of digital point transfer and image coordinate observations, on different levels of interactive performance resp. of automation. The questions were further elaborated only partially in the planning phase as it was felt that the methods to be used by participants are anyhow going to be too diverse for definite conclusions on any single question. Using the terms of statistical analysis, it was seen from the very beginning that the project is going to be a mixture of exploratory data analysis and confirmatory data analysis, with a short list of some predefined tests but with a long list of open-ended questions.

The project proceeded according to the following time schedule:

- December 1992: Selection of FORSSA block to be used as a test material.
- February 1993: Scanning of the photographs by Landesvermessungsamt Baden-Württemberg in Stuttgart, Germany
- May 1993: Check of the digital image material at the pilot centre
- June 1993: Distribution of the material to the participants
- February 1994: Most of the results returned from the participants
- May 1994: Review of the preliminary results at the Workshop in Hanasaari, Helsinki
- June 1994: Decision to extend the study on natural tie-points
- Fall 1995: Final reports from the participants
- February 1995: Completion of experiments on natural tie-points

The results of the test are presented in this report. After this introduction, in Chapter 2, a short review is given of the state of the art of digital aerial triangulation as it was in 1992. The initial set up of the project and the Forssa test area are described in Chapters 3 and 4. The task of the participants and the delivered material are explained in Chapter 5. Then follow overviews of the methods for analysis and of the measurements made by individual participants, Chapters 6 and 7. The detail analysis of the results is made in Chapter 8, followed by conclusions in Chapter 9. The reports written by individual participants are collected in Appendix A.

3 State of the Art of Digital Aerial Triangulation in 1992

3.1 Hardware and software prerequisites

Concerning hardware, digital aerial triangulation is dependent on good quality image scanner and computer with sufficient memory capacity and speed for handling large image files. For interactive work a graphical display with sufficient quality is also required. These prerequisites have well been met already for some time, but disk memory units with sufficient capacity have been expensive until very recently. The situation has changed very rapidly and today (spring 1996) a disk unit with 9 GB capacity can be purchased for about USD 3000. In 9 GB we could store about 35 aerial images with 15 μm resolution in an uncompressed 8 bit format. Thus the whole Forssa block of this research project would easily fit simultaneously on a single disk unit.

Concerning software and methodology, the measurement part of digital aerial triangulation is concerned with only three items: 1) to find and select suitable image details for tie point, 2) to identify and measure the image coordinates such details in all overlapping images concerned and 3) to identify and measure the image coordinates of ground control points, signalized or not. The identification and measurement of the image coordinates of ground control points may also be treated as a separate problem which may or may not be included in automation efforts. The basic techniques required for these issues have become available through the development of image processing methods during the past two decades. Some essential points are reviewed below.

3.2 Early studies on image correlation

Image correlation, that is, finding the image coordinates for a homologous point from two or more photographs, is the corner stone in building systems for automatic aerial triangulation. Research on this topic has been done by *Hobrough* already in 1959 in the context of automatic stereo plotting. The technique was implemented in a form of an electronic cross-correlation device. A thorough paper on the theory of digital image correlation was given by *Helava* 1976. The techniques were implemented already earlier (*Helava and Chapelle*, 1972) in an analytical stereoplotter by Bendix, called AS-11B-X automated stereomapper, that was designed for automatic collection of digital elevation data.

The paper by *Förstner* (1982) forms a foundation for least squares correlation by introducing its basic formulation as an adjustment problem. The formulation includes template matching and correlation of two images and especially a rigorous derivation of the geometric precision of digital image correlation. At the same ISPRS Helsinki Symposium *Thurgood and Mikhail* (1982) treat the same problem and also introduce the least squares method for geometric

positioning, with the goal to achieve sub-pixel precision. Their research included an empirical study using simulated or synthetic images. As they conclude, "results indicated that both human and algorithmic operators are capable of extracting high-precision geometric information from digital images, provided that the targets to be measured are sufficiently well defined". The numerical results demonstrated a sub-pixel accuracy that was in most of the cases better than 1/10 of a pixel.

3.3 *Digital point transfer for aerial triangulation*

The empirical studies by *Ackermann* (1983, 1994) demonstrated for the first time that very high accuracy point transfer is possible for relative orientation. His research included the use of least squares area correlation and use of CCD-cameras on-line in the Zeiss Planicomp C100 analytical stereoplotter. The results demonstrated accuracy better than 4 μm . This corresponds to less than 1/5 of the 20 μm pixel size that was used.

The paper by *Ackermann* and *Schneider* (1986) reported results on digital aerial triangulation in two practical blocks having sizes of 26 and 28 photographs. The instrumentation was the same as used in *Ackermann* (1984). Visually selected image patches were digitized with the CCD-cameras and stored on a computer disk for the algorithmic digital point transfer. The authors conclude: "The transfer errors of image coordinates are only in the order of 3 μm or better. Thus, it is shown that digital transfer of natural tie points can raise conventional aerial triangulation to the high precision level which so far was only obtainable with signalised points."

The paper by *Helava* (1987) introduced a new instrument "Digital Comparator Correlator System (DCCS) by *Helava Associates Incorporated*. DCCS included a special software for digital aerial triangulation. The technical realisation was very similar compared to the approach used in *Ackermann* and *Schneider* (1986): Image patches for tie points and control points were digitized with a CCD-camera and the final point transfer was made algorithmically.

DCCS used *Förstner* operator (*Padeiras et al.*, 1994; *Förstner*, 1985; *Förstner*, 1986) for automatic selection of suitable tie points, and the final measurements were done using object-space multi-image least squares correlation, with a reference to (*Grün*, 1985). According to the paper, "a hierarchical, or 'pyramid', approach is used for the pull-in task", i.e. coarse matching.

3.4 *Towards automatic digital aerial triangulation*

In the context of DCCS the following quotation reflects *Helava's* opinion about automation at that time: "An almost fully automatic operation appears feasible, but not practical at this time. While the DCCS does manage to run through photographs fully automatically, it does not do so

consistently. The automatic mode can be made more reliable by capturing larger image patches and using more sophisticated processing. However, the cost of required resources makes this approach impractical at this time. A semiautomatic mode, with occasional assistance and monitoring by the operator, is more economical."

As reported by *Miller et al.* (1992), the procedures for digital aerial triangulation were also implemented in the fully digital stereo comparator/compiler (DSCC) in the mid 1980s. According to the paper, "these capabilities are very similar to those implemented in the DCCS (*Helava*, 1987). There is very little information available on this development because it was done as part of an in-house project for the Defence Mapping Agency in USA.

The paper by *Sarjakoski* (1986) studied on a conceptual level fully digital and fully automatic systems for aerial triangulation. It stated that "progress in digital image storage and processing technologies proposes that fully digital and automatic systems for aerial triangulation can be built already". The main focus in the paper was how expert-system technology could be utilised in implementing these systems. Exploitation of heuristic, auxiliary knowledge was considered to be useful. This approach was further elaborated (1988) in the more narrow context of photogrammetric block adjustment systems.

The work by *Tsingas* (1991,1992) represents the first empirical research on fully automatic digital aerial triangulation. It proceeds on the "softcopy-line", i.e., full photographs are scanned, not only image patches. The selection of tie points is based on the *Förstner* operator that is applied on predefined overlap areas. Full automation was reached for selection of tie points and also for their image coordinate measurements. The accuracy level of 3.5 μm in image coordinates was reached using images with 15 μm pixel size, thus satisfying very high requirements for aerial triangulation.

4 Set-up and goal of the project

It was decided at the very beginning of the project that an existing large-scale photogrammetric block covering an urban area would be used in the test. The use of existing photography was seen necessary for timely start-up of the project. As a drawback, the accuracy of the geodetic co-ordinates for signalised targets was limited to the "standard quality" in contrast to nearly error-free coordinates of many test fields.

The project was decided to be implemented in a form of a multi-site comparative test project, so that the Finnish Geodetic Institute would act the as the pilot centre taking care of the general arrangements, the distribution of the test material, and also of the collection and analysis of the results

from the participating institutes. Regarding the methods to be used in digital aerial triangulation, participants were advised to use any approach and system they consider suitable for the purpose.

The use of a high quality photogrammetric scanner for digitizing the photographs was considered to be necessary, in order to guarantee geometrically good material of digital images.

The main method for comparing the geometrical accuracy of the triangulation results would be the use of check points having geodetically determined coordinates. For point densification, i.e., for applications where the coordinates of triangulated points are of interest, this method is obviously the most reliable, as it measures directly the quality of the end-product. In this method the effect of object definition will be included in the error estimates. When dealing with digital imagery, the object definition is usually dependent on the pixel size that had to be considered in the investigation.

Orientation elements of images determined by triangulation will be used in fully digital environments in the subsequent process phases, like interactive or automatic data collection and orthophoto production. Therefore it is important to know their metric quality. However, because the applications are ground related, i.e., we are dealing with position determination on the ground, the metric quality of the orientation elements can be evaluated by using geodetic check points as above. The errors of the orientation elements will be propagated to the coordinates of the check points. It was thus considered that in this study check point analysis will give a reliable indication also of the quality of orientation elements.

It is also important to compare the performance of digital aerial triangulation with the methods being widely used at the moment. Therefore comparative measurements were carried out using analytical plotters and monocomparators.

Already in the planning phase it could be seen that the systems to be used in the test would mainly be of experimental nature or still in development and often couldn't exploit the digital technology fully. Due to this, the purpose of the project was set to find lines for further development rather than to give final answers. For the same reason, the reporting and analysis of the operational aspects of digital aerial triangulation are very fragmentary and limited to the reports by each participant.

5 Test Area

In the search for an appropriate test area, the aim was to find an urban area with a dense geodetic network and covered by a recent large scale photography. Such a block was found in the small Finnish town of Forssa. The

selected wide angle colour photography in scale 1 : 4000 had been made for practical purposes; but, at the same time, a dense geodetic network had been signalised for collecting some quality information. The total block consists of 60 images in 7 strips with 60 % side and end laps. Due to problems with a high amount of image data, a small sub block of 4 strips and 28 images (7 in each strip) was chosen for the test. The side lap, which was approximately 34 %, varied between 24% - 49 %. The geometrical configuration of the block is presented in Figure 1.

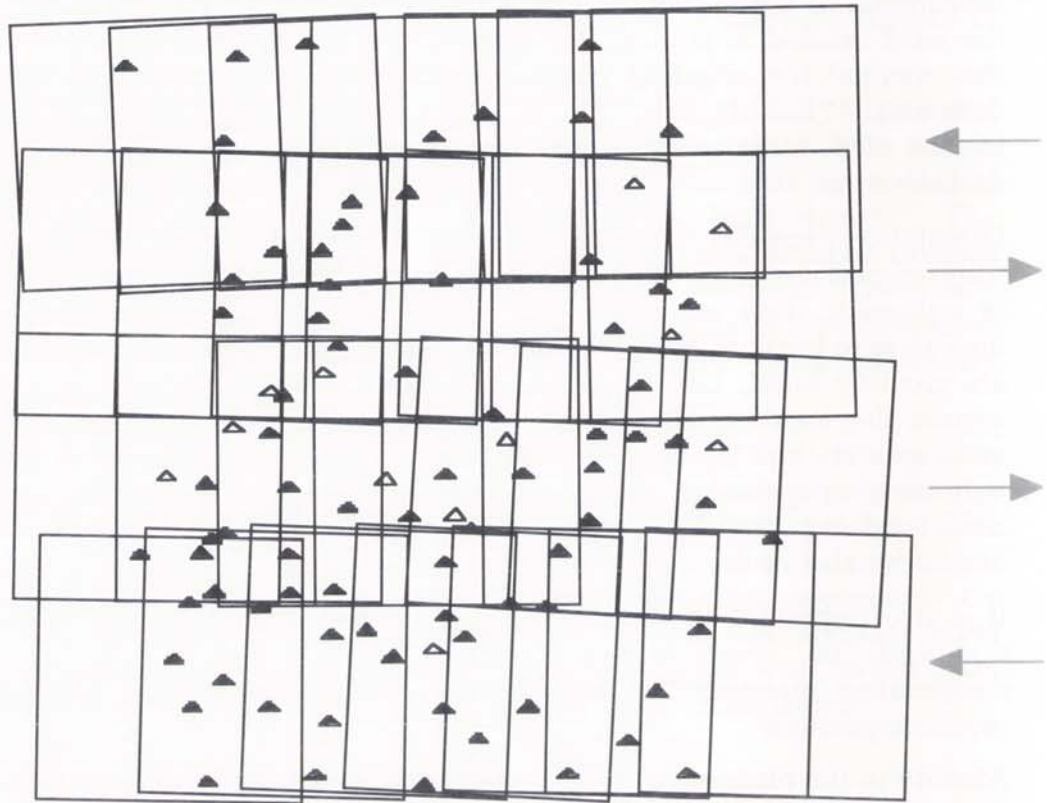


Figure 1 – The Forssa test block and the location of the control and check points.

Black triangles mean XYZ-, and white triangles XY-points. The arrows show the flight directions on the strips.

The block was flown in east-west direction. The top and bottom strips were flown towards the west and the two strips inside the block towards the east. Additional information about the block is available in Table 1.

The geodetic points had been signalised using white, cross shaped signals. The arms of these signals were 60 cm x 10 cm. The width of the arms corresponded to only 25 μ m in image scale. For digital imagery, especially when using different pixel sizes, large circular signals might be better. The signals were painted mainly on asphalt. Some of them were made of cardboard and had sand or grass in the background.

The test area itself is a flat urban area with rural surroundings. Except for some bigger houses (blocks of flats) in the centre of the town and some factories, the houses are small one family buildings with a garden. The rural area is mainly field, but, due to the time of photography, without vegetation. Forested areas are small.

Table 1 – Flight parameters of test block Forssa.

Time of photography	3.5.1989 11:40
Flying height above ground	600 m
Scale of photography	1 : 4000
Camera	Wild RC 20/23
Principal distance	153.19 mm
Film	positive colour
Number of strips	4
Number of images/strip	7
End lap	60 %
Side lap	34 % (24% – 49%)

In this report, the ground coordinate system is defined as a left hand system, the X-axis pointing to the east and the Y-axis to the north.

5.1 Image material

The photography was made under a light cloud, which can be noticed from the light shadows. On the other hand, the original colour diapositives were relatively hard, and some decrease in illumination in the corners can be observed.

The selected colour diapositives were scanned as black-and-white images in Landesvermessungsamt Baden-Württemberg in Stuttgart/Germany with a Zeiss PS1 PhotoScan using 15 μ m pixel size. At that time, the installation was quite new, and only limited experience had been collected. However, the scanning succeeded rather well, except for some minor radiometric disturbances. For instance, changes in grey scale in different image zones and

striping could be observed. However, in aerotriangulation single errors of this kind are not severe.

The 30 μm pixel image set was created from the 15 μm data by averaging every 2x2 pixel window. The decrease in image quality through lower resolutions did not cause any loss in the number of measurable signals.

The images of this small block occupied almost 7 GB storage space with 15 μm pixel size, and less than 2 GB with 30 μm pixel size. It was stored for delivery on 2.3 GB Exabyte tapes. The data was uncompressed.

5.2 *Signalised ground points*

The test area was covered by a dense geodetic network of 97 signalised points, the location of which can be seen in Figure 1.

The plane coordinates of these points were determined mainly by using traverse measurements. The heights were measured by levelling. All the control points and check points were selected from this group.

Because the network was measured for practical purposes in different phases, there was no precise information available about the metric quality of the points. It can be assumed that the mean coordinate errors of the points were below 20 mm. In the analysis of the results a value of 15 mm has been used.

5.2.1 *Control points*

Two control point configurations (Figure 2) were selected from the set of signalised ground points. The dense control was formed by 14 xyz-points on the borders of the block. Because of the small size of the block, no control inside the block is necessary. The analysis is mainly based on dense control configuration.

The sparse control was created using 4 xyz-points and 4 z-points at the ends of the strips. The selected configuration is not acceptable for accurate aerotriangulation. However, it is interesting to see how different methods react on sparse control. Especially systems using high amounts of tie points might be less sensitive to the quality of ground control.

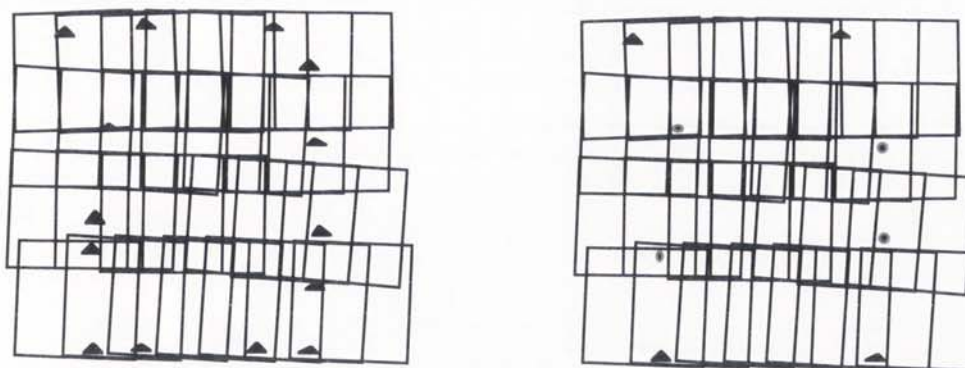


Figure 2 – Dense and sparse control point configurations. Black triangles mean XYZ-, and black circles Z-points.

5.2.2 Check points

In an ideal case, the ground coordinates of the check points should be free of all errors. However, they were selected from the same group of points as the control points, so their errors have an effect on the root mean square values (RMS) calculated from the differences between the given and the adjusted ground coordinates. On the other hand, one of the main interests in this research is to compare the results of different types of measurements. In such a case, the changes of RMS values are more important. The effect of inaccurate check point coordinates on RMS values can be estimated by the following formula:

$$m_x = \sqrt{m_{xc}^2 - m_c^2} \quad (1)$$

m_x = true mean error of adjusted coordinates

m_{xc} = root mean square error from differences between adjusted coordinates and check point coordinates

m_c = known mean error of check point coordinates

The analysis in Chapter 5.2.3 and the achieved results have shown that the mean errors of the plane coordinates of the check points are below 15 mm.

Based on this, some realistic combinations of m_c , m_{xc} , and the outcome m_x are listed in Table 2. In the "worst case" ($m_c = 15$ mm, $m_{xc} = 20$ mm and $m_x = 13$ mm), the m_x is affected by about 30%. This must be kept in mind when interpreting the results in the rest of this report. However, in this project the differences between different methods and systems are more interesting than the "absolute" values.

Table 2 – True mean errors (m_x) from formula (1) with different assumptions of check point accuracy (m_c) and calculated root mean square errors (m_{xc}). The values are in mm.

m_c	m_{xc}	m_x
10	20	17
10	30	28
10	40	39
15	20	13
15	30	26
15	40	37

5.2.3 Checking of individual points

The quality of check points and control points, as well, was controlled for outliers making adjustments, where also all the check points were treated as control points. The rigid structure of such a block is able to reveal errors in ground coordinates and targeting. Naturally, the differences on ground points reflect only the discrepancies between geodetic and photogrammetric systems. However, single anomalies are more probable in geodetic traverses and centring of signals than in photogrammetric systems.

The adjustments were performed using additional parameters and the ESPA block adjustment software of the pilot centre. In order to minimise the effects of photogrammetric error sources, the data sets were selected according to the best metric and image quality, as well as, to the highest amount of measured check points. Thus, this control was made using analogue imagery (i.e. Wild BC1 and Zeiss PK1 measurements of two different participants). The blocks were adjusted using an assumed standard deviation 15 mm for ground coordinates and $4 \mu\text{m}$ (= 16 mm on the ground) for image observations. The assumed accuracy of 15 mm corresponds to the expected real accuracy.

In addition to the adjustments above, the results from the original block adjustment of the complete block (61 images in 7 strips with 60 % side lap), made by the SITO company in 1989, were available for this check. In this case, the measurements were made with a BC 1 analytical plotter.

The adjusted coordinates were compared against the given ground coordinates. The points with a difference of at least three times the RMS value of the corresponding coordinate, were taken for a closer inspection. If the difference in the other cases exceeded twice the RMS value in the same direction, the point was finally discarded. So, six points (4942, 5022, 5023, 5047, 5929 and 6004) were excluded from the check point set. The results of SITO fully support these exclusions.

The RMS values of the check points in the whole block are displayed also in Table 3. The values indicate the compatibility of photogrammetric and geodetic systems with given accuracy assumptions.

Table 3 – RMS values on check points (used as control points), and the number of measured and rejected check points in the first phase.

Measurement	Control point accuracy [mm]	s_0 [μ m]	rmsX [mm]	rmsY [mm]	rmsZ [mm]	Points measured	Points rejected
BC1	15	3.3	9	11	7	83	8
PK1	15	3.3	8	10	6	88	6

5.2.4 Selection of check points

Because the participants had measured slightly different point configurations, the question was raised, whether only points having been measured in all the cases should be included in the analysis. However, this would have led to a high reduction in the number of check points (about 50 %) and the inclusion of only those points, which are easy to identify and measure and measurable also on 30 μ m imagery. On the other hand, the comparisons between different adjustments would not be correct, if the check point sets were different, even if the effect were small. As a compromise, the check points measured in all 7 most accurate (15 μ m imagery) and, at the same time, most interesting cases were selected. Thus 50 XY- and 41 Z-coordinates could be included. These check points were used in both control cases.

This kind of selection rejects points, which are difficult to recognise and measure. As a result, the calculated estimates are too optimistic in this respect. However, as shown in Chapter 9.8, the effect is very small, excluding the heights in 30 μ m imagery.

6 Task of the Participants

All the participants received the following material:

- 28 digital images with pixel size of 15 μm in raw format on 4 Exabyte tapes
- 28 digital images with pixel size of 30 μm in raw format on an Exabyte tape
- Ground coordinates (X, Y, Z) of 14 control points
- Approximate image coordinates of control and check points
- Image coordinates of proposed tie points for optional use
- Camera calibration certificate
- Ground points marked on low resolution paper prints of the images
- Sketch of the image block
- Map of the area including the signalised ground points
- Scanner calibration and image header files
- Instructions for measurements

The task of the participants was to perform photogrammetric aerotriangulation with both image data sets. Because the aim of the test was to investigate all varieties of the item, there were no instructions concerning the measuring process and method. The given tie point configuration was also optional, because of the requirements of different methods. The adjustment software and method was set free. Fixed items were:

- Usage of six parameter transformation for inner orientation
- Usage of given dense and sparse control
- Adjustment with and without additional parameters

In all other points the participant could use the best choice of the method he had. The participants had the possibility to make, in addition to the basic two measurements and eight adjustments, other measurements and calculations.

Two of the participants made also comparative measurements on a monocomparator and an analytical plotter using the original diapositives. In these measurements a large number of the tie points were signalised check points, so the results represent best obtainable accuracy in practical aerial triangulation. They give good reference for judging the potential of digital triangulation.

7 Method of Analysis

Being an empirical investigation, the accuracy potential has been investigated by calculating error estimates in two different ways. The empirical values can be achieved by comparing the true values with the defined unknowns, and the theoretical estimates by using the law of error propagation.

The accuracy concept of aerotriangulation is not unambiguous, but it depends on the application for which the measurements have been made, and on the parameters to be defined. In point densification, the accuracy of the computed ground coordinates is of main interest. In other cases, where aerotriangulation is only an intermediate phase, like in mapping or in the measurement of digital elevation models, the accuracy of exterior orientation is close to the final results. However, these two groups of determined parameters have a strong correlation with each other.

7.1 Ground coordinates

Since the ground coordinates of the check points are known, the root mean square error (RMS) value for each coordinate, calculated using formula (2), can be used as an accuracy estimate.

$$RMS_X = \sqrt{\frac{\sum (X_c - X_g)^2}{n}} \quad (2)$$

where

X_c = calculated value

X_g = given value

n = number of check points

In this investigation, the RMS values are biased because of errors in given values. Their influence has been discussed in Chapter 5.2.2.

7.2 Known distances

The geodetic network had been measured mainly using traverse measurements. So, the distances between neighbouring points in each traverse, calculated from given coordinates, are as accurate as the distance measuring accuracy, here approximately 5 mm. These distances can be regarded as ground truth. The RMS values for distances RMS_s can be calculated with formula (2), if the coordinates X are replaced by distances s , and n equals to the amount of distances.

If we consider only the horizontal components of the distances and assume that the differences ΔX and ΔY between geodetic and photogrammetric coordinates belong to the same normally distributed population, the corresponding coordinate error RMS_C can be calculated using formula (3):

$$RMS_C = RMS_s / \sqrt{2} \quad (3)$$

This value is referenced to the end points of the given distances and not to the whole block. Therefore, it is not affected by block deformations, and it sets the limit for the available coordinate accuracy of the used system. It is also a good tool for checking the quality of measurements on signals.

7.3 *Parameters of exterior orientation*

The use of accuracy estimates of the parameters of exterior orientation is not quite direct. The parameters themselves are usually only indirect information, from which the final ground coordinates are derived. Additional affecting factors are, for instance, the correlation between the parameters of exterior orientation on the same and on neighbouring images. However, with a similar geometry of the blocks, the estimates should be well comparable.

In this investigation, no true values for exterior orientation parameters were available, so the comparisons base on the theoretical mean errors determined in the block adjustments. Due to the problems above and the quality of conclusions to be drawn, the analysis has been limited to the coordinates of the projection centres.

8 **Measurements of the participants**

In all, 21 participants joined the test and received the material. At the end, 13 participants, which are listed below, submitted the results to the pilot centre.

Agricultural University of Norway	(NLH)	Norway
École Polytechnique Fédérale de Lausanne	(EPFL)	Switzerland
Eidgenössische Technische Hochschule Zürich	(ETH)	Switzerland
Finnish Geodetic Institute	(FGI)	Finland
Helsinki University of Technology	(HUT)	Finland
Institut Géographique National	(IGN)	France
Kungliga Tekniska Högskolan	(KTH)	Sweden
National Land Survey of Sweden	(NLSS)	Sweden
Technical University Munich	(TUM)	Germany

Technische Universität Wien	(TUW)	Austria
Université Laval	(UL)	Canada
University of Stuttgart	(TUS)	Germany
University of Trondheim	(NTH)	Norway

The participants made 155 different block adjustments. They were based on measurements, which can be divided into three main groups:

1. **Completely visual methods (VM).** Measurements are made on a screen in the same way as on an analytical plotter. They can be made in stereoscopic or monoscopic mode. When comparing to conventional methods, the advantages are the flexibility in treatment and display of images. The disadvantages are mainly related to a decrease in image quality.
2. **Semiautomatic methods (SM).** In this group automatic image matching has been used in some form in different tasks of image block measurement. The most common way is to match any kinds of homologous points on multiple images. Another automated task is the measurement of fiducial marks and signals, mainly using template matching. Essential in this group is that the approximate values of points must be known in advance or gained using manual pointing.
3. **Automated methods (AM).** The basic difference, as compared to semiautomatic methods, is the automatic selection of tie points and acquisition of approximate image coordinates. In its most advanced form, the method is practically fully automatic. In the current status, at least the measurement of signalised points requires human interference.

Most of the systems in this test belong to groups 1 and 2; and only one participant used a system, which belongs to group 3. The latter is based also on a different concept, in which the drawbacks of the less accurate measurements using feature based matching are compensated through a high amount of clustered measurements. Other participants have used area based matching (mainly least squares matching), if any. The different structure of the measured blocks leads to some problems in the analysis of accuracy.

In the methods belonging to the groups 1 and 2, and also in measurements with analogue imagery, the tie points were mostly signals or similar small well-defined natural objects, which can be easily found in large scale imagery. In some cases the amount of observations on signalised points (check points and control points) was over 60 % of all the observations.

In some cases, the full capacity available of automation of the system was not used, and the measurement has been classified according to the used level.

The nature of different measurements varied. Systems may have been commercial or experimental, and under development. The experience level of the operators ranged from students to professional operators. These factors

make the analysis more difficult, but the high number of participants and measurements compensate this problem somewhat.

Some of the results are, because of some error in the treatment of observations, clearly erroneous over large areas of the block. They have been excluded and are not analysed further in this report.

8.1 Measurements of individual participants

Detailed descriptions of each system, written by the participants, are available in Appendix A. However, short descriptions will be made here to facilitate the reading of this report and to stress the specialities of each system.

The cases have been named using the following sort key order in the sub groups:

1. Pixel size in μm (15, 30)
2. Control point configuration (dense (D), sparse (S))
3. Additional parameters (without (N), with (P))

An example of the numbering in a typical case is presented in Table 4. For instance NLH 2 means an adjustment of NLH using 15 μm imagery, dense control and additional parameters. Several participants have made more than 8 basic adjustments, and the numbering scheme is correspondingly different. Detailed information about the numbering is available in Appendix B.

Table 4 – An example of a typical numbering scheme.

Case number	1	2	3	4	5	6	7	8
Pixel size	15	15	15	15	30	30	30	30
Control	D	D	S	S	D	D	S	S
Additional parameters	N	P	N	P	N	P	N	P

Each system has been classified to one of the groups (VM, SM or AM) described in the previous chapter. Most of the measurements have been made using both signalised and natural tie points. In some cases the block adjustment is completely based on natural tie points, which will be mentioned if applicable.

École Polytechnique Fédérale de Lausanne (EPFL)

The measurements have been made using Intergraph ImageStation and Leica DPW systems. Both are commercially available semi automatic systems. The

measuring resolution of DPW system is one pixel. The adjustments have been made in all cases with additional parameters.

The BC 1 and DSW 100 (with DCCS software) measurements have been made for comparison.

- EPFL 1 – 2 Wild BC1 analytical plotter measurements using analogue imagery. The cases have often been referred to with the name BC 1. (VM)
- EPFL 3 – 4 Helava DSW 100 measurements. (SM)
- EPFL 5 – 6 Leica DPW measurement. (SM)
- EPFL 7 – 8 Intergraph ImageStation measurements. (SM)
- EPFL 9 – 12 Adjustments with natural tie points.

Eidgenössische Technische Hochschule Zürich (ETH)

The measuring system was the self built DIPS II. The semi automated system includes also the automatic measurement of fiducial marks and signalised points using automatic template matching. In the block adjustment, two different sets for additional parameters were used (12 and 44 parameters). Only the results from adjustments with 12 parameters have been used for the comparisons. (SM)

Finnish Geodetic Institute (FGI)

The used system was a self developed digital photogrammetric workstation, where automation was used in image matching. The matching is based on a cross-correlation method. The block was measured using different approaches:

1. Completely visual or semi automatic measurements.
2. Different densities of tie points (17–34 points/image).
3. Different number of visual observations per signalised ground point.
4. Use of natural or signalised points as tie points

- FGI 1–8 Visual observations. (VM)
- FGI 9–16 Points were measured visually on the first images. On the following, correlated with the first observations. (SM)
- FGI 17–24 Like FGI 9–16, but the tie points were natural details (no signals). (SM)
- FGI 25–26 Like FGI 9–16, but all the points have been measured visually and then correlated to corresponding observations on other images. (SM)
- FGI 27–34 Like FGI 9–16, but the number of tie points (natural) has been increased from 27 to 34 per image. (SM)

FGI 35-36 Like FGI 25-26, but using tie points like in FIG 27-34. (SM)

Helsinki University of Technology (HUT)

The experimental system was developed in the institute. For monoscopic visual measurements, variable measuring marks were available. The block adjustments were performed without additional parameters. (SM)

Institut Géographique National (IGN)

The 15 μ m data was measured using a self developed system on a Vaxstation (IGN 1-4) (SM). The 30 μ m data was measured on a Matra Traster T10 (IGN 5-8). (VM)

Kungliga Tekniska Högskolan (KTH)

Measurements were made completely visually using ERDAS software (KTH 1-4) (VM) and semiautomatically using a system developed in the institute (KTH 5-9) (SM). The semi automatic system includes template matching on fiducial marks and signals.

Agricultural University of Norway (NLH)

The measurements were made visually using ERDAS OrthoMAX block triangulation software. The measurements were made without stereoscopic viewing and area based image matching, even if they were included in the system. (VM)

National Land Survey of Sweden (NLSS)

Measurements were made visually on Teragon system. (VM)

University of Trondheim (NTH)

The measuring system was ERDAS with the remote sensing module. (VM)

Technical University Munich (TUM)

The measurements were made visually with two measuring resolutions, 1 pixel (TUM 1-4) and 1/3 pixel (TUM 5-8). One control point in dense configuration was not measured, which makes the comparison to other measurements slightly biased. (VM)

University of Stuttgart (TUS)

The measurements on digital imagery were made using visual and automated methods. In the automated measurements, the special features were automatic selection of tie points, feature based matching and high number of tie points. A basic difference, as compared to other methods, is also the way tie points are used. The points are in small patches, which correspond to

single points in the other methods. Very typically, the points were measured on only two images.

The Zeiss PK1 measurements were made in a conventional way for comparison.

TUS 1-4	Zeiss PK1 monocomparator measurements using analogue imagery. The cases have often been referred to with the name PK1. (VM)
TUS 5-12	Visual observations on digital images. (VM)
TUS 13-16	Automatic measurements using 15 μm data (272 points per image). (AM)
TUS 17-20	Automatic measurements using 30 μm data (237 points per image). (AM)
TUS 21-24	Automatic measurements using 30 μm data (131 points per image). (AM)

Technische Universität Wien (TUW)

The method is based on feature based matching, but, in this case, unlike TUS, the number of points corresponds to conventional cases. (SM)

Université Laval (UL)

The measurements were made completely visually using Leica DVP system. The measuring resolution of 1/2 pixel is lower than in most systems. In addition to normal bundle block adjustment (UL 1-8), also adjustment using independent models was used (UL 9-12). (VM)

8.2 Additional measurements for comparison purposes

The comparative measurements with diapositives were made with Zeiss mono comparator PK1 at TUS and Wild BC1 analytical plotter at EPFL using standard methods. In addition to these, one set of measurements was made by EPFL using Helava DSW100 (DCCS) system, which includes also a scanner (12,5 μm pixel size). The descriptions of these measurements can be found in Appendix A.

9 Analysis and Results

The pilot centre calculated, from the adjusted check point coordinates delivered by the participants, the differences to the given coordinates, and then the RMS values using formula (2). The delivered coordinates were checked for gross errors by excluding points, which had differences exceeding three times the RMS of the corresponding coordinate in that adjustment.

The horizontal distances between neighbouring traverse points and their RMS values were calculated by the pilot centre. Because these values were intended to be used as a kind of quality control for observations of check points, the results were analysed only in the cases, where dense control and additional parameters were used. Due to the low number of distances, all the known distances were included.

Each image data set was usually adjusted in four different versions. In the analysis, calculations using dense control and additional parameters have been used mostly. The sparse control is not capable of controlling systematic or small gross errors, and the results show clear instabilities. Therefore, these adjustments have been used only for investigating special items. However, all the results are presented in Appendix B.

Some of the adjustments included gross errors, which made their inclusion into the comparison unreasonable.

Sometimes in the analysis of the results, comparisons have been made between selected cases. This limitation often gives more useful information and better readability. Therefore, in most extreme cases, the comparisons are made only between measurements made by a single participant. In these cases many block parameters, like point locations, number of points, measuring method and adjustment method, remain the same throughout the whole series. The advantages of this can be seen in the stable behaviour of the series.

9.1 Comparative triangulations

The results of comparative triangulations are presented in Table 5.

Table 5 – The RMS values [mm] for X, Y and Z coordinates from check point coordinates as well as for plane coordinates (rms_C) from short distances in comparative triangulations.

pix = pixel size [μm]

D/S = dense/sparse control

P/N = with/without additional parameters

s_0 = standard error in the block adjustment [μm]).

Instrument	pix	D/S	P/N	s_0	rms_X	rms_Y	rms_Z	rms_C
PK1		D	N	3,7	17	22	46	17
PK1		D	P	3,5	15	20	35	17
PK1		S	N	3,7	31	27	60	21
PK1		S	P	3,5	19	29	32	18
BC1		D	P	3,3	22	20	36	20
BC1		S	P	3,1	45	33	40	18
DSW	12,5	D	P	5,5	27	33	97	25
DSW	12,5	S	P	5,4	67	58	160	25

The best results were achieved with PK1 measurements. The used block is very favourable for it. The instrument is very accurate; and the lack of stereovision is not crucial, when a lot of signalised points are available as tie points. The PK1 measurements offer a good reference for comparisons in this investigation.

The BC1 measurements produced, in plane, slightly less accurate results than PK1. Due to the stereoscopic observations, the Z-coordinates are more accurate in relation to achieved planimetric accuracy. This represents the most usual solution of today.

DSW results are, in plane, about 50 % worse than in other cases. In Z, the errors are even 2 to 3 times worse. The system represents the first generation of digital systems.

The instability of the block in adjustments with sparse control is clear. The differences to dense control vary a lot. Also the means of coordinate differences prove clear block deformations.

The values in column rmsC, are in the most accurate cases (BC1 and PK1 measurements with dense control and additional parameters), very close to the accuracy of plane coordinates. This proves the following facts:

- The block does not have significant deformations.
- The achievable accuracy of the densified points (signalised check points) is limited by the measuring accuracy of these points, not by the accuracy of the block.
- The errors of the check point coordinates cannot have a significant effect on calculated RMS values.

9.2 Triangulation using 15 μ m images

The results from the adjustments using 15 μ m imagery with dense control and additional parameters are presented in Table 6.

The table includes all the delivered cases. Except for some clearly erroneous adjustments, they will be analysed in the following chapters.

9.2.1 Coordinate accuracy from check points

Planimetric accuracy

The results with 15 μ m pixel size, dense control, and additional parameters are presented in Figure 3. In plane coordinates, the RMS values, the variations of which are relatively small, are around 20 mm. An explanation for bigger values in TUM 2 is the one pixel measuring resolution, and in TUV 2 the low number of points when using feature based matching.

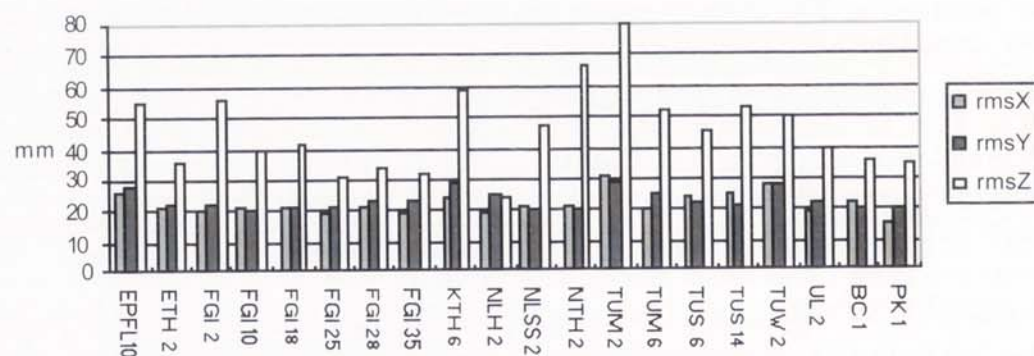


Figure 3 – RMS values from 15 μ m pixel size data, as well as from BC1 and PK1 measurements when using dense control and additional parameters.

Table 6 – The results from adjustments on 15 μm imagery with dense control and additional parameters. The theoretical accuracy estimates in cases of TUS are from calculations without additional parameters. In the table:

s_o = standard error [μm]

$\text{rms}_x, \text{rms}_y, \text{rms}_z$ = RMS values of X, Y and Z coordinates [mm]

n_{xy} = number of used check points in plane

n_z = number of used check points in height

m_x, m_y, m_z = theoretical accuracy estimates for ground points [mm]

$m_{x_0}, m_{y_0}, m_{z_0}$ = theoretical accuracy estimates for coordinates of the projection centres [mm]

Case	s_o	rms_x	rms_y	rms_z	rms_C	n_{xy}	n_z	m_x	m_y	m_z	m_{x_0}	m_{y_0}	m_{z_0}
EPFL 7	5,5	29	26	54	20	48	39						
EPFL12	5,6	29	26	56	20	48	39						
ETH 2	3,8	21	22	36	19	50	41	16	19	40	50	47	50
ETH 3	3,8	21	24	37	19	50	41	16	19	42	57	53	57
FGI 2	3,9	20	22	56	16	49	41	20	21	47	56	57	31
FGI 10	3,4	21	20	40	17	49	41	17	18	42	48	49	27
FGI 18	3,7	21	21	41	19	49	40	19	20	44	53	53	29
FGI 25	2,9	19	21	31	16	50	41	12	14	30	34	34	20
FGI 28	4,2	21	23	34	18	49	41	18	19	40	41	41	25
FGI 35	3,6	19	23	32	17	50	41	14	16	32	31	31	20
HUT 5	6,0	32	30	73	21	50	41	29	26	56	87	87	48
IGN 1		68	177	63	36	46	37						
KTH 6	5	24	29	59	21	45	37						
NLH 2	3,9	19	25	24	17	50	41	18	15	43	48	62	38
NLSS 2	3,8	21	20	47	15	50	41						
NTH 2	5,5	21	20	67	16	49	41	32	26	74	101	117	63
TUM 2	6,9	31	29	79	20	48	39	30	33	79			
TUM 6	5,8	20	25	52	19	48	39	25	28	66			
TUS 6	3,9	24	22	45	22	50	41	17	18	40	52	52	29
TUS 14	6,2	25	21	53	22	50	41	25	27	59	30	38	25
TUW 2	3,2	28	27	50	23	49	41						
UL 2		19	22	40	19	50	41						

In comparison to measurements using analogue imagery, the best results are at the same level with the BC1 measurements, and only slightly worse than the PK1 results. The test block with signalised check points is favourable for visual methods in general, and especially for monocomparator measurements. The influence of tie point quality will be discussed later in Chapter 9.6.

In a comparison between the different measurements of a single participant no big differences can be found. The increase of measuring efforts, like in FGI, seems to have no influence in planimetric accuracy.

Height accuracy

In the Z-coordinate, the variation is bigger, which can be seen also in Figure 3, as well as in Figure 4, which shows the height to plane accuracy relation. In height the big errors have often been achieved using visual methods (FGI 2, NLSS 2, NTH 2, TUM 2, TUM 6, TUS 6 and UL 2). An exception from this is NLH 2. Also, in other cases of the same participant, the same phenomenon can be seen, if additional parameters have been used. One reason is the participant's own additional parameter set, but it does not explain the whole phenomenon.

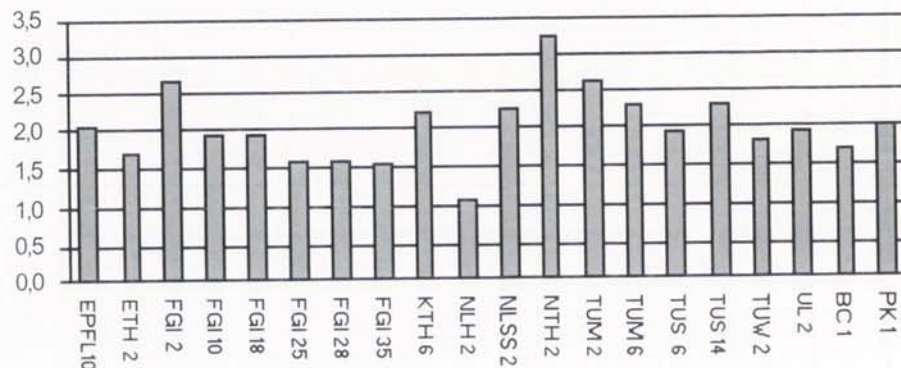


Figure 4 – Height to plane accuracy relation with 15 µm imagery, dense control, and additional parameters. For comparison, also corresponding BC1 and PK1 results are shown.

The best height to plane accuracy relations (ETH 2, ETH 3, FGI 25, FGI 28 and FGI 35), except for NLH 2, have been achieved using automation and image matching also on check points. It seems that matching improves the parallax measurements, and, at the same time, the height definition. In the series of FGI, the intensity of signal measurements increases from left to right, and the phenomenon is well observable. The importance of parallax measurement accuracy is visible also with analogue imagery, when stereoscopic viewing on BC1 gives better relative height accuracy than monoscopic measurements on PK1.

9.2.2 Plane coordinate accuracy from distances

The RMS values calculated using formula (3) are presented in Figure 5. They follow the same trend as the values calculated from check point coordinates (Figure 3), but their magnitude is on an average 4 mm below. There are two main reasons for this difference. The values calculated from short distances are less affected by block deformations, and the given distances are, due to correlation between neighbouring points, more accurate than the given ground coordinates.

The small difference between both estimates also proves the quality of check point coordinates.

The slightly higher values from TUS in interactive (TUS 6) and automated (TUS 14) measurements, and from TUW indicate, that the pointing accuracy on signalised points has not been as accurate as in the measurements of other participants. This could explain some disagreements between the theoretical and the empirical values in the TUS measurements.

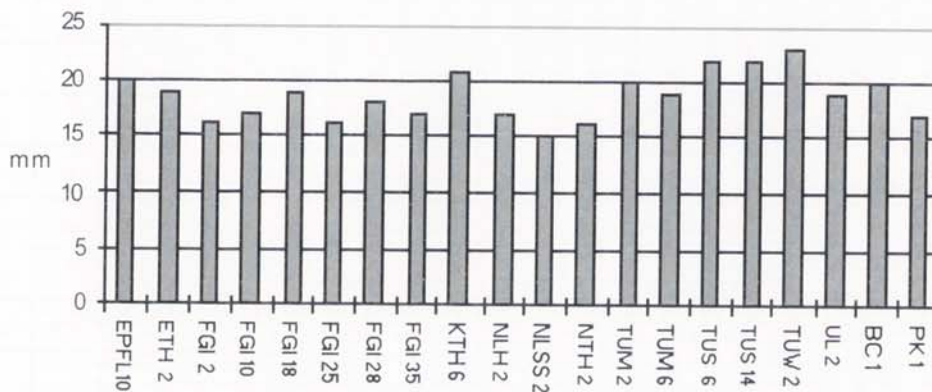


Figure 5 – Estimated local coordinate errors calculated from short distances, when 15 μ m imagery, dense control, and additional parameters have been used.

9.3 Triangulation using 30 μ m images

The results with 30 μ m data are treated here only shortly. A more thorough analysis is in Chapter 9.4, where the effect of pixel size will be discussed.

Table 7 – Results from adjustments on 30 μm imagery with dense control and additional parameters. The theoretical accuracy estimates in cases of TUS are from calculations without additional parameters. In the table:

s_0 = standard error [μm]

$\text{rms}_X, \text{rms}_Y, \text{rms}_Z$ = RMS values of X, Y and Z coordinates [mm]

n_{xy} = number of used check points in plane

n_z = number of used check points in height

m_X, m_Y, m_Z = theoretical accuracy estimates for ground points [mm]

$m_{X_0}, m_{Y_0}, m_{Z_0}$ = theoretical accuracy estimates for coordinates of the projection centres [mm]

Case	s_0	rms_X	rms_Y	rms_Z	rms_C	n_{xy}	n_z	m_X	m_Y	m_Z	m_{X_0}	m_{Y_0}	m_{Z_0}
EPFL 5	5,5	50	45	73	44	48	39						
EPFL11	5,6	52	48	72	48	48	39						
ETH 8	7,5	31	69	68	29	48	39	30	36	75	92	87	55
ETH 9	7,6	31	68	68	29	48	39	32	38	82	107	107	62
FGI 6	5,3	27	23	37	12	48	40	27	28	64	76	77	43
FGI 14	4,2	24	26	33	20	50	41	21	22	51	60	61	33
FGI 22	4,4	23	25	31	19	50	41	22	23	53	63	63	35
FGI 26	3,4	19	24	33	15	49	40	15	16	35	41	40	24
FGI 32	4,6	22	26	30	19	49	40	19	21	44	45	44	28
FGI 36	3,7	22	24	30	19	49	40	15	16	34	33	33	21
HUT 6	8,9	47	45	83	40	49	40	47	43	83	129	129	71
IGN 3		29	27	54	20	47	38						
KTH 2	8	26	33	54	20	46	39						
KTH 9	5	27	32	79	31	42	36						
NLH 6	4,8	18	21	30	19	50	41	22	18	51	57	45	46
NLSS 6	4,6	27	26	37	17	49	40						
NTH 6	6,9	19	24	61	15	47	38	41	32	87	113	138	73
TUS 10	5,3	24	28	74	31	50	41	20	21	51	68	67	35
TUS 18	11,7	42	44	111	29	50	41	46	49	108	59	74	46
TUS 22	10,6	36	35	97	29	50	41	42	44	99	62	73	45
TUW 6	4,5	25	27	39	14	46	37						
UL 6		25	33	37	20	47	38						

9.3.1 Coordinate accuracy from check points

The results from 30 μm data with dense control and additional parameters (Figure 6) have somehow a different nature than the corresponding results using 15 μm data. The variations of RMS values between different cases are, in general, larger, and the height to planimetric accuracy relation (Figure 7) is smaller. One explanation is that the geometric quality of the images does not decrease much with larger pixel size, but the pointing accuracy on signals is more affected due to the size and shape of the signals. The problem will be discussed in more detail in Chapter 9.4.

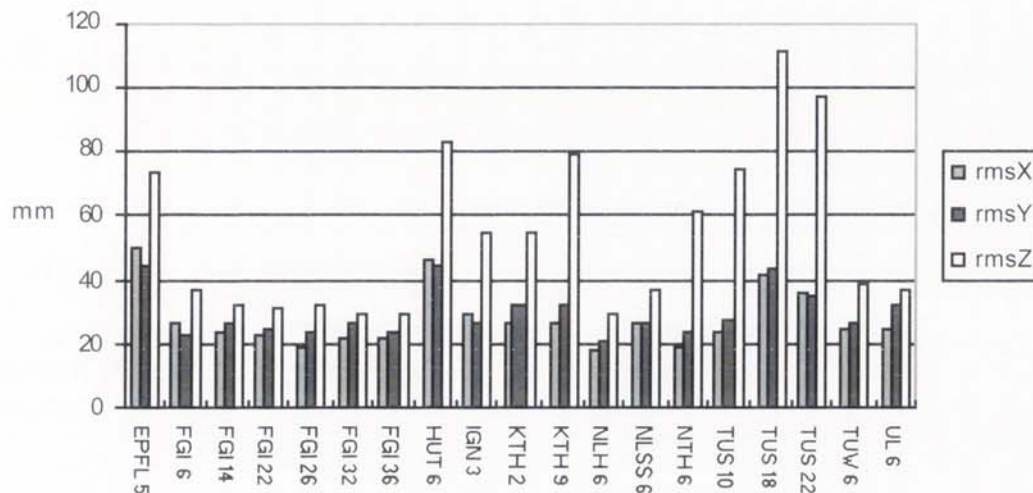


Figure 6 – RMS values from 30 μm pixel size data when using dense control and additional parameters.

An increase in the number of observations should improve the metric quality. However, in TUS 18 (237 points/image) and TUS 22 (131 points/image) the behaviour is unexpected. Here, the reason is the quality of the tie points. In TUS 22 (a subset of TUS 18), only 20 best tie points per image patch have been used, when in TUS 18, all the measured points are included in the adjustment.

Another anomaly, which can be explained in these results, is the case EPFL 5. Here the reason is the measuring resolution of 1 pixel.

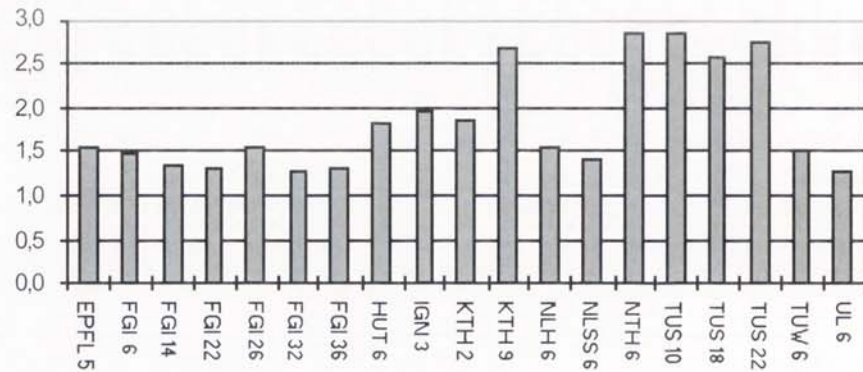


Figure 7 – Height to plane accuracy relation with 30 μ m imagery, dense control, and additional parameters.

9.3.2 Plane coordinate accuracy from distance

The accuracy estimates for measured ground coordinates have also, with 30 μ m data, the same nature as with the 15 μ m imagery. Also here, the variation is much larger, which indicates problems in measurements and the quality of signals on 30 μ m imagery. The corresponding values calculated from the check point coordinates are now about 6 mm larger. Nevertheless, the lowest values are at same level as with 15 μ m imagery.

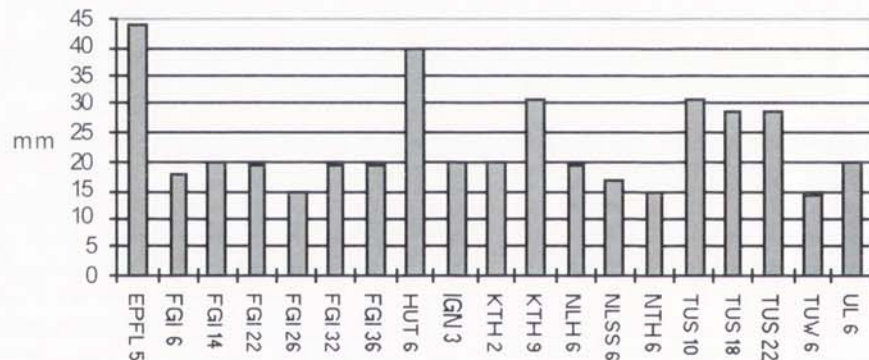


Figure 8 – Estimated local coordinate errors calculated from short distances, when 30 μ m imagery, dense control, and additional parameters have been used.

9.4 Effect of pixel size

The influence of pixel size has been investigated by comparing corresponding adjustments with 15 and 30 μm data. The comparison is here limited to the cases, where dense control and additional parameters have been used. In some cases the comparison is not possible, due to gross errors in one of the cases or the lack of corresponding adjustment.

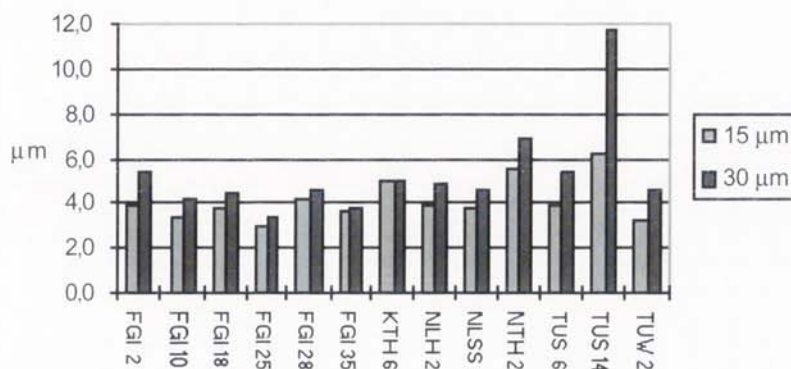


Figure 9 – The standard errors s_0 from adjustments with 15 and 30 μm data when using dense control and additional parameters. The names refer to cases with 15 μm data.

The changes in the standard error vary much. In visual cases (FGI 2, NLH 2, NLSS 2, NTH 2 and TUS 6) the changes are on the level of 1 μm . In cases FGI 10 ... FGI 35 the increased number of area based matches decreases the difference to almost zero. The big change in TUS 14 is a result of feature based matching, the accuracy of which is nearly constant in pixel units. In TUV 2 the matching method is the same as in TUS 14, but due to a much lower number of feature based matched points, the effect of visually observed signalised points is still dominant. In KTH 6 the reason for the zero difference might be the fact that the values have been given as rounded-off to whole μm s; or some error, because neither the measuring method nor the theoretical and empirical RMS values support it.

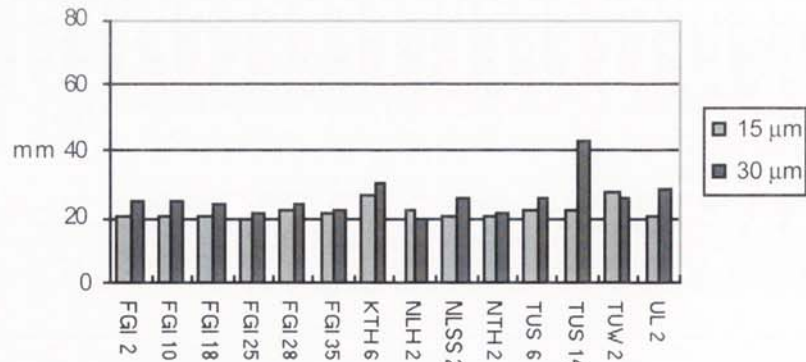


Figure 10 – The RMS values of plane coordinates from adjustments with 15 and 30 μm data when using dense control and additional parameters. The names refer to cases with 15 μm data.

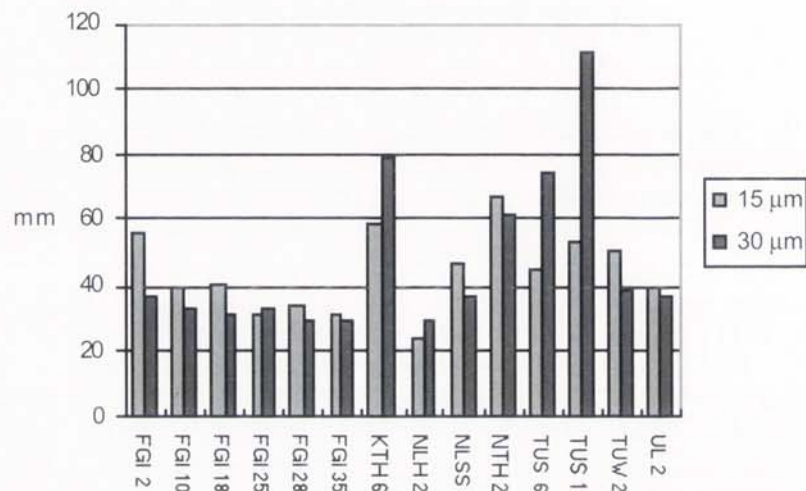


Figure 11 – The RMS values of height coordinates from adjustments with 15 and 30 μm data when using dense control and additional parameters. The names refer to cases with 15 μm data.

The RMS values (Figure 10 and Figure 11) show a quite unexpected pattern. The height accuracy with 30 μm imagery is in most cases (9 of 14) better than with 15 μm imagery. If large changes, which can be explained as a special feature of the method, like in TUS 14, or gross errors are left out, the phenomenon is even clearer. On the other hand, the planimetric accuracy is, in general, slightly worse with 30 μm data.

The basic differences between 15 and 30 μm imagery are the better quality of signals on 15 μm imagery and the larger area on the ground for area based matching and also for visual observations on 30 μm imagery. The former property explains well the differences in planimetric accuracy. On the other hand, the series of FGI show that the quality and the amount of measurements make the difference very small.

It is difficult to explain the behaviour of height accuracy. There is also no clear evidence that visual or digital measurements would behave differently. The larger matching window on the ground could be a weak explanation. The signals are mostly painted on the street (= horizontal plane without texture), and so the larger window may allow better parallax measurements.

The results above show that, in point densification, practically the same accuracy can be achieved with both pixel sizes. It requires, however, suitable methods and a high quality of measurements.

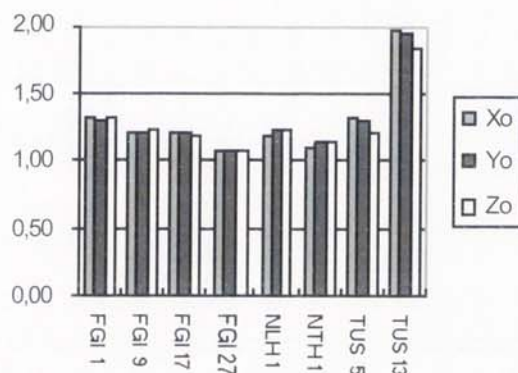


Figure 12 – The relation (30 μm /15 μm) of theoretical accuracy estimates for coordinates of projection centres. The results are from cases with dense control and without additional parameters.

The changes in theoretical estimates of projection centres (Figure 12) show the same trend as the empirical estimates of X- and Y-coordinates on the ground. The values are, in general, approximately 20 % larger with 30 μm imagery; but, with a high number of accurate measurements, the changes remain below 10 %. Also in this respect, the 30 μm imagery seems to be well acceptable for accurate photogrammetric triangulation. However, the choice of the method must be correct.

9.5 Effect of measuring resolution

The measuring resolution has been different practically in each system. In most cases it was smaller than $1/4$ of a pixel, often $1/8$ or $1/10$. In some cases, it was not given or it could vary within single measurements. The measurements with lower resolution ($1 - 1/3$ pixel) are, in case of dense control and additional parameters, presented in Figure 13.

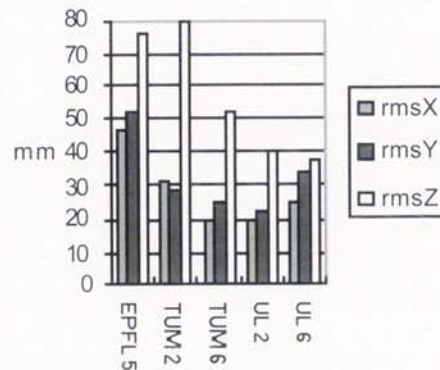


Figure 13 – Results from measurements with low resolution ($1 - 1/3$ pixel) when using dense control and additional parameters. EPFL 5 = $30\text{ }\mu\text{m}/1$ pixel, TUM 2 = $15\text{ }\mu\text{m}/1$ pixel, TUM 6 = $15\text{ }\mu\text{m}/1/3$ pixel, UL 2 = $15\text{ }\mu\text{m}/1/2$ pixel and UL 6 = $30\text{ }\mu\text{m}/1/2$ pixel.

In TUM 6 and UL 2 the accuracy is at the same level as in most other cases with $15\text{ }\mu\text{m}$ data. The effect of low resolution can be regarded as a rounding-off error, the mean error of which is 0.29 of the measuring unit (Hirvonen 1971). In case of $1/2$ pixel resolution and $15\text{ }\mu\text{m}$ pixel size, it causes an additional random error of $2.2\text{ }\mu\text{m}$ into the measured coordinates. It has only a minor effect also in accurate block triangulations.

With $30\text{ }\mu\text{m}$ pixel size, a $1/2$ pixel resolution, corresponding to a $4.4\text{ }\mu\text{m}$ random error, has already a greater effect on the adjusted coordinates. This can be seen in UL 6. Figure 10 also shows that the decrease in plane accuracy from UL 2 to UL 6 is larger than in the other comparable cases. In height (Figure 11) the $30\text{ }\mu\text{m}$ data is still at the level of $15\text{ }\mu\text{m}$ data.

One pixel resolution with $30\text{ }\mu\text{m}$ data leads already to remarkable errors (EPFL 5).

It can be concluded that, in aerotriangulation, the measuring resolution must be better than $10\text{ }\mu\text{m}$, and in the most accurate cases below $5\text{ }\mu\text{m}$. These values are still high, when compared with conventional photogrammetric systems. In them, the measuring accuracy and the resolution are usually at the same level; and very often the resolution is higher than the accuracy.

9.6 Effect of tie point quality

In this investigation, many of the tie points are signals, which are easy to measure accurately. Therefore, the effect of tie point quality on the block has been questioned. To answer this question, some participants have recalculated the block adjustment so that all the signalised tie points are excluded. The check point coordinates have then been defined using spatial intersections.

In FGI 17–24, corresponding in other respects to FGI 9–16, each signalised tie point was replaced by a natural detail in the vicinity of the signal. All other observations in both groups were the same.

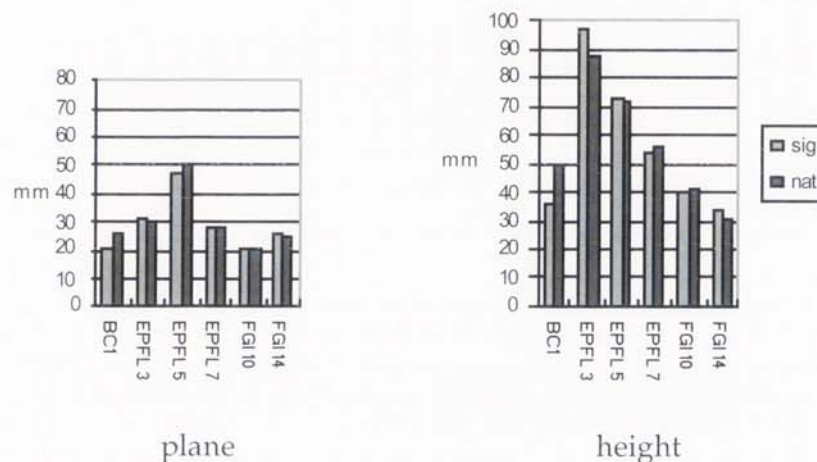


Figure 14 – RMS values of plane and height coordinates in measurements of EPFL and FGI, when all possible (i.e. signalised and natural = sig) and only natural (nat) tie points have been used. The blocks have been adjusted using dense control and additional parameters.

In cases of FGI, the s_0 value increased, with both pixel sizes, on an average by $0.3 \mu\text{m}$, when natural tie points were used. This indicates that the quality of natural points is slightly poorer than the quality of signals. However, $0.3 \mu\text{m}$ on original image scale corresponds to only 1 mm on the ground.

With $15 \mu\text{m}$ data (FGI 10), the RMS values were on an average 1 mm larger. On the other hand, with $30 \mu\text{m}$ data (FGI 14), the RMS values were, when using natural tie points, on an average 1 mm smaller. The changes are so small that they can be regarded as insignificant.

In EPFL all the measurements were readjusted so that the signalised tie points were left out (EPFL 9–12). As a side effect, at the same time, the amount of tie points was also reduced. The s_0 value increased in every case.

Especially in BC1, the change is absolutely and relatively large, from 3,3 μm to 3,7 μm . With DSW (EPFL 3) and ImageStation (EPFL 7) measurements, the increase is 0,1 μm , and in DPW (EPFL 5) 0,5 μm . The reduction of signalised points in visual measurements (BC1) has a clear effect on RMS values of all three coordinates, but, in digital systems, the changes are, in plane, relatively small. However, in height, the variation is much larger, and drawing conclusions is difficult.

In spite of some uncertainties in cases of EPFL, the results above show that in systems based on digital imagery and methods, natural tie points give practically the same accuracy as signalised tie points. Even if the item has not been investigated here, it can be expected that the accuracy of tie point measurements and of the whole block, at the same time, decreases, when the measurements are made using monocular visual observations.

9.7 Effect of control point density

The importance of control point density decreases, when in-flight GPS measurements are in wide use. However, the sensitiveness to control point density is also an indication of the general quality of the methods.

It could be expected that the sensitiveness to different control point configurations would depend on the quality of tie point measurements and on the amount of measured points. This has been investigated by calculating the differences from RMS values on check points between adjustments with dense and sparse ground control. Even if the instability with sparse control makes the drawing of conclusion difficult, some trends can be seen.

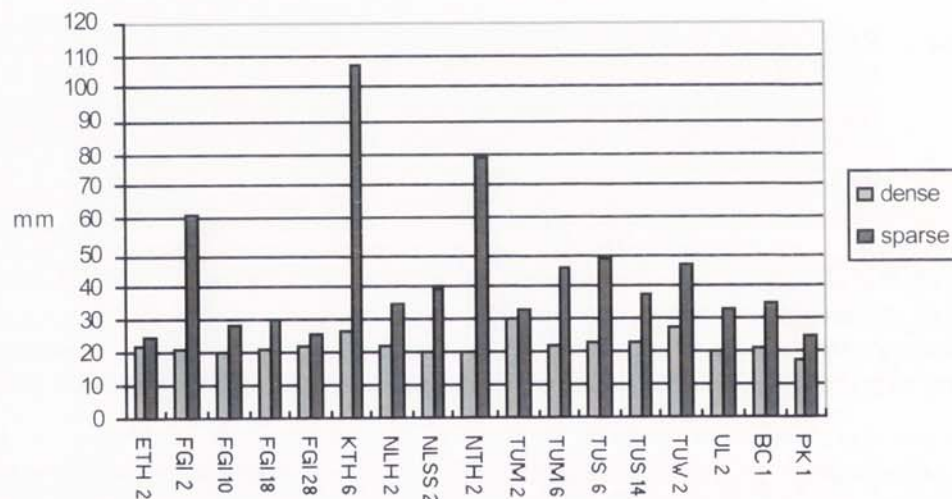


Figure 15 – The RMS values of plane coordinates on check points with dense and sparse control and additional parameters. In digital cases, the pixel size is 15 μm . The names of the cases refer to adjustments with dense control and additional parameters.

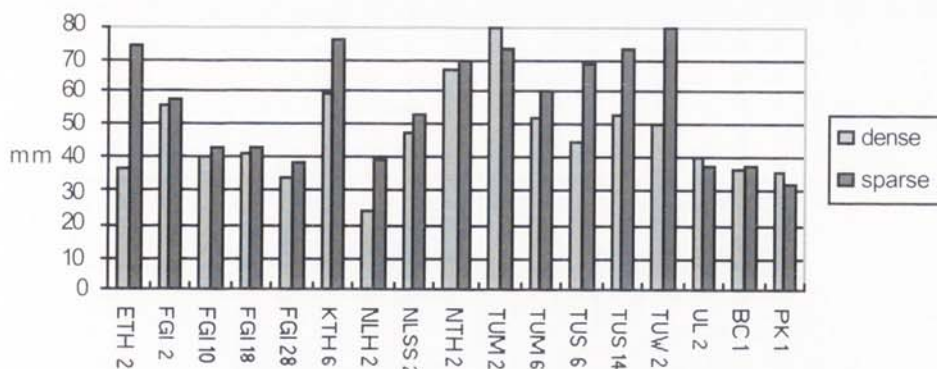


Figure 16 – The RMS values of height coordinates on check points with dense and sparse control and additional parameters. In digital cases, the pixel size is 15 μ m. The names of the cases refer to adjustments with dense control and additional parameters.

In 15 μ m data, the decrease in accuracy with sparse control is only some mm in the best cases. The amount of observations does not seem to be important, whereas the quality of observations has, in general, a positive effect. The changes with analogue imagery are smaller than with digital imagery.

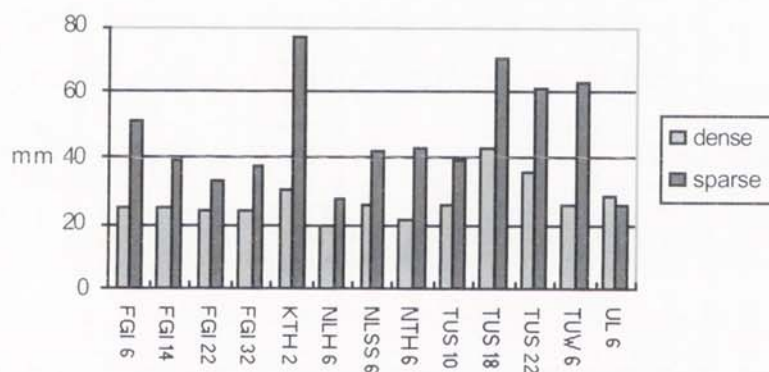


Figure 17 – The RMS values of plane coordinates with dense (with additional parameters) and sparse (without additional parameters) control. The pixel size is 30 μ m. The names of the cases refer to adjustments with dense control and additional parameters.

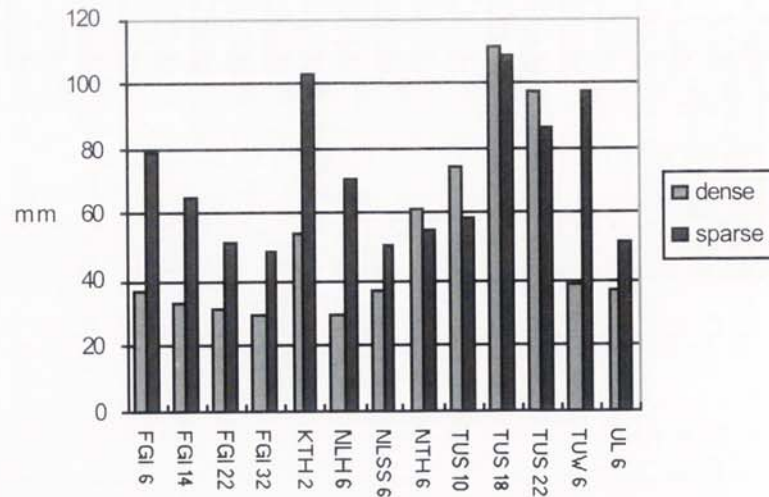


Figure 18 – The RMS values of height coordinates with dense (with additional parameters) and sparse (without additional parameters) control. The pixel size is 30 μm . The names of the cases refer to adjustments with dense control and additional parameters.

The 30 μm data is more sensitive to the density of ground control and the use of additional parameters than 15 μm data. Therefore the comparisons were made between the best cases in both control types, in dense cases using adjustments with additional parameters, and in sparse cases without. The trends are in plane the same as with the 15 μm data, but the decrease in accuracy is larger in sparse cases. The behaviour in the height is quite different. In the cases, where the height accuracy has been poor with dense control (NTH 6, TUS 10, TUS 18 and TUS 22), it even gets better if sparse control has been used. Two of the four cases have been measured visually and two automatically.

9.8 Effect of bad imaging of signals

The reduction of the check point set to points measured by all the participants means that several points with low contrast and deformed shape have been left out. Its influence has been investigated by comparing the RMS values achieved with the selected point set, and the corresponding values with all measured check points, except those 6, which were regarded as gross errors. For this purpose, cases with a high amount of measured check points were selected. This led to measurements made by TUS. The amount of measured check points was 71–73 XY-points and 60–62 Z-points, when digital imagery was used. The corresponding values in PK1 measurements were 76 and 64. The higher number comes from the better image quality of the original analogue imagery.

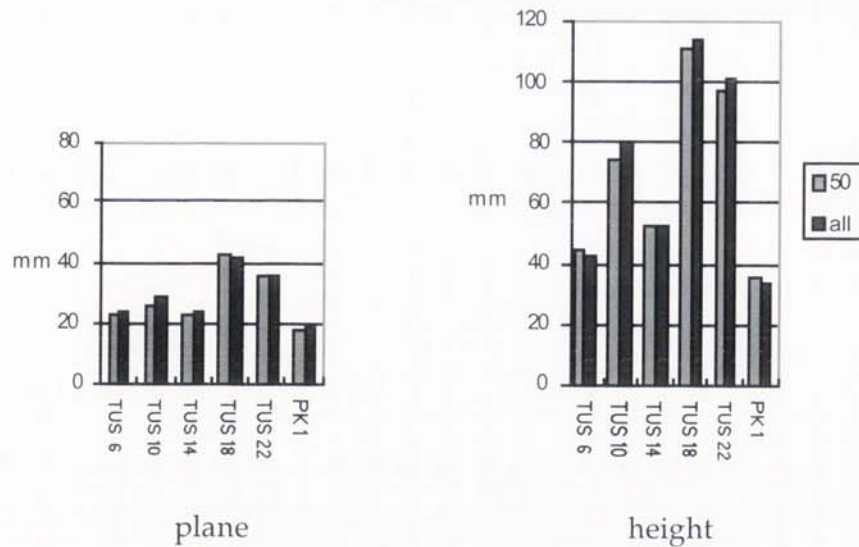


Figure 19 – The RMS values of ground coordinates from used (50) and complete (all) check point sets.

The differences between both check point sets show that the additional (more than twenty) “bad” check points affect the RMS values in plane only slightly. The increase is on an average about 1 mm. In height, there is a clear difference between pixel sizes. With 30 μ m imagery, TUS 10, TUS 18, and TUS 22, the increase is on an average 5 mm, whereas, in other cases, there are no essential differences.

The results above show that the limitation to 50 check points leads in case of 30 μ m imagery to slightly smaller RMS values in height. In all other cases the effect is neglectable.

9.9 Theoretical accuracy estimates

Some participants have been able to submit also theoretical accuracy estimates for the unknowns of the block adjustments. These values can be used for controlling the quality of the used mathematical models and of the check point coordinates. Because of the errors in check point coordinates, the empirical accuracy estimates are biased, and the comparisons between theoretical and empirical estimates are not quite correct.

The theoretical accuracy estimates provide also accuracy information about the elements of exterior orientation.

9.9.1 Elements of exterior orientation

The accuracy of exterior orientation can be regarded as a quality measure of a block adjustment. Especially, it gives good information for comparing two

similar block adjustments with each other. In more general cases, the correlation between orientation parameters of an image and its neighbouring images are needed. However, separate series of measurements of single participants give good insight into the behaviour of accuracy estimates.

In the following, some cases are shown to give an idea of the behaviour of error estimates. Only the coordinates of the projection centres have been taken into consideration here. The rotation parameters behave in a similar way.

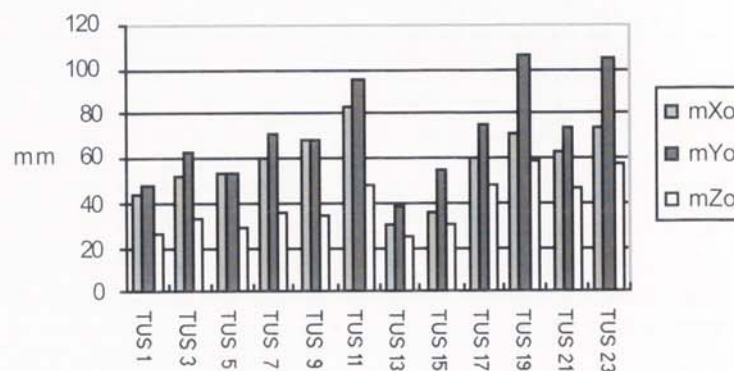


Figure 20 – Theoretical error estimates for the coordinates of the projection centres in adjustments of TUS. The values are from cases with dense and sparse control without additional parameters.

Figure 20 shows the values of the accuracy estimates from the measurements made in TUS. They are from cases, where no additional parameters have been used, because only these values were available. The values for cases with additional parameters would differ only slightly from corresponding values, if dense ground control were used. With sparse control, the values would be larger.

It can be seen that the best theoretical accuracy for projection centres has been achieved using feature based matching, 15 μ m imagery and dense control (TUS 13). The corresponding PK1 measurement (TUS 1) is clearly less accurate. The inconsistency with the estimates achieved using check point coordinates is partly due to different pointing accuracy on check points. However, with digital data, in visual measurements (TUS 5) and automated measurements (TUS 13), the visual pointing method of the check points has been the same in both cases, and the discrepancy is still similar. It seems that the accuracy of individual elements of exterior orientation is not sufficient to describe block accuracy.

When comparing the accuracy estimates in Figure 20, one has to remember that, in cases where feature based matching has been used, in addition to control points, also signalised check points have been measured visually. These points alone give a fairly good block structure. The accuracy estimates

are thus better than in cases where only feature based matched tie points are used.

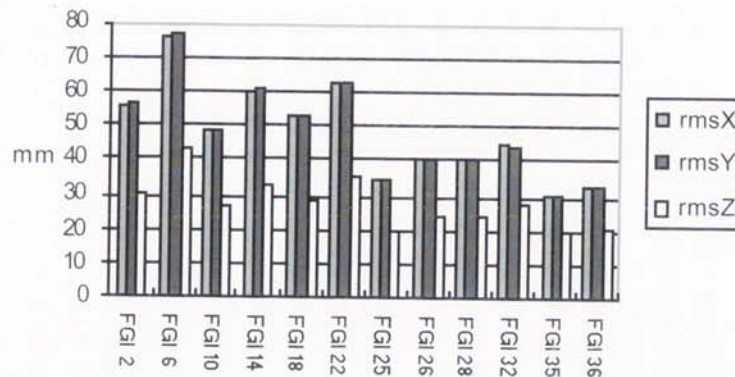


Figure 21 – Theoretical error estimates for the coordinates of the projection centres in adjustments of FGI with additional parameters.

The measurements of FGI, in cases with additional parameters and dense control, in Figure 21, show similar properties as in the cases of TUS. The most important factor for achieving high theoretical accuracy seems to be the number of observations. If the number of observations is high enough (FGI 35 and FGI 36), the importance of pixel size (and image quality) is very low. On the other hand, the quality of measurements is clearly visible in accuracy estimates, if the number of observations is low.

The discrepancies between the accuracy of exterior orientation and the RMS values of ground points are not so evident here as in previous cases of TUS. The reason is the block structure, which does not differ so much from case to case. However, the variation in the accuracy estimates of the parameters of exterior orientation is much larger than in the RMS values of the check points. So, also in these cases, the accuracy of exterior orientations and of ground coordinates do not seem to have linear dependency.

9.9.2 Ground points

The theoretical estimates for ground point accuracy and corresponding empirical RMS values have been compared only in cases with dense control and with additional parameters. In cases of sparse control the empirical values are due to block deformations often biased, and not applicable here. The theoretical values of TUS are from adjustments without additional parameters, and thus slightly larger than corresponding values with additional parameters.

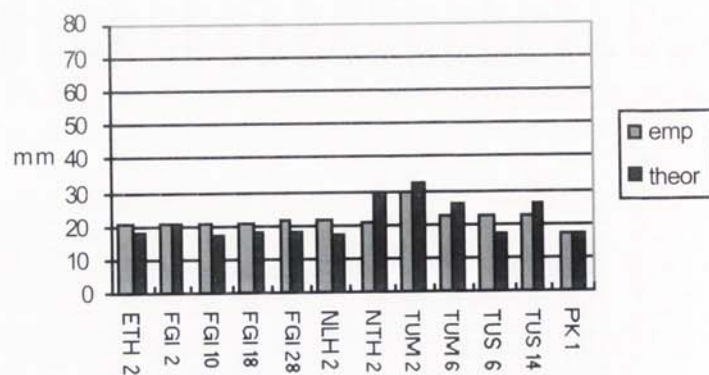


Figure 22 – Empirical (emp) and theoretical (theor) accuracy estimates of plane coordinates of ground points with 15 μ m imagery, when using dense control and additional parameters. The cases FGI 2, NLH 2, TUM 2, TUM 6, TUS 6 and PK1 are mainly visual methods.

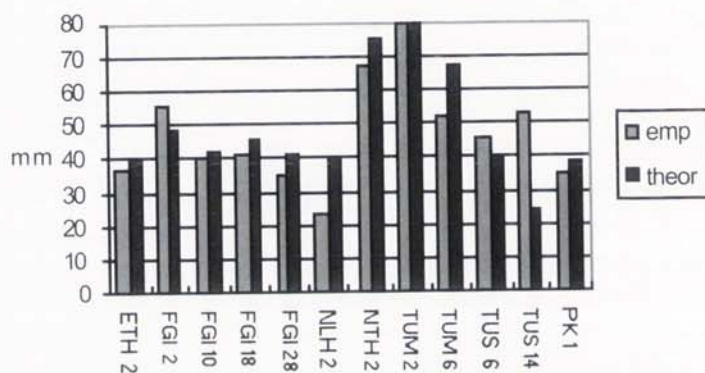


Figure 23 – Empirical (emp) and theoretical (theor) accuracy estimates of heights of ground points with 15 μ m imagery, when using dense control and additional parameters. The cases FGI 2, NLH 2, TUM 2, TUM 6, TUS 6 and PK1 are mainly visual methods.

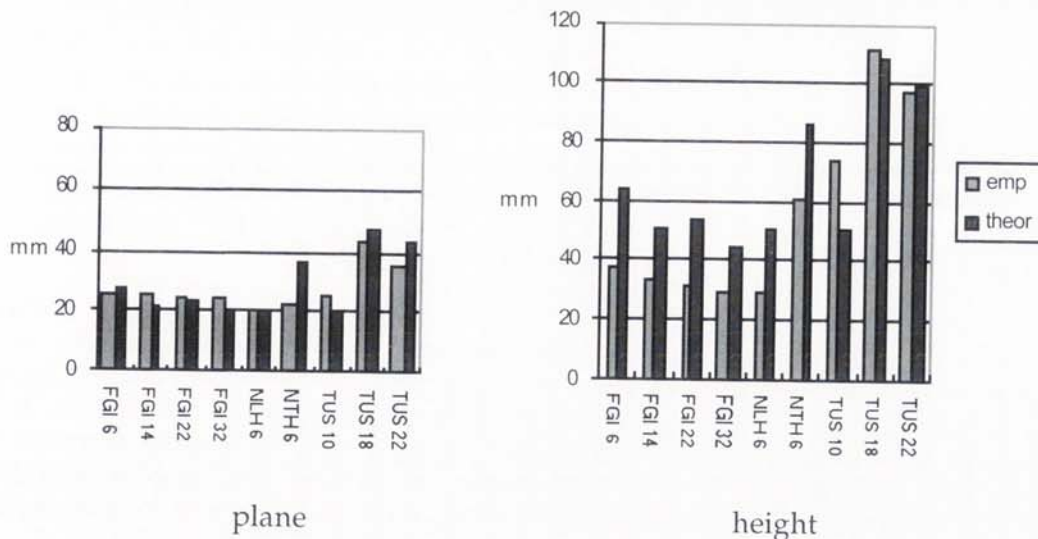


Figure 24 – Empirical (emp) and theoretical (theor) accuracy estimates of heights of ground points with 30 μ m imagery, when using dense control and additional parameters. The cases FGI 6, NLH 6, NTH 6 and TUS 10 are mainly visual methods.

Figures 22–24 show the empirical and theoretical accuracy estimates of ground coordinates. They do not give, in detail, any clear impression of the relationship between the two groups of values. Partly, because they refer to different values. The theoretical values refer to all unknown ground points, but the empirical values only to the signalled check points. This difference is very essential in TUS 14, TUS 18 and TUS 22. Some general conclusions can be drawn.

- Theoretical errors for plane coordinates are, in general, smaller than empirical errors. The main reason are the errors of the check point coordinates. The effect might be in the order of 2 mm. A difference of this magnitude comes in the most accurate cases from check point coordinate errors of 10 mm. This fits quite well with the considerations made in Chapter 5.2.
- The heights, especially with 30 μ m data, seem to be more accurate than the theoretical values let one assume. An explanation might be the good quality of parallax measurements, when area based matching has been used. The mathematical models do not take into account the correlation, which apparently exists on homologous image patches, and the parallax measuring method. In completely visual methods the trend seems to be, if not very clearly, slightly inverse.

10 Conclusions

This project on digital aerial triangulation was implemented as a multi-site comparative test project. Nearly all of the triangulations carried out by the participants would satisfy normal requirements of any mapping or data collection project. This is a very positive outcome, especially when the large variety of the methods and systems and also the experimental nature of these systems is taken into account. The main results of this test project are related to accuracy. The following detailed conclusions can be made:

- Digital aerial imagery seems to have the potential for accurate aerotriangulation. In the best realisations, the accuracy is at the same level with the most accurate conventional methods. With the proper usage of automation, which means a high amount of tie points, high quality coordinate measurements on the image, an even distribution of tie points, and good ties between image strips, the accuracy potential of digital imagery exceeds that of analogue data and conventional methods.

In this test, pixel size was, in most of the cases, a less important factor than expected. It is in the most accurate methods, almost neglectable. On the other hand, pixel size is, in systems using feature based matching for tie point measurements, the most critical factor.

- A measuring resolution of half a pixel is sufficient also with small amounts of observations, if the pixel size is 15 μm .
- In methods using area based matching, signalised tie points are not significantly better than natural details.
- Planimetric accuracy is in completely visual methods using digital imagery, in the best cases, at the same level with more advanced methods. The heights are in most cases slightly poorer.
- The relation of height to plane accuracy is smaller when area based image matching has been used on tie point measurements than in visual methods.
- The used theoretical accuracy estimates give too large values for height accuracy. The reason is the incorrect stochastic model used in block adjustments.
- Sensitiveness to sparse ground control is, when using digital methods, very often larger than with conventional analogue methods.

The conclusions above have been drawn from the results and experience obtained in this case. It is especially characterized by the use of large scale photography in urban area. The results could be different in other conditions and with different project parameters. The most important parameters are the scale of the photography, the block size, the shape and size of the signals, and the use of in-flight GPS measurements. In these respects, there are many opportunities for further research.

Concerning operational aspects, the project reassured that digital aerial triangulation is a working concept. A good accuracy is achievable by manual, semiautomatic or nearly fully automatic methods. The tests by participants have been made with systems that are nearly three years old by the time this report comes out of print. Since 1993, a lot of progress has already been made regarding the capabilities of systems for digital aerial triangulation. Therefore it is not considered justified to evaluate the operational aspects much further here. As many of the participants of the test struggled with limited disk capacities and sluggish systems, the situation has changed very rapidly. In this respect, it is a general opinion that we have just stepped over a critical threshold for using digital photogrammetric methods in daily production.

The design and implementation of more productive systems has also been alleviated by research since 1993: many papers have been published on image compression, image matching, line photogrammetry, automatic selection of tie points, etc. A thorough understanding of these issues is necessary for automatic and robust systems for digital aerial triangulation.

11 Acknowledgements

The authors thank Landesvermessungsamt Baden-Württemberg in Stuttgart/Germany for the scanning of the imagery, and the authorities of the City of Forssa for the delivery of the photography and the coordinate information for this test. Special thanks go to all the participants who have delivered their results for the final analysis.

The authors wish to thank Prof. Dr. F. Ackermann, Prof. Dr. Ø. Andersen, Prof. Dr. I. Dowman, Prof. Dr. O. Kölbl and Prof. Dr. K. Torlegård as referees of OEEPE for their remarks and suggestions. The remaining errors and omissions are, of course, solely the responsibility of the authors.

12 References

Ackermann, F., 1983. High precision digital image correlation. Proceedings of the 39th Photogrammetric Week, Institute for Photogrammetry, Stuttgart University, Stuttgart, pp. 231–243.

Ackermann, F., 1984. Digital Image Correlation: Performance and Potential Application in Photogrammetry. *The Photogrammetric Record*, 11(64), pp 429–439.

Ackermann, F. and W. Schneider, 1986. High Precision Aerial Triangulation with Point Transfer by Digital Image Correlation. *International Archives of Photogrammetry and Remote Sensing*, Vol. 26, Part 3/1, Rovaniemi, pp.18–27.

Förstner, W., 1982. On the Geometric Precision of Digital Correlation. International Archives of Photogrammetry and Remote Sensing, Vol. 24-III, Helsinki, pp. 176-189.

Förstner, W., 1985; Prinzip und Leistungsfähigkeit der Korrelation und Zuordnung von Bildern. Proceedings of the 40th Photogrammetric Week, Institute for Photogrammetry, Stuttgart University, Stuttgart.

Förstner, W., 1986. A Feature based Correspondence Algorithm for Image Matching. International Archives of Photogrammetry and Remote Sensing, Vol. 26, Part 3/3, Rovaniemi, pp. 150-166.

Grün, A., 1985. Adaptive Least Squares Correlation: A Powerful Image Matching Technique. South African Journal of Photogrammetry, Remote Sensing and Cartography, 14(3), pp. 175-187.

Helava, U. and *W. Chapelle*, 1972. Epipolar-Scan Correlation, Bendix Technical Journal, 5(1), pp. 19-23.

Helava, U., 1976. Digital Correlation in Photogrammetric Instruments. A paper presented for the XIII International Congress for Photogrammetry, Helsinki, 26 p.

Helava, U., 1987. The Digital Comparator Correlator System (DCCS). Proceedings of the Intercommission conference on Fast Processing of Photogrammetric Data, Interlaken, pp. 404-418.

Helava, U., 1991. Prospects in Digital Photogrammetry. The Photogrammetric Journal of Finland. 12(2), pp. 57-64.

Hirvonen, R., 1971. Adjustment by least squares in Geodesy and Photogrammetry. Frederick Ungar Publishing Co., New York.

Hobrough, G., 1959. Automatic Stereo Plotting. Photogrammetric Engineering, 24(5), pp. 763-769.

Miller, S., *U. Helava* and *K. Devenecia*, 1992. Softcopy Photogrammetric Workstations. Photogrammetric Engineering and Remote Sensing, 58(1), pp. 77-83

Paderes, F., *E. Mikhail* and *W. Förstner*, 1984. Rectification of Single and Multiple Frames of Satellite Scanner Imagery Using Points and Edges as Control. NASA Symposium on Mathematical Pattern Recognition and Image Analysis, June 1984, Houston.

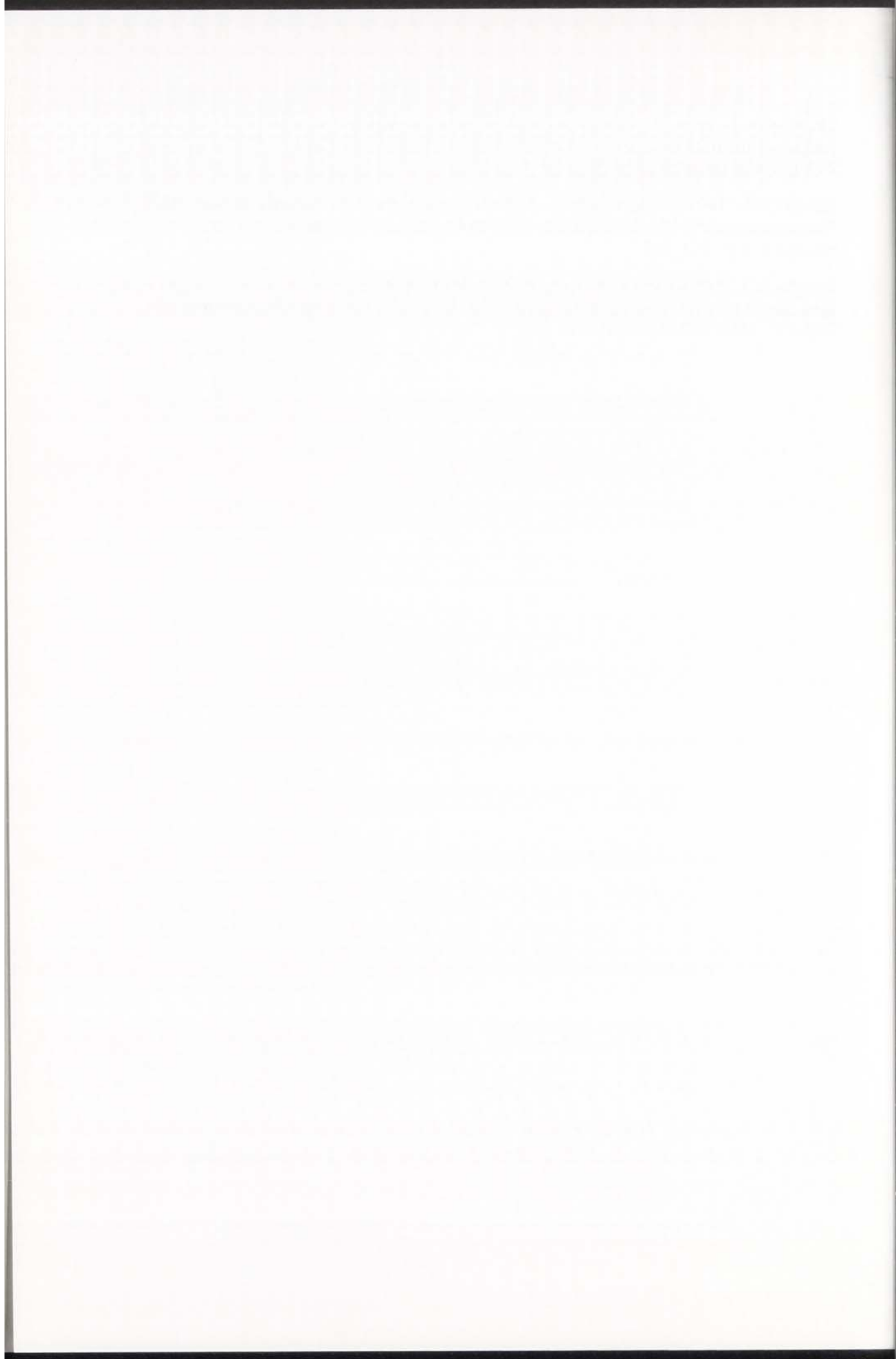
Sarjakoski, T., 1986. Potential of Expert-System Technology for Aerial Triangulation. International Archives of Photogrammetry and Remote Sensing, Vol. 26, Part 3/3, Rovaniemi, pp. 212-224.

Sarjakoski, T., 1988. Automation in Photogrammetric Block Adjustment Systems - On the Role of Heuristic Information and Methods. Acta Polytechnica Scandinavica, Ci 88, Helsinki, 125 p.

Thurgood, J. and E. Mikhail, 1982. Photogrammetric Analysis of Digital Images. International Archives of Photogrammetry and Remote Sensing, Vol. 24-III, Helsinki, pp. 576-590

Tsingas, V., 1991, Automatische Aerotriangulation. Proceedings of the 43rd Photogrammetric Week, Institute for Photogrammetry, Stuttgart University, Stuttgart, pp. 253-268.

Tsingas, V., 1992, Automatisierung der Punktübertragung in der Aerotriangulation durch mehrfache digitale Zuordnung. Deutsche Geodätische Kommission, Reihe C, Heft 392, Munich, 110 p.



Appendix A

The tabulated results of all the adjustments

Appendix B

Reports of the Participants

1. *O. Kölbl, M. Crosetto*
École Polytechnique Fédérale de Lausanne
2. *T. Kersten, D. Stallmann*
ETH-Hoenggerberg/Zurich
3. *J. Lammi*
Finnish Geodetic Institute
4. *J. Heikkinen*
Helsinki University of Technology
5. *E. Beauvillain*
Institut Géographique National, St-Mandé
6. *H. Wiman*
KTH-Stockholm
7. *Ø. Andersen, L. E. Blankenberg, I. Maalen-Johansen*
Agricultural University of Norway
8. *J. Talts*
National Land Survey of Sweden
9. *I. Hådem*
University of Trondheim
10. *C. Heipke*
Technical University of Munich
11. *V. Tsingas*
University of Stuttgart
12. *F. Rottensteiner, R. Prinz*
Technical University of Vienna
13. *J.-P. Agnard, P.-A. Gagnon, M. Boulianne*
Laval University, Quebec/Canada

THE UNIVERSITY OF CHICAGO
LIBRARY
1100 EAST 58TH STREET
CHICAGO, ILL. 60637
TEL. 773-936-5000

DATE
BY

1. *[Faint text]*

2. *[Faint text]*

3. *[Faint text]*

4. *[Faint text]*

5. *[Faint text]*

6. *[Faint text]*

7. *[Faint text]*

8. *[Faint text]*

9. *[Faint text]*

The tabulated results of all the adjustments.

The column labels mean:

Case	= name of the case
15/30	= pixel size, 15 or 30 μm
D/S	= ground control, D = dense, S = sparse
P/N	= adjustment with (P) or without (N) additional parameters
obs	= number of observations / image
s0	= standard error of unit weight [μm]
rmsX, rmsY, rmsZ	= RMS values from check point coordinates [mm]
rmsC	= RMS value of plane coordinates from short distances [mm]
nxy	= number of XY check points
nz	= number of Z check points
rej	= number of rejected check points
mX, mY, mZ	= theoretical accuracy for ground coordinates [mm]
mXo, mYo, mZo	= theoretical accuracy for coordinates of the projection centres [mm]
mOm, mPh, mKa	= theoretical accuracy for rotations of the camera [mrad]

EPFL

- EPFL 1-2 Wild BC1 analytical plotter measurements using analogue imagery.
- EPFL 3-4 Helava DSW 100 measurements.
- EPFL 5-6 Leica DPW measurement.
- EPFL 7-8 Intergraph ImageStation measurements.
- EPFL 9 Adjustments with natural tie points only (BC1).
- EPFL 10 Adjustments with natural tie points only (DSW 100).
- EPFL 11 Adjustments with natural tie points only (DPW).
- EPFL 12 Adjustments with natural tie points only (ImageStation).

Empirical estimates:

Case	15/30	D/S	P/N	obs	s0	rmsX	rmsY	rmsZ	rmsC	nxy	nz	rej
EPFL 1		D	P	27	3,3	20	22	36	20	49	40	1
EPFL 2		S	P	27	3,1	23	44	37	18	50	41	0
EPFL 3		D	P	30	5,5	33	27	97	25	49	40	1
EPFL 4		S	P	30	5,4	55	62	125	25	49	40	0
EPFL 5	30	D	P	34	11,2	50	45	73	44	48	39	1
EPFL 6	30	S	P	34	11,2	79	78	72	46	49	40	0
EPFL 7	15	D	P	26	5,5	29	26	54	20	48	39	0
EPFL 8	15	S	P	26	5,4	63	39	60	20	48	39	0
EPFL 9		D	P	17	3,7	24	26	49	19	47	38	1
EPFL10		D	P	21	5,6	34	25	88	24	48	39	0
EPFL11	30	D	P	25	11,7	52	48	72	48	48	39	0
EPFL12	15	D	P	17	5,6	29	26	56	20	48	39	0

ETH

ETH 2, 5, 8 and 11 Adjustments with an additional parameter set of 12 parameters.

ETH 3, 6, 9 and 12 Adjustments with an additional parameter set of 44 parameters.

Empirical estimates:

Case	15/30	D/S	P/N	obs	s0	rmsX	rmsY	rmsZ	rmsC	nxy	nz	rej
ETH 1	15	D	N	25	3,9	33	28	39	20	49	40	1
ETH 2	15	D	P	25	3,7	21	22	36	19	50	41	0
ETH 3	15	D	P	25	3,5	21	24	37	19	50	41	0
ETH 4	15	S	N	25	3,8	40	30	51	20	49	40	1
ETH 5	15	S	P	25	3,7	20	30	74	19	50	41	0
ETH 6	15	S	P	25	3,5	31	37	77	19	50	41	0
ETH 7	30	D	N	25	7,7	36	67	69	29	48	39	0
ETH 8	30	D	P	25	7,5	31	69	68	29	48	39	0
ETH 9	30	D	P	25	7,6	31	68	68	29	48	39	0
ETH 10	30	S	N	25	7,4	44	162	69	30	48	39	0
ETH 11	30	S	P	25	7,3	32	154	64	31	46	39	2
ETH 12	30	S	P	25	7,5	27	157	62	30	46	39	2

Theoretical estimates:

Case	15/30	D/S	P/N	obs	mX	mY	mZ
ETH 1	15	D	N	25	18	18	40
ETH 2	15	D	P	25	18	18	39
ETH 3	15	D	P	25	18	18	42
ETH 4	15	S	N	25	26	26	45
ETH 5	15	S	P	25	30	30	46
ETH 6	15	S	P	25	31	31	62
ETH 7	30	D	N	25	32	32	74
ETH 8	30	D	P	25	33	33	75
ETH 9	30	D	P	25	35	35	82
ETH 10	30	S	N	25	46	46	82
ETH 11	30	S	P	25	55	55	87
ETH 12	30	S	P	25	60	60	125

FGI

- | | |
|-----------|--|
| FGI 1-8 | Visual observations. |
| FGI 9-16 | Points were measured visually on the first images. On the others, correlated with the first observations. |
| FGI 17-24 | Like FGI 9-16, but the tie points have been natural details. |
| FGI 25-26 | Like FGI 9-16, but all the points have been measured visually and then correlated to corresponding observations on other images. |
| FGI 27-34 | Like FGI 9-16, but the number of tie points has been added from 27 to 34 per image. |
| FGI 35-36 | Like FGI 25-26, but using tie points like in FIG 27-34. |

Empirical estimates:

Case	15/30	D/S	P/N	obs	s0	rmsX	rmsY	rmsZ	rmsC	nxy	nz	rej
FGI 1	15	D	N	17	4,2	22	21	53	17	49	41	1
FGI 2	15	D	P	17	3,9	20	22	56	16	49	41	1
FGI 3	15	S	N	17	4,2	22	57	58	17	49	41	1
FGI 4	15	S	P	17	3,9	36	79	58	18	49	41	1
FGI 5	30	D	N	17	5,6	26	25	45	18	49	41	1
FGI 6	30	D	P	17	5,3	27	23	37	12	48	40	2
FGI 7	30	S	N	17	5,6	51	51	79	18	49	41	1
FGI 8	30	S	P	17	5,3	66	77	80	24	49	41	1
FGI 9	15	D	N	17	3,7	22	20	37	19	48	40	2
FGI 10	15	D	P	17	3,4	21	20	40	17	49	41	1
FGI 11	15	S	N	17	3,7	29	31	37	20	48	40	2
FGI 12	15	S	P	17	3,4	31	26	43	18	49	41	1
FGI 13	30	D	N	17	4,4	25	27	37	20	50	41	0
FGI 14	30	D	P	17	4,2	24	26	33	20	50	41	0
FGI 15	30	S	N	17	4,3	32	45	65	22	50	41	0
FGI 16	30	S	P	17	4,2	30	46	44	22	49	40	1
FGI 17	15	D	N	17	3,9	22	23	39	21	50	41	0
FGI 18	15	D	P	17	3,7	21	21	41	19	49	40	1
FGI 19	15	S	N	17	4,0	28	29	38	21	50	41	0
FGI 20	15	S	P	17	3,7	35	25	43	19	48	39	2
FGI 21	30	D	N	17	4,7	23	25	35	20	50	41	0
FGI 22	30	D	P	17	4,4	23	25	31	19	50	41	0
FGI 23	30	S	N	17	4,7	26	38	51	21	50	41	0
FGI 24	30	S	P	17	4,4	29	49	39	20	50	41	0
FGI 25	15	D	P	37	2,9	19	21	31	16	50	41	0
FGI 26	30	D	P	36	3,4	19	24	33	15	49	40	1
FGI 27	15	D	N	34	4,4	22	24	36	20	49	41	1
FGI 28	15	D	P	34	4,2	21	23	34	18	49	41	1
FGI 29	15	S	N	34	4,4	29	27	38	21	48	40	2
FGI 30	15	S	P	34	4,2	24	28	38	18	48	40	2
FGI 31	30	D	N	34	4,8	24	26	42	19	50	41	0
FGI 32	30	D	P	34	4,6	22	26	30	19	49	40	1
FGI 33	30	S	N	34	4,8	39	36	49	21	49	40	1
FGI 34	30	S	P	34	4,7	32	42	39	21	49	40	1
FGI 35	15	D	P	54	3,6	19	23	32	17	50	41	0
FGI 36	30	D	P	54	3,7	22	24	30	19	49	40	1

Theoretical estimates:

Case	15/30	D/S	P/N	obs	mX	mY	mZ	mXo	mYo	mZo
FGI 1	15	D	N	17	20	21	48	56	57	31
FGI 2	15	D	P	17	20	21	47	56	57	31
FGI 3	15	S	N	17	34	42	61	66	91	44
FGI 4	15	S	P	17	39	56	69	78	113	55
FGI 5	30	D	N	17	27	27	64	74	75	42
FGI 6	30	D	P	17	27	28	64	76	77	43
FGI 7	30	S	N	17	42	47	77	89	122	59
FGI 8	30	S	P	17	49	58	82	105	153	74
FGI 9	15	D	N	17	17	18	42	49	49	27
FGI 10	15	D	P	17	17	18	42	48	49	27
FGI 11	15	S	N	17	26	29	49	56	65	33
FGI 12	15	S	P	17	30	35	51	63	72	37
FGI 13	30	D	N	17	21	21	50	59	59	33
FGI 14	30	D	P	17	21	22	51	60	61	33
FGI 15	30	S	N	17	24	25	58	65	65	38
FGI 16	30	S	P	17	25	28	61	73	72	42
FGI 17	15	D	N	17	19	19	45	52	52	29
FGI 18	15	D	P	17	19	20	44	53	53	29
FGI 19	15	S	N	17	30	33	54	63	73	37
FGI 20	15	S	P	17	34	40	57	72	81	43
FGI 21	30	D	N	17	22	23	53	62	62	34
FGI 22	30	D	P	17	22	23	53	63	63	35
FGI 23	30	S	N	17	36	40	65	76	87	45
FGI 24	30	S	P	17	41	48	69	86	97	51
FGI 25	15	D	P	37	12	14	30	34	34	20
FGI 26	30	D	P	36	15	16	35	41	40	24
FGI 27	15	D	N	34	18	19	41	39	40	25
FGI 28	15	D	P	34	18	19	40	41	41	25
FGI 29	15	S	N	34	25	28	46	45	53	30
FGI 30	15	S	P	34	28	33	47	51	59	33
FGI 31	30	D	N	34	19	21	44	42	43	27
FGI 32	30	D	P	34	19	21	44	45	44	28
FGI 33	30	S	N	34	27	31	49	48	57	33
FGI 34	30	S	P	34	30	36	51	56	64	37
FGI 35	15	D	P	54	14	16	32	31	31	20
FGI 36	30	D	P	54	15	16	34	33	33	21

HUT

Empirical estimates:

Case	15/30	D/S	P/N	obs	s0	rmsX	rmsY	rmsZ	rmsC	nxy	nz	rej
HUT 1	15	D	N	17	6,5	39	35	67	23	50	41	0
HUT 2	15	S	N	17	6,7	84	61	83	22	50	41	0
HUT 3	30	D	N	17	9,0	48	44	83	36	47	38	3
HUT 4	30	S	N	17	9,2	78	68	93	43	49	40	1
HUT 5	15	D	P	17	6,0	32	30	73	21	50	41	0
HUT 6	30	D	P	17	8,9	47	45	83	40	49	40	1

IGN

IGN 1-2 Measurement on a self developed digital photogrammetric workstation.

IGN 3-4 Matra Traster T10 measurements.

Empirical estimates:

Case	15/30	D/S	P/N	obs	s0	rmsX	rmsY	rmsZ	rmsC	nxy	nz	rej
IGN 1	15	D	P	20		68	177	63	36	46	37	1
IGN 2	15	S	P	20		117	118	97	41	47	38	0
IGN 3	30	D	P	20		29	27	54	20	47	38	0
IGN 4	30	S	P	20		32	31	53	19	46	37	1

KTH

KTH 1-4 Visual measurements using ERDAS software.

KTH 5-9 Semiautomatic measurements on a self developed digital photogrammetric workstation.

Empirical estimates:

Case	15/30	D/S	P/N	obs	s0	rmsX	rmsY	rmsZ	rmsC	nxy	nz	rej
KTH 1	30	D	N	13	7	100	45	103	25	47	40	2
KTH 2	30	D	P	13	8	26	33	54	20	46	39	3
KTH 3	30	S	N	13	7	100	45	103	25	47	40	2
KTH 4	30	S	P	13	8	23	31	55	19	46	39	3
KTH 5	15	D	N	15	5	25	32	74	21	45	37	2
KTH 6	15	D	P	15	5	24	29	59	21	45	37	2
KTH 7	15	S	N	15	5	43	62	124	33	46	38	1
KTH 8	15	S	P	15	8	85	125	76	30	45	38	2
KTH 9	30	D	P	15	5	27	32	79	31	42	36	2

NLH

Empirical estimates:

Case	15/30	D/S	P/N	obs	s0	rmsX	rmsY	rmsZ	rmsC	nxy	nz	rej
NLH 1	15	D	N	21	4,0	20	26	61	17	50	41	0
NLH 2	15	D	P	21	3,9	19	25	24	17	50	41	0
NLH 3	15	S	N	21	4,0	36	33	67	18	50	41	0
NLH 4	15	S	P	21	3,8	39	30	39	19	50	41	0
NLH 5	30	D	N	21	4,9	18	21	68	19	50	41	0
NLH 6	30	D	P	21	4,8	18	21	30	19	50	41	0
NLH 7	30	S	N	21	5,0	21	34	71	19	50	41	0
NLH 8	30	S	P	21	4,7	21	29	108	20	50	41	0

Theoretical estimates:

Case	15/30	D/S	P/N	obs	mX	mY	mZ	mXo	mYo	mZo
NLH 1	15	D	N	21	19	16	40	49	57	36
NLH 2	15	D	P	21	18	15	43	48	62	38
NLH 3	15	S	N	21	30	26	45	65	64	42
NLH 4	15	S	P	21	28	26	55	63	78	49
NLH 5	30	D	N	21	22	19	48	58	70	44
NLH 6	30	D	P	21	22	18	51	57	45	46
NLH 7	30	S	N	21	35	30	55	78	79	51
NLH 8	30	S	P	21	34	31	68	77	96	59

NLSS

Empirical estimates:

Case	15/30	D/S	P/N	obs	s0	rmsX	rmsY	rmsZ	rmsC	nxy	nz	rej
NLSS 1	15	D	N	16	4,0	23	20	50	16	49	40	1
NLSS 2	15	D	P	16	3,8	21	20	47	15	50	41	0
NLSS 3	15	S	N	16	4,0	29	22	48	18	50	41	0
NLSS 4	15	S	P	16	3,7	42	37	53	19	49	40	1
NLSS 5	30	D	N	16	5,0	27	26	37	17	49	40	1
NLSS 6	30	D	P	16	4,6	27	26	37	17	49	40	1
NLSS 7	30	S	N	16	4,8	32	49	50	18	50	41	0
NLSS 8	30	S	P	16	4,5	51	103	80	17	50	41	0

NTH

Empirical estimates:

Case	15/30	D/S	P/N	obs	s0	rmsX	rmsY	rmsZ	rmsC	nxy	nz	rej
NTH 1	15	D	N	13	5,6	22	25	57	17	48	40	2
NTH 2	15	D	P	13	5,5	21	20	67	16	49	41	1
NTH 3	15	S	N	13	5,5	34	105	78	17	49	41	1
NTH 4	15	S	P	13	5,5	46	101	70	17	50	41	0
NTH 5	30	D	N	14	6,9	18	29	57	16	47	38	2
NTH 6	30	D	P	14	6,9	19	24	61	15	47	38	2
NTH 7	30	S	N	14	7,0	36	49	55	19	48	39	1
NTH 8	30	S	P	14	7,0	70	57	51	19	48	39	1

Theoretical estimates:

Case	15/30	D/S	P/N	obs	mX	mY	mZ	mXo	mYo	mZo
NTH 1	15	D	N	13	32	26	75	102	119	63
NTH 2	15	D	P	13	32	26	74	101	117	63
NTH 3	15	S	N	13	60	54	94	141	144	84
NTH 4	15	S	P	13	70	61	95	150	149	89
NTH 5	30	D	N	14	40	32	86	111	136	72
NTH 6	30	D	P	14	41	32	87	113	138	73
NTH 7	30	S	N	14	71	64	108	160	168	99
NTH 8	30	S	P	14	83	72	109	170	174	104

TUM

TUM 1-4 Measurements with a resolution of 1 pixel.

TUM 5-8 Measurements with a resolution of 1/3 pixel.

Empirical estimates:

Case	15/30	D/S	P/N	obs	s0	rmsX	rmsY	rmsZ	rmsC	nxy	nz	rej
TUM 1	15	D	N	26	6,9	30	30	85	19	48	39	1
TUM 2	15	D	P	26	6,9	31	29	79	20	48	39	1
TUM 3	15	S	N	26	6,9	36	33	92	20	46	38	3
TUM 4	15	S	P	26	6,8	34	32	73	20	46	38	3
TUM 5	15	D	N	26	5,8	19	26	54	19	48	39	1
TUM 6	15	D	P	26	5,8	20	25	52	19	48	39	1
TUM 7	15	S	N	26	5,7	43	47	52	23	43	36	6
TUM 8	15	S	P	26	5,6	37	53	61	23	45	38	4

Theoretical estimates:

Case	15/30	D/S	P/N	obs	mX	mY	mZ
TUM 1	15	D	N	26	30	34	79
TUM 2	15	D	P	26	30	33	79
TUM 3	15	S	N	26	66	77	104
TUM 4	15	S	P	26	66	77	103
TUM 5	15	D	N	26	26	28	67
TUM 6	15	D	P	26	25	28	66
TUM 7	15	S	N	26	55	64	86
TUM 8	15	S	P	26	54	63	85

TUS

TUS 1-4 Zeiss PK1 monocomparator measurements using analogue imagery.

TUS 5-12 Visual observations on digital images.

TUS 13-16 Automatic measurements using 15 μm data (272 points per image).

TUS 17-20 Automatic measurements using 30 μm data (237 points per image).

TUS 21-24 Automatic measurements using 30 μm data (131 points per image).

Empirical estimates:

Case	15/30	D/S	P/N	obs	s0	rmsX	rmsY	rmsZ	rmsC	nxy	nz	rej
TUS 1		D	N	17	3,7	17	22	46	17	48	40	2
TUS 2		D	P	17	3,5	15	20	35	17	49	40	1
TUS 3		S	N	17	3,7	31	27	60	21	50	41	0
TUS 4		S	P	17	3,5	19	29	32	18	49	40	1
TUS 5	15	D	N	16	4,0	20	25	32	19	49	40	1
TUS 6	15	D	P	16	3,9	24	22	45	22	50	41	0
TUS 7	15	S	N	16	4,0	27	51	45	22	50	41	0
TUS 8	15	S	P	16	3,8	55	40	68	22	50	41	0
TUS 9	30	D	N	16	5,5	22	32	56	31	49	40	0
TUS 10	30	D	P	16	5,3	24	28	74	31	50	41	0
TUS 11	30	S	N	16	5,6	42	36	59	33	49	41	1
TUS 12	30	S	P	16	5,3	33	35	104	31	50	41	0
TUS 13	15	D	N	272	6,2	35	26	43	23	50	41	0
TUS 14	15	D	P	272	6,2	25	21	53	22	50	41	0
TUS 15	15	S	N	272	6,2	38	40	59	23	49	41	1
TUS 16	15	S	P	272	6,2	35	40	73	21	50	41	0
TUS 17	30	D	N	237	11,8	49	43	83	31	50	41	0
TUS 18	30	D	P	237	11,7	42	44	111	29	50	41	0
TUS 19	30	S	N	237	11,8	67	74	109	31	50	41	0
TUS 20	30	S	P	237	11,7	51	107	127	30	50	41	0
TUS 21	30	D	N	131	10,7	41	37	68	32	50	41	0
TUS 22	30	D	P	131	10,6	36	35	97	29	50	41	0
TUS 23	30	S	N	131	10,7	58	65	87	32	50	41	0
TUS 24	30	S	P	131	10,6	45	101	120	30	50	41	0

Theoretical estimates:

Case	15/30	D/S	P/N	obs	mX	mY	mZ	mXo	mYo	mZo	mOm	mPh	mKa
TUS 1		D	N	17	17	18	38	44	47	26	4,1	4,1	1,5
TUS 2		D	P	17									
TUS 3		S	N	17	27	30	45	51	62	33	4,8	4,5	1,9
TUS 4		S	P	17									
TUS 5	15	D	N	16	17	18	40	52	52	29	4,6	4,9	1,6
TUS 6	15	D	P	16									
TUS 7	15	S	N	16	27	32	47	60	70	36	5,4	5,3	2,1
TUS 8	15	S	P	16									
TUS 9	30	D	N	16	20	21	51	68	67	35	6,0	6,5	2,0
TUS 10	30	D	P	16									
TUS 11	30	S	N	16	34	41	63	82	95	47	7,4	7,5	2,8
TUS 12	30	S	P	16									
TUS 13	15	D	N	272	25	27	59	30	38	25	3,4	2,7	1,0
TUS 14	15	D	P	272									
TUS 15	15	S	N	272	30	35	63	36	53	30	4,0	2,8	1,3
TUS 16	15	S	P	272									
TUS 17	30	D	N	237	46	49	108	59	74	46	6,6	5,3	2,0
TUS 18	30	D	P	237									
TUS 19	30	S	N	237	55	63	115	70	106	57	8,2	5,7	2,5
TUS 20	30	S	P	237									
TUS 21	30	D	N	131	42	44	99	62	73	45	6,6	5,7	2,1
TUS 22	30	D	P	131									
TUS 23	30	S	N	131	52	60	107	73	105	56	8,1	6,1	2,6
TUS 24	30	S	P	131									

TUW

Empirical estimates:

Case	15/30	D/S	P/N	obs	s0	rmsX	rmsY	rmsZ	rmsC	nxy	nz	rej
TUW 1	15	D	N	21	3,2	33	32	72	24	49	41	1
TUW 2	15	D	P	21	3,2	28	27	50	23	49	41	1
TUW 3	15	S	N	21	3,2	52	40	78	26	48	40	2
TUW 4	15	S	P	21	3,2	49	45	80	23	49	41	1
TUW 5	30	D	N	19	4,8	26	29	45	15	46	37	1
TUW 6	30	D	P	19	4,5	25	27	39	14	46	37	1
TUW 7	30	S	N	19	4,5	47	76	97	40	45	36	2
TUW 8	30	S	P	19	4,5	73	46	35	17	45	36	2

UL

UL 1-8 Bundle block adjustment.

UL 9-12 Adjustment with independent models.

Empirical estimates:

Case	15/30	D/S	P/N	obs	s0	rmsX	rmsY	rmsZ	rmsC	nxy	nz	rej
UL 1	15	D	N	29		23	23	48	20	50	41	0
UL 2	15	D	P	29		19	22	40	19	50	41	0
UL 3	15	S	N	29		32	23	61	21	50	41	0
UL 4	15	S	P	29		32	33	37	19	50	41	0
UL 5	30	D	N	29		27	32	36	21	47	38	3
UL 6	30	D	P	29		25	33	37	20	47	38	3
UL 7	30	S	N	29		26	26	51	21	50	41	0
UL 8	30	S	P	29		41	29	84	22	50	41	0
UL 9	15	D	N			26	26	42	21	49	40	1
UL 10	15	S	N			42	42	82	21	50	41	0
UL 11	30	D	N			34	34	52	25	50	41	0
UL 12	30	S	N			76	53	66	26	50	41	0

Graphical representations of all the results.

In the names of the digital cases caseses:

15, 30 = pixel size in μm

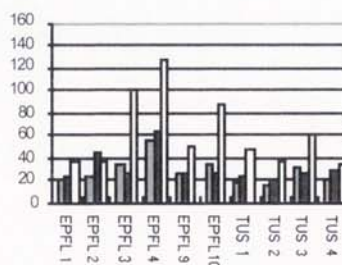
D = dense control

S = sparse control

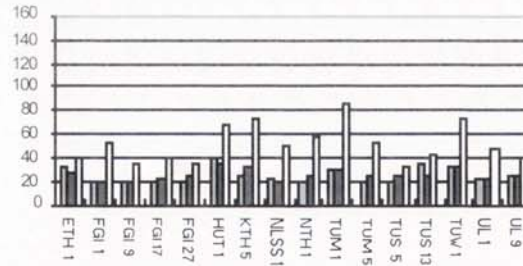
N = block adjustment without additional parameters

P = block adjustment with additional parameters

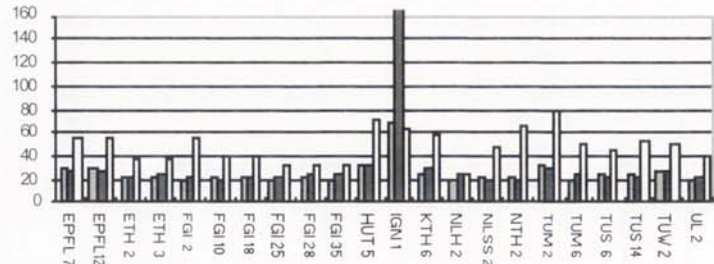
Comparative cases



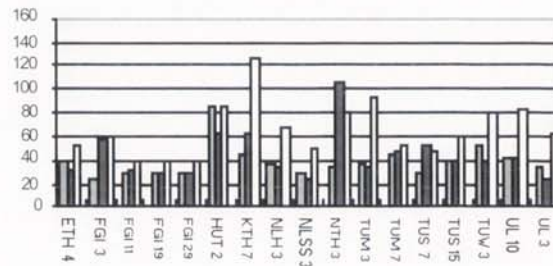
15_D_N



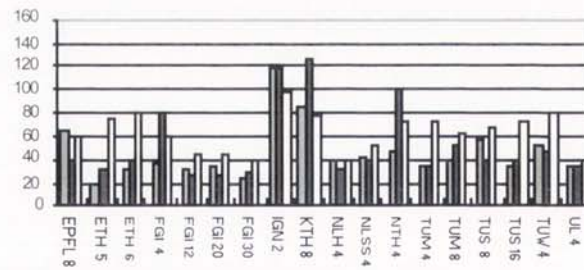
15_D_P



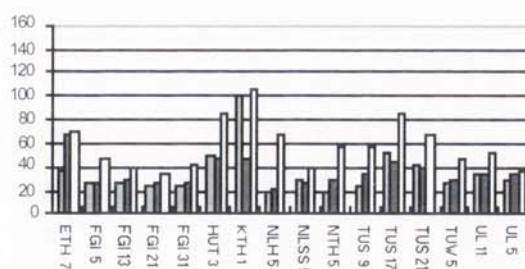
15_S_N



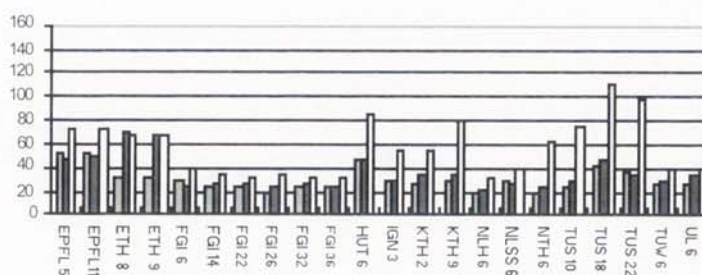
15_S_P



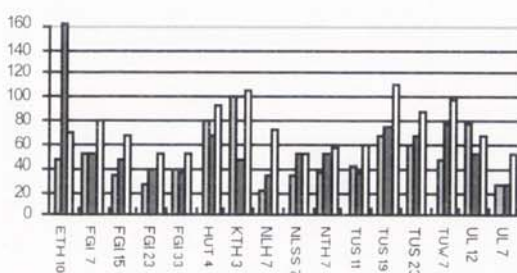
30_D_N



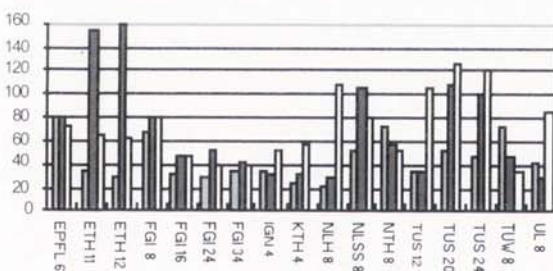
30_D_P



30_S_N



30_S_P



THE UNIVERSITY OF CHICAGO
LIBRARY

100 EAST 57TH STREET
CHICAGO, ILL. 60637

DATE
BY

100 EAST 57TH STREET
CHICAGO, ILL. 60637

DATE
BY

100 EAST 57TH STREET
CHICAGO, ILL. 60637

DATE
BY

Reports of the participants.

1. EPFL / O. Kölbl, M. Crosetto
2. ETH / T. Kersten, D. Stallmann
3. FGI / J. Lammi
4. HUT / J. Heikkinen
5. IGN / E. Beauvillain
6. KTH / H. Wiman
7. NLH / Ø. Andersen, L.E. Blankenberg, I. Maalen-Johansen
8. NLSS / J. Talts
9. NTH / I. Hådem
10. TUM / C. Heipke
11. TUS / V. Tsingas
12. TUW / F. Rottensteiner
13. UL / J.-P. Agnard, P.-A. Gagnon, M. Boulianne

Digital Aerotriangulation with Commercial Software Products

O. Kölbl, M. Crosetto

Institut de photogrammétrie

École Polytechnique Fédérale de Lausanne – Switzerland

1 Introduction

Digital aerotriangulation has in the last years aroused an extraordinary interest in various research institutes and most of the participants in the OEEPE test used their own developments. In parallel, industry has for some time been offering instruments and software packages for digital aerotriangulation which have found a considerable range of applications in practice. One of the first instruments to come on the market was definitely the DCCS (Digital Correlator Comparator System), presented for the first time in 1987 in Baltimore at the congress of the American Society of Photogrammetry (cf. [1]). At that time, it was hardly possible to store several aerial photographs; consequently, the DCCS does not store whole aerial photographs but small image segments centered around the measuring points. However, the software enables an automatic point transfer to the neighboring pictures with the help of correlation procedures. This instrument brought a considerable increase in efficiency for practical work. It met with a certain degree of success in Europe; however, only few institutions have a sufficient quantity of models for triangulation to justify the acquisition of such a special instrument. Later on, the DCCS software was integrated into the DSW100 scanner.

It was only later that digital photogrammetric workstations with integrated software for aerotriangulation came onto the market: the Helava DPW around 1991 and at about the same time the Intergraph ImageStation.

The Institute of Photogrammetry of the EPF-Lausanne, which was recently able to acquire instruments for digital photogrammetry, took the opportunity of the OEEPE test to use various software packages available to the public. This was in the hope of exchanging experience with other users of such software packages. Unfortunately, the presentation of the test results showed that the Institute of Photogrammetry was the only participant to have used the software packages by Helava and Intergraph. All others concentrated on their own developments. Consequently, the working conditions were in fact very different. As the Institute of Photogrammetry has only limited experience with the different software packages, it found it difficult to exhaust the potential of these products. On the other hand, this very lack of practical experience means that one judges the comparative efficiency of the user interface much more critically.

In spite of these limitations, we would like to try to demonstrate, by means of this test, the actual efficiency of the commercial software products.

The Institute of photogrammetry participated in the test with the following instruments:

- DCCS software integrated in the Helava scanner DSW100
- Photogrammetric workstation DPW by Helava
- ImageStation by Intergraph

Additionally, the block was measured on the analytical plotter BC1 for comparison.

2 DCCS, the digital correlator comparator system by Helava

2.1 Short presentation of the instrument

As already mentioned, the DCCS represents one of the oldest systems for digital triangulation. The original version was presented in 1987. Helava subsequently offered the DCCS software in the DSW100 scanner. That means that one now has a scanner which can also be used directly for aerial triangulation.

The DSW100 digital scanner consists of a scanning unit (fig. 1 : 1), a control monitor (2), a monitor for the display of images (3) and a digitizing tablet (4). The system is driven by a 486 PC in Unix.



Figure 1

General view of the Helava-Leica scanner DSW100 with the scanning unit (1), the control monitor (2), the monitor for the display of images (3) and the digitizing tablet (4).

The proper scanning unit consists of an image carriage for the format 23 x 23 cm (cf. fig. 2). For the illumination a halogen lamp is used, the light of which is transmitted by fiber optic into the illumination system. The illumination system has been changed several times. At one time, great efforts were made to get diffused light by using an Ulbricht sphere. Later on, the use of color filters required modifications and a filter wheel was mounted directly above the aerial photographs. As these filters absorb considerable light, the Ulbricht sphere had to be eliminated.

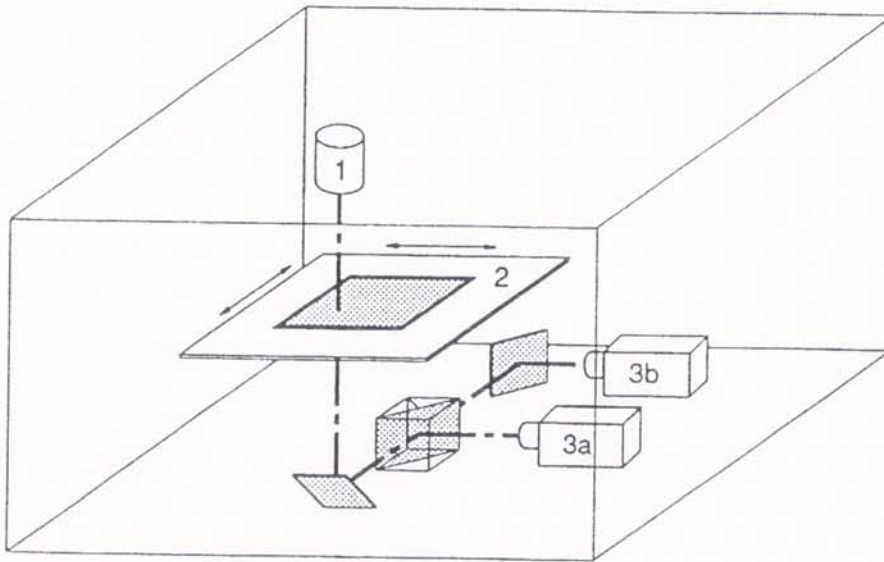


Figure 2

Schematic view of the scanning unit of the DSW100 Helava-Leica with the illumination unit (1), the plate carrier (2) and the 2 digital cameras (3a,b).

When doing an aerotriangulation, one is limited to black-and-white reproductions of the aerial photographs. For the image scanning itself, one uses 2 digital cameras with matrix sensors of 480 x 480 pixels of the type Pulnix. The 2 cameras have different lenses ($f = 135$ and $f = 105$ mm) which allow a scanning with pixel sizes of 12.5×12.5 or 25×25 μm .

2.2 Principle of image triangulation on the DCCS

Aerial triangulation on the DCCS is characterized by storage of image segments and automatic transfer of points. The aerial photograph to be treated is introduced into the

scanner. This instrument is directed by the digitizing tablet on which one normally places a paper copy of the aerial photograph in order to guide the operator.

With the help of this digitizing tablet, the operator selects regions which will be measured subsequently. The corresponding image segments are digitized and displayed on the monitor. A floating mark also displayed on the monitor makes it possible to exactly pinpoint the measuring point. For the first image this work is limited to the selection of points. It is only for the next image that the points are transferred and that the relative orientation is calculated.

An interest operator can be used for the selection of the measuring points. The process of image correlation itself is not described in detail in the literature, but it is based on the 'relaxation' method developed by Helava (cf. [1]). One stores only one image segment for one measuring point; this segment will be conserved and will always be available for the measurements in connection with the subsequent images. Consequently, points can be transferred without any limitations to neighboring strips or even to cross strips.

2.3 Detailed working procedure on the DCCS

The image triangulation runs essentially according to the following procedure :

- 1) Introduction of the aerial photograph onto the image carrier of the scanner
- 2) Measurement of the fiducial marks for inner orientation; the film carriage is automatically driven to the fiducial marks, but the measurements have to be done visually.
- 3a) First image of a strip only: selection and measurement of the tie points and control points and storage of the corresponding image sections. When selecting the tie points, it is possible to use an interest operator in order to determine the exact position of the points.
- 3b) Following images :
 - automatic positioning of the points in the overlapping zone to the previous pictures
 - monitoring of the segments of homologous images (segment of the image currently in work and previously stored segment; cf. fig. 3)
 - automatic image correlation and determination of the position of the tie points with possibility of control by the operator.
 - computation of the relative orientation to the preceeding image and display of the residual parallaxes after the measurement of 5 points.
 - selection and storage of new image segments presenting the tie points to the next images and eventual additional control points. This work is done with one image only, as under point 3a.

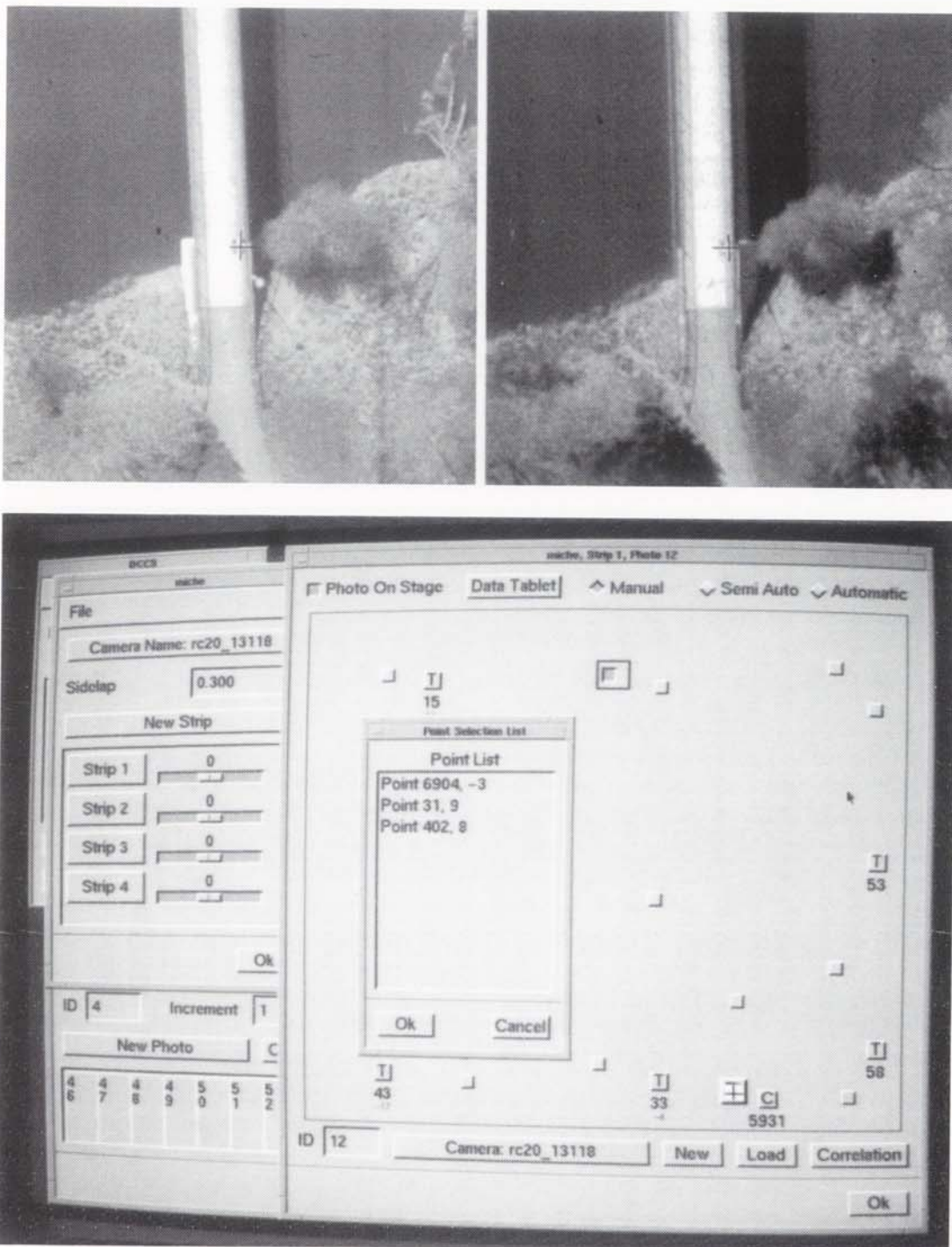


Figure 3 – Presentation of the working environment for aerial triangulation on the scanner DSW100 with the software package DCCS. Above, the display monitor with 2 corresponding image sections serving for measurements and below the control monitor with the information on residual parallaxes (right window) and a sketch of the block configuration (left window).

2.4 *Experiences with the DCCS*

The Institute has the DCCS software package integrated into a DSW100 scanner, instead of the original instrument; the advantage is that it is not necessary to acquire a special instrument only for aerial triangulation. Handling of the instrument is relatively simple and enables the user to obtain a satisfying production after a short introduction (cf. also [2]).

For the practical work, the original color photographs were used. The block shows a very regular structure with a strong side lap. Consequently, it was possible to present the working environment for aerial triangulation on the scanner DSW100 with the software package DCCS. Above, the display monitor with 2 corresponding image sections serving for measurements and below the control monitor with the information on residual parallaxes (right window) and a sketch of the block configuration (left window).

It is possible to choose the tie points directly on the instrument. However, it appeared appropriate to choose 4 tie points at the position of the schema points (Gruber points) in order to ensure that a sufficient number of points would finally be available. By definition, the selection of the points is limited to one image only; therefore, the operator cannot judge whether a point chosen to be measured is effectively on the ground or may be visible on the neighboring image, as it might only be a scratch or any other defect of the emulsion.

This difficulty is amplified by the rather mediocre image reproduction on the monitor; the segment shown corresponds to an image size of 5 x 5 mm on the original film.

Nevertheless, the DSW100 also has considerable advantages; it proved that one can work fairly efficiently in regions which are not too difficult. The Rijkswaterstaat in Delft has published figures according to which about 40 models can be handled per day (8 hours) (cf. [2]). This is also due to the fact that the transfer of points to neighboring strips can be done very efficiently. However, there is a lack of quality control for this point transfer as it is not controlled numerically. Within a model, the relative orientation is computed from the 5th measuring point onwards and the residual parallaxes are displayed. This function is very satisfying as long as the points are sufficiently wide apart. When they are too close, they are summarized within a group of points and the residual parallaxes can only be visualized by opening a special menu field. One might also regret that no absolute orientation can be done, as this would considerably simplify the location of points given by their coordinates.

It can also be considered as an advantage that the aerial photographs not be digitized as a whole; however, it is not easy to know whether the results of the aerial triangulation can be transferred without any special precautions onto digital or analytical stereo plotters for a further use. If one continues to work with digitized photographs, uncertainties might result concerning the inner orientation. Similar questions arise when transferring the orientation elements directly onto an analytical plotter. It would certainly not be wise to completely leave out the use of control points for the individual models. This, however, requires either that points be marked onto the aerial photographs or the elaboration of sketches. These precautions are not required if all operations are done with digital images, which means that the aerial triangulation is also performed with photographs which have been first digitized.

Another disadvantage is the relatively slow motion of the image carriage. Displacing the image by 20 cm requires about 10 sec. Queries in the image menu during the measuring procedure also require considerable response times. The remeasurement of points in a previously measured image is also rather cumbersome, as the photograph has to be re-introduced in the instrument and the whole measuring procedure has to be rerun from the beginning.

3 Aerial triangulation on the DPW (Digital Photogrammetric Workstation) by Helava-Leica

3.1 Short description of the instrument

The photogrammetric workstation DPW by Helava-Leica is based on a general-purpose computer. Partially, this has been a PC with an Intel 480 processor. However, most of the workstations use Sun Spark computers. The software 'Socet Set', which represents a universal program system, includes all photogrammetric operations such as image orientation, stereoplotting, automatic derivation of digital terrain models, computation of orthophotos and mosaiking. The basic computer is sufficient for all these operations, without any additional processor. Only the possibility of stereo observation requires additional means. In the most simple case, adding a stereo viewer can be sufficient; the homologous images are then displayed side by side. The complete stereo station uses a Tektronix screen for stereo observation based on the polarization principle. This screen needs a special processor card. Earlier models used the Vitec board; today, the Dupont-Pixel-Card is mostly used. If desired, it is also possible to use the flicker principle with an interlaced monitor. It should be mentioned in this context that aerial triangulation does not strictly require stereo observation.

The Institute of photogrammetry has a Sun Spark 10/41 computer on which the Socet Set software was loaded. This computer has only a very limited local disk capacity and is exploited within a network. For image storage, it was necessary to use an external disk server controlled by a Cray computer (Nestor); this processor is operated by the Computer Center of the University. The efficiency of data access was not optimal, due to the special configuration of the network. The photogrammetric workstation was used with a split screen and a stereo viewer. A trackball was used for the displacement of the measuring mark. Furthermore, the 3-button mouse of the computer was available. Another version of the digital workstation includes handwheels.

3.2 Principle of aerial triangulation on the DPW

Whereas the DCCS software was specially designed to optimize aerial triangulation, the DPW performs aerial triangulation according to the principle of relative orientation of 2 successive images. The operator is however supported by a correlation algorithm for the elimination of parallaxes. This algorithm has proved to be fairly reliable and works quite quickly.

The measuring points can be marked in the digital images, which facilitates the transfer of points and their documentation. However, only 2 images are available for the measuring procedure. It is also possible to perform control computation during the measurements; this however requires interruption of the measuring process and initiation of the computation.

3.3 Working procedure for aerial triangulation on the DPW

Essentially, the operations for a block triangulation are the following:

1. Loading of the digital images on the workstation, possible conversion of the images into the internal format of the Helava software and generation of the image pyramid.
2. Measuring of inner orientation (semi-automatically, that means that the fiducial marks are automatically introduced on the screen, whereas the pointing has to be done by the operator).
3. Selection of the tie points and positioning of the control points; the parallaxes can be automatically eliminated allowing either the left or the right measuring mark to be displaced (cf. Fig. 4).

The selection of the tie points can be supported by the use of an interest operator.

Points already measured in a previous model can be located with the help of their point number.

4. Closing of the measuring mode, computation and monitoring of the residual parallaxes.

3.4 Experience with the DPW

When used to working with classical photogrammetrical instruments, one is surprised that aerial triangulation can be performed on a mere general-purpose computer. The speed of the operations depends essentially on the efficiency of the computer system. It is specially important that the display of images and image sections be done very rapidly. The computer configuration of the Institute of photogrammetry, with an external disk server, showed considerable shortcomings in this context. This problem is increased by the fact that the images used for measurement are not compressed.

The correlation algorithm proved to be very reliable and a visual correction was necessary in only about 10% of cases. These errors can be easily corrected as the corresponding images are monitored and can be presented 1:1, 1 pixel corresponding to 1 picture element on the screen. However, a sub-pixel enlargement did not prove to be very useful. In this context, it should be noted that the image measurements were quite efficient when using only the 'monocular' mode. The only advantage of stereoscopic observation is that the operator has an improved perception of the model space, which requires that the left and right images be properly separated.

The Helava system uses Motiv as user surface. The windows for the display of data and the presentation of images were designed on that basis (cf. photo of the screen). In this way, however, one obtains a rather unsatisfying user interface; numerous windows contain comparatively little information; stronger compacting would make it possible to have much more information available. For example, the operator does not have access to the residual parallaxes during image measurements. That is rather cumbersome if re-measurements are necessary. The absolute orientation, which would facilitate the search of control points or check points according to predetermined values, is rather complex and in certain cases the absolute orientation did not converge, meaning that no orientation was computed. In general, one gets the impression that the user interface could be considerably improved and it also seems to be a disadvantage that only one enlargement be available for point measuring and that the change to another enlargement require several manipulations. It would be helpful to have the possibility of simultaneous display of several image sections with different enlargements and even the possibility of displaying a third image to facilitate the points transfer to neighboring strips. Nevertheless, one has to admit that digital image triangulation on this workstation is surprisingly efficient compared to the same work on analytical plotters. However, the possibilities of the system are still limited.

4 Aerial triangulation on the ImageStation by Intergraph

4.1 Short description of the instrument

The photogrammetric workstation by Intergraph represents a special development based on the processor Clipper 6487 or the new version with the processor 6887 developed by Intergraph. The 6487 has a processing capacity of about 30 Mips. Additionally, one has the parallel processor Vitec 50 for image operations and a hardware board for the compression and decompression of images. The mass storage of the workstation used at the Institute has a disk capacity of 5 Giga-bytes. The workstation is equipped with a high-quality image screen of 1200 x 1800 pixels and allows the monitoring of 24-bit color images. For stereo viewing, one uses 'Crystal Liquid Eye Shutter' glasses; the corresponding stereo images are monitored in an interlaced mode.

The system operates under UNIX with a special Clipper processing system. The software package of photogrammetry available at the Institute of photogrammetry represents a pre-release with automatic image correlation.

4.2 Principle of aerotriangulation on the ImageStation

Methodologically, aerial triangulation on the ImageStation is very similar to the operations on the DPW by Helava-Leica. On the ImageStation, one can also only handle a model formed of 2 images simultaneously. However, the operator has a much stronger support and the operations occur much more rapidly. The operator has access simultaneously to 3 different enlargements of the 2 homologous images (cf. Fig. 5). In this way, the operator can have a view of the whole aerial photograph, enlarged image sections

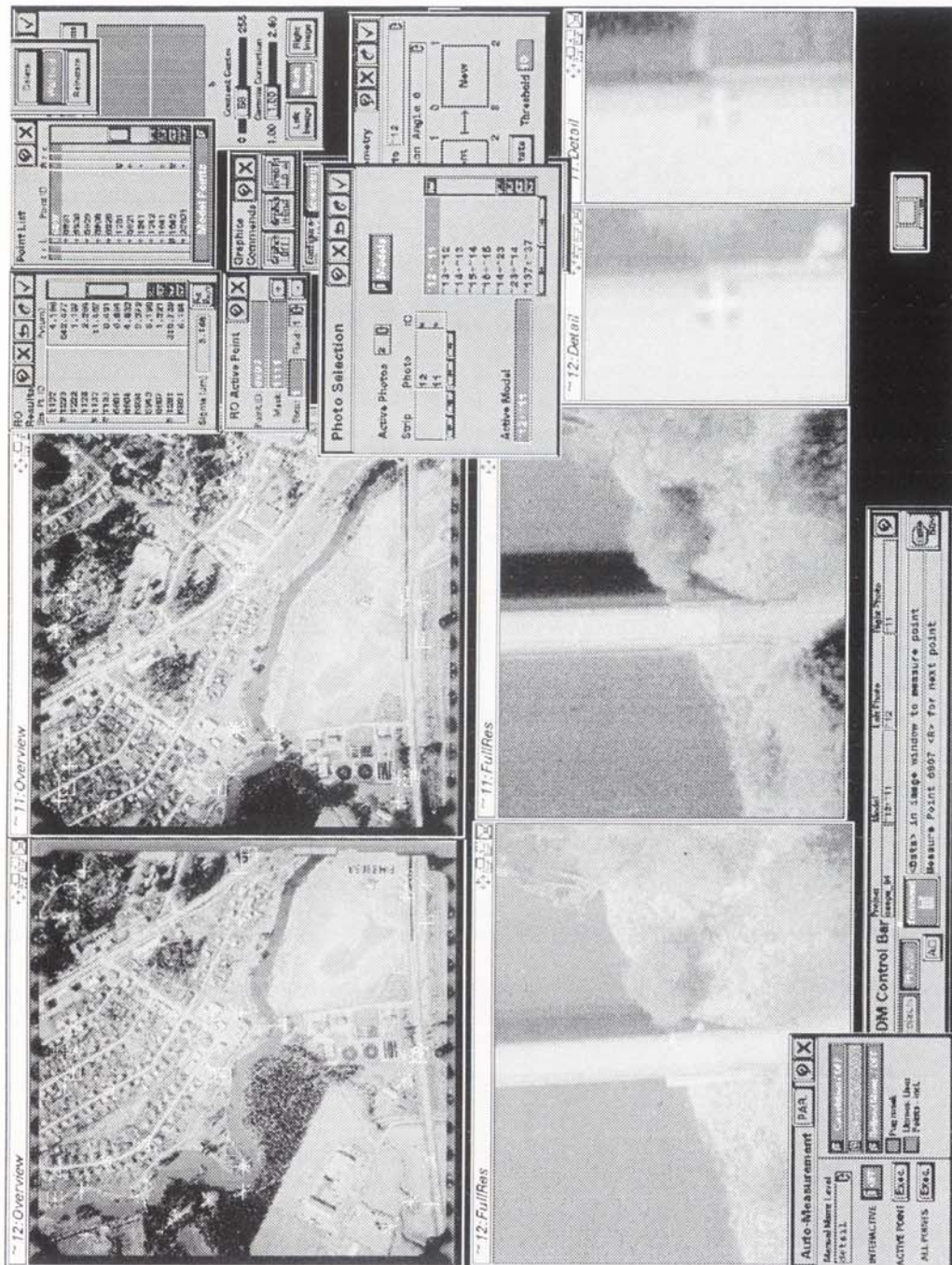


Figure 5 – Screen copy showing the working environment on the Intergraph ImageStation for relative orientation for aerial triangulation. The upper part shows an overview of the 2 corresponding aerial photographs. In the lower part are reproduced detail views and the 2 windows and an overview of the residual parallaxes. The windows are activated successively. The working environment can be defined freely by the user and can also include stereo windows (flicker principle).

for which one pixel of the image corresponds to one pixel on the screen or sub-pixel enlargements. A special algorithm computes a convolution for image smoothing in order to avoid the appearance of a chessboard in the sub-pixel enlargement. The image does not appear to be very sharp, but the points can be measured with a fairly high degree of precision. The simultaneous presentation of the pictures in various sections enables very efficient work. For this, it is obviously necessary that the hardware be able to display an image section within less than a second.

As already mentioned, the ImageStation also allows the monitoring of stereo images according to the flicker principle. This technique is rather satisfying when observing a whole stereo model. For aerial triangulation, one can observe in stereo 1 or 2 window sections of a stereo model. However, the operator intuitively got the impression that the stereo measurement is not very reliable. This might be due to the rather small image section or to the fact that images are not resampled according to epipolar lines. It might also be that the glasses do not completely separate the images. As a result, the stereo mode was not used for the test measurements.

The elimination of parallaxes on the image station is also supported by an automatic correlation algorithm. Already after the measurements of 2 or 3 points for relative orientation, one can initiate the automatic transfer of points measured in a previous model. In this way, one obtains the orientation of the whole model. A program for elimination of blunders controls the quality of the parallax measurements and eliminates mismatching; in 50% to maybe 90% of cases, a rather good relative orientation is already obtained in less than 1-2 min. Further transfer points can be added, an operation which can be supported by automatic image matching and by using an interest operator for point selection. If the model was not properly orientated by the automatic matching algorithm, it is necessary either to pinpoint the blunders and measure these points visually or to reject the whole automatic measurements and transfer all points visually. After relative orientation it is possible to add an absolute orientation; this absolute orientation is performed automatically when a sufficient number of control points were already measured in the previous image and have been transferred during the relative orientation.

The ImageStation has a special processor for data compression. Image data are only decompressed for displaying. The data compressions enable data reduction by a factor of about 4-5 which means that a rather large block digitized with a small pixel size (e.g. 15 μm) does not require an excessive disk space. All 28 pictures of the block 'Forssa' with a pixel size of 15 μm have been stored on a disk of 2 Giga-bytes.

4.3 Detailed working procedure on the ImageStation

These characteristics results in the following basic working procedure, which is very similar to that on the DPW :

1. Loading of the digital images on the workstation, possible conversion of the images into the internal format and generation of the image pyramid.
2. Measuring of the inner orientation; this procedure runs completely automatically

from the 2nd image on and requires about 1 min per picture.

3. Selection of 2 to 3 tie points and visual elimination of the parallaxes; subsequently, full automatic relative orientation which permits a completely automated transfer of image points already localized in one of the two images. Afterwards, additional tie points and control points can be measured. Parallaxes are automatically eliminated, which means that the left or the right floating mark is displaced according to previous specifications. The proper selection of the tie points can be left to the computer by using an interest operator within a narrow field around the floating mark. Residual parallaxes are computed after each measurement and then displayed.
4. Absolute orientation of the model. This has an advantage if a great number of points have to be measured with predefined coordinates. If enough control points have already been measured in the previous model, then the absolute orientation is performed automatically on the basis of the measurements made during relative orientation. Residual errors after absolute orientation are recomputed after each measurement and monitored, provided that 3 points are already measured. Points predefined by their coordinates are also automatically located in the images in order to facilitate point measurements.

4.4 Experiences with the ImageStation

After a relatively short introduction, one obtains the impression that digital aerotriangulation on the ImageStation is very efficient. One of our students remarked that this type of work is like a video game. Effectively, the opening of various windows of image sections systematically after the previous measuring defines very clearly the measuring process and drives the operator without giving too much constraints. The arrangement of the menus on the screen can be organized very freely and allows a thorough control of the measuring operations. Furthermore, several operations are performed largely automatically. The production rate in practice rises to about 60 models a day. Data compression also appears as a great advantage.

However, image correlation for points transfer did not prove to be very reliable and led to several miscorrelations. This might be due to the fact that the Institute of Photogrammetry only has a prototype of the software. It is most probable that by a better choice of parameters one could avoid many of these problems, but there are no appropriate instructions for the tuning of the parameters.

As on the DPW, the problem of transfer of points to neighboring strips has not been solved yet. The addition of a third image or the storage of image segments as with the DCCS software could be of great assistance. Stereo observation was not really satisfying either. Finally, the blunder detection can be rather cumbersome, especially when a great number of points were measured in a model. It is also inconvenient that points to be remeasured cannot be called from the menu in which residual parallaxes are monitored. Nevertheless, aerial triangulation on the ImageStation proved to be very efficient.

5 Analysis of the results of the block 'Forssa'

As already described, 4 different instruments were used for aerotriangulation. On the analytical plotter BC1 and on the DCCS one worked with the original color photographs, whereas digitized image data were used on the DPW (30 μm pixel size) and the ImageStation (15 μm pixel size). On the ImageStation, data compression made it possible to store the whole block of 28 pictures on a disk of 2 Gigabytes.

5.1 Image measurements

As far as they were visible, all control points and check points were measured during aerial triangulation. Additionally, 3 points (4 on the DCCS) were measured as tie points in the schema points of relative orientation, that means a total of 18 resp. 24 tie points per model. This high number of points appeared necessary to ensure reliable connections between images; in this context it should be taken into consideration that the points were chosen ad hoc without control of visibility on the neighboring images.

On the DPW and the DCCS, measurements were mainly done with the help of automatic image correlation for the transfer of the tie points whereas on the ImageStation Intergraph the correlation algorithm was only used for the first 2 strips. Several matching errors occurred which needed to be corrected, so that the time required when using the matching algorithm was finally longer than when using a purely visual method.

Table 1 gives an overview of the time required for the image measurements on the instruments; according to this compilation, somewhat more than an hour was necessary for a model on the analytical plotter BC1, whereas on the ImageStation only 20 min. were required as an average. These time estimations are relatively long compared to earlier mentioned values and show the lack of practice. Nevertheless, the relation given should correspond rather well to the fact that one can work about 3 times faster on the ImageStation than on an analytical plotter.

The software package PATB had been used for block adjustment for all the different measurements. All software packages for the triangulation measurements allowed the transfer of the measuring data into this adjustment program without any difficulties.

The results of the block adjustment are summarized in Table 2. Highest precision has been achieved with the analytical plotter BC1 whereas results on the ImageStation and the DCCS are somewhat lower but very close. The precision on the digital workstation DPW is considerably lower as a pixel size of only 30 μm has been used on this station, whereas on the ImageStation a pixel size of 15 μm was used.

Table 1 – Overview on the different instruments used for the aerotriangulation with a comparison of the characteristics.

Name	DSW100 (DCCS)	DPW	ImageStation	BC1
Manufacturer	Helava	Helava	Intergraph	Leica
Characteristics	Scanner	Digital Workstation	Digital Workstation	Analytical Plotter
Type of images	Analogical photographs	Digital images	Digital images	Analogical photographs
Treatment of image	∞ im. sect. 512x512 pixels	2 pictures	2 pictures	2 pictures
Data compression	Not necessary	Optional	Yes	–
Presentation	1 enlargement	1 enlargement	3 or more enlargements	1 enlargement
Automation	Correlation 1 point	Correlation 1 point	Correlation ∞ point	–
On-line control	Rel. o. within strip	Relative orientation	Rel. + abs. orientation	–
Used pixel size	12.5 μm	30 μm	15 μm	–
Working time	40'	40'	20'	80'

Table 2 – (legend on next page)

Instrument	Pixel size [μm]	Type control	Auto- calibration	Redund.	σ_0 [μm]	μ_x [cm]	μ_y [cm]	μ_z [cm]	Check planim.	Check altim.
BC1	–	4 – 8	4 P	961	3.10	4.7	3.0	3.9	90	75
BC1	–	14 – S	4 P	987	3.25	2.7	2.2	3.8	80	69
BC1	–	14 – S	4 P	709	3.73	2.9	2.9	4.2	80	68
BC1	–	22	4 P	1011	3.18	2.7	2.4	3.7	76	60
DCCS	12.5	4 – 8	3 P	880	5.38	6.2	5.7	12.9	79	66
DCCS	12.5	14 + S	3 P	906	5.45	2.7	3.5	10.0	69	60
DCCS	12.5	14 – S	3 P	661	5.59	2.7	3.4	8.7	69	59
DCCS	12.5	22	3 P	930	5.62	2.9	3.7	8.4	65	51
ImageStation	15	4 – 8	3 P	767	5.43	4.2	6.3	6.7	83	66
ImageStation	15	14 + S	2 P	794	5.45	3.0	2.9	5.5	73	60
ImageStation	15	14 – S	2 P	559	5.63	3.0	2.8	5.9	73	60
ImageStation	15	22	2 P	818	5.48	3.2	2.8	4.7	69	52
DPW	30	4 – 8	5 P	963	11.19	7.6	9.4	7.6	81	68
DPW	30	14	7 P	987	11.15	4.8	6.2	7.5	71	62
DPW	30	14	7 P	746	11.74	5.2	6.4	8.0	71	62
DPW	30	22	4 P	1014	11.19	4.6	5.3	7.1	67	55

Legend for Table 2 :

Comparison of the results of the aerial triangulation on the different instruments.

BC1 = analytical plotter Aviolyt BC1.

DCCS = aerotriangulation software integrated in the scanner DSW100 of Helava.

ImageStation = digital photogrammetric workstation of Intergraph.

DPW = digital photogrammetric workstation of Helava.

The column 'Type control' indicates the number of control points used :

4-8 = 4 planimetric control points and 8 height points.

14 = 14 control points in planimetry and height (cf. also fig. 6).

+S = signalized check points have been used as tie points in the block adjustment

-S = the signalized check points were not used as tie points in block adjustment; the coordinates of the check points have been computed by intersection after adjustment.

22 = number of control points used; this special configuration has been chosen to compensate better for eventual systematic errors in terrestrial control points.

In the column 'Autocalibration' are given the number of parameters used with the program PATB; maximum allowed parameters were 12.

'Redund.' = number of redundancies in block adjustment.

's0' is the standard error of unit weight in block adjustment.

'mx, my, mz' give the mean square error on the residuals of the check points.

The number of check points in the planimetry and height is given in the last 2 columns.

5.2 Considerations on systematic errors

If one analyzes the results in more detail, one has the impression that the block shows considerable deformations. If one compares the residual errors on the check points when using different configurations of control points, one obtains a surprising pattern. Fig. 6a shows the residual errors on the check points when using the passpunkt configuration 4/8, which means 4 points in planimetry and 8 in height, whereas Fig. 6b shows the corresponding errors when using 14 control points. If one computes the difference between the residual errors as presented in Fig. 6c one obtains the impression that there is an interruption between strips 3 and 4. It was not possible to do a more detailed analysis of these systematic deformations with the available software package; moreover, to a great extent these deformations had been assimilated by the additional parameters.

5.3 *Utility of signalized transfer points*

The block 'Forssa' was equipped with a considerable number of control points which were signalized in the terrain. With a few exceptions the whole block could have been adjusted without additional tie-points relying only on the signalized control points and check points as tie-points. In principle, this is very favorable for the precision as it is generally stated that aerotriangulation on analytical plotters supplies higher precision with signalized transfer points. For digital photogrammetry, the point transfer is in general achieved by correlation procedures and one assumes that, with this technique, one obtains the same high precision as when using signalized transfer points for analytical photogrammetry.

The measurements on the block 'Forssa' done by the Institute of Photogrammetry tends to argue for a control of this hypothesis, as sufficient natural transfer points have been measured beside the signalized control and check points. Practically, the procedure was as follows : in a first run all signalized check points were eliminated from block adjustment except of course the 14 control points. The orientation elements determined in this way for the aerial photographs were then used to compute the point coordinates of all the signalized points without any further modification of the orientation elements. Table 2 gives an overview of the results obtained. For this comparison, adjustments with 14 control points are indicated with +S, which means that the signalized control points have been included in the adjustment, whereas -S means that the signalized transfer points have been eliminated from the adjustment. One remarks that on the analytical plotter BC1 a precision reduction of about 10% can be observed when eliminating the signalized check points. This difference is not very great and might be due to the type of terrain showing urban area and residential area which supplies numerous natural transfer points of rather high quality. The difference in precision for all other instruments is even smaller than on the analytical plotter. Consequently, it seems difficult to answer definitely the question on the utility of signalized control points in digital photogrammetry when requiring highest precision.

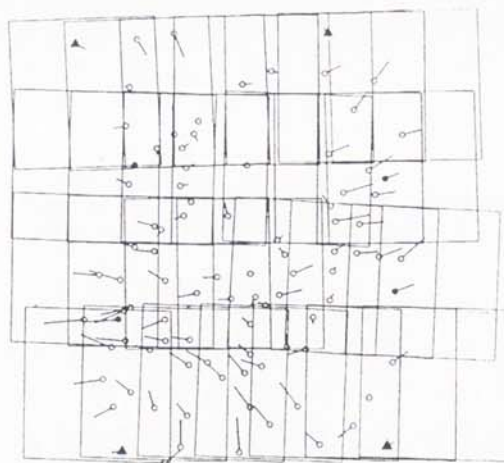
6 **Conclusions**

The presentation confirms the efficiency of digital photogrammetry for aerotriangulation. Although the test measurements in the Institute of Photogrammetry do not permit one to achieve the same efficiency as in other institutions which use this technique on a routine basis, it confirms its high potential. Digital photogrammetry opens in this respect new perspectives for point densification.

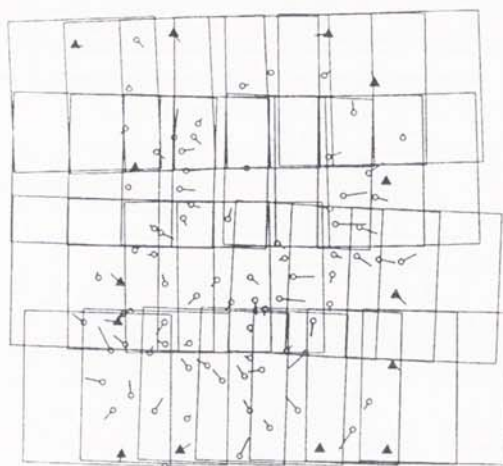
It is remarkable that this work has been performed with commercial products after a relatively short introduction period. Doubtless the development in this field of digital aerotriangulation have not yet been fully accomplished and various developments of University Institutes might serve to stimulate instrument industry. For routine applications, fairly efficient products are already available today.

The initiative for this OEEPE test occurred at a time when digital photogrammetry was not yet generally accepted. Doubtless this work has contributed to promoting a larger use of this technique, on the basis of its higher efficiency.

6a Residual errors in the check points when using 4 planimetric control points (triangles) and 4 additional height control points.



6b Residual errors using 14 control points



6c Differences of coordinates between 6a and 6b. The residuals show a surprisingly systematic pattern.

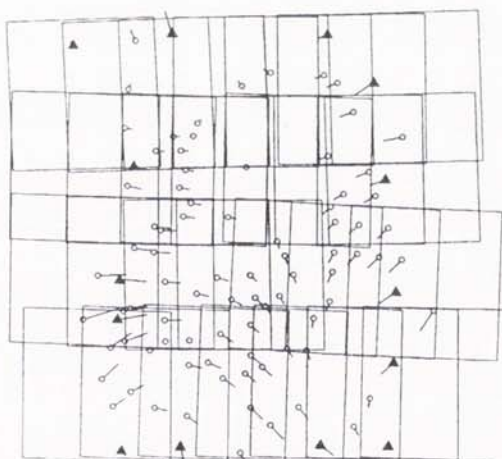


Figure 6 – Overview of the Helsinki block and the residual errors on the check points.

References

- [1] *Helava, U.V.* (1987) 'Digital Correlator Comparator System'. Proceedings of 'Fast Processing of Photogrammetric Data', June 2-4, Interlaken/Switzerland, pp 404-418.
- [2] *Han, C. S.* (1992) 'Digital Photogrammetry at the Survey Department'. International Archives of Photogrammetry Vol. 29 Part B2, pp. 297-301.
- [3] *Kaiser, D.* (1991) 'ImageStation : Intergraph's Digital Photogrammetric Workstation'. Digital Photogrammetric Systems - Wichmann, pp. 188-197.
- [4] *Madani, M.* (1992) 'The Intergraph ImageStation Photogrammetric System'. ITC Journal 1992-1, pp. 87-92.
- [5] *Miller, S.B., Walker A.S.* (1993) 'Further Developments of Leica Digital Photogrammetric Systems by Helava'. ACSM/ ASPRS Convention, New Orleans, February 15-18, Vol. 3, pp. 256-263.
- [6] *Jaakkola, J.* 'OEEPE Research project - Aerotriangulation Using Digitized Images - Preliminary Results', ISPRS Comm. III Symposium, München 1994, pp. 416-421

Semi-automatic aerotriangulation with digital OEEPE image data at the Digital Photogrammetric Station DIPS II of ETH Zurich

Thomas Kersten, Dirk Stallmann

Institute of Geodesy and Photogrammetry, Swiss Federal Institute of Technology
ETH-Hoenggerberg, CH-8093 Zurich, Switzerland

Abstract

With the development of higher-resolution scanners, faster image-handling capabilities, and higher-resolution screens, digital photogrammetric workstations promise to rival conventional analytical plotters in functionality, i.e. degree of automation in data capture and processing, and in accuracy. The availability of high quality digital image data offers the capability to perform accurate semi-automatic or automatic triangulation of digital aerial photo blocks on digital photogrammetric workstations instead of analytical plotters.

In this paper, we present investigations using hard- and software, and results of the Institute of Geodesy and Photogrammetry, ETH Zurich on the OEEPE test project "Aerotriangulation using digitized images". For this international experiment the delivered two data sets of digital images were processed with components of the Digital Photogrammetric Station DIPS II using own software packages. The measurement of the fiducial marks, signalised and natural tie points was performed by least squares template and image matching. The self-calibrating bundle adjustment yielded an estimated standard deviation of the image coordinates of about 1/4th of the pixel size for both data sets. An empirical accuracy of $\mu_{xy} = 26 \text{ mm}$ and $\mu_z = 38 \text{ mm}$ was obtained in object space from the check points with the $15 \mu\text{m}$ digital data set.

1 Hardware and software components

For the investigations with the test data, basic hardware components of the Digital Photogrammetric Station DIPS II (Grün/Beyer, 1990) of the Institute of Geodesy and Photogrammetry were used. DIPS II consists of 2 file servers and 16 Sun workstations linked to each other via Ethernet with some external components for digital image acquisition and output. DIPS II serves as a platform for all research and development projects of the Institute. At the current stage, a total of 15 GByte for is available data storage. For the OEEPE test 2 GByte could be effectively used.

The relevant used programs, which are developed in the Institute, are summarized in the following:

- A viewing tool for the display of the images, manual measurement of image points, and extraction of Regions Of Interest (ROIs) from images.
- A Least Squares Matching (LSM) tool for measuring fiducial marks, signalised and natural points.
- A program for bundle adjustment with self calibration and analysis of the observation data.
- Different programs for affine transformations, corrections of the image point observations (earth curvature, refraction, and distortion), changing rasterfile and data formats, etc.

2 Preprocessing of digital image data

For point positioning in aerial triangulation only parts of the whole image are interesting for measurements, i.e. fiducial marks for transformations into image coordinates, signalised points with known 3-D coordinates for transformations into object space, and tie points along strip and across strip direction for reliable connection of the images. The input and output of large digital images (i.e. 256 Mbyte) and their display require large disk storage and consume long I/O time. Due to these aspects, the concept in our investigations was to use only ROIs of the images for the measurements. Therefore, patches of the eight fiducial marks, all visible signalised points and selected tie points were extracted automatically in each digital image using approximate pixel coordinates provided by the pilot center or measured manually before extraction. For the extraction the images were temporarily stored on disk. For all ROIs no image enhancement was performed.

The patch size of each extracted ROI was 64×64 pixels ($30\mu\text{m}$) and 128×128 pixels ($15\mu\text{m}$). Only for tie points of the $30\mu\text{m}$ image data, which were manually selected in the six "von Gruber" positions in each image, the patch size was 512×512 pixels. Excluding fiducial marks the average number of image patches per image was 25.

3 Mono image point measurement by template and image matching

The image point measurement for all points (fiducials, signalised and tie points) was performed by matching in the patches. The used algorithm is known as constrained Least Squares image Matching (LSM), which allows point measurements with subpixel accuracy, and is described in Grün/Baltsavias (1988). The matching was performed interactively with the LSM tool using a window-based interface to the algorithm. This allows all algorithm parameters (e.g. patch size etc.) to be set to optimum values for a particular matching problem, plus assessment of the result by visual inspection for quality control: if a point could not be matched satisfactorily with the chosen parameters, then an alternative optimum set was found – usually a smaller or larger patch size or restricted image shaping transformation.

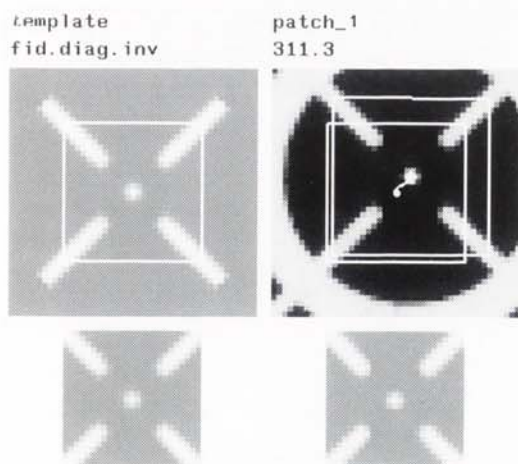


Figure 1 – Template matching of fiducial marks (30 mm image data)

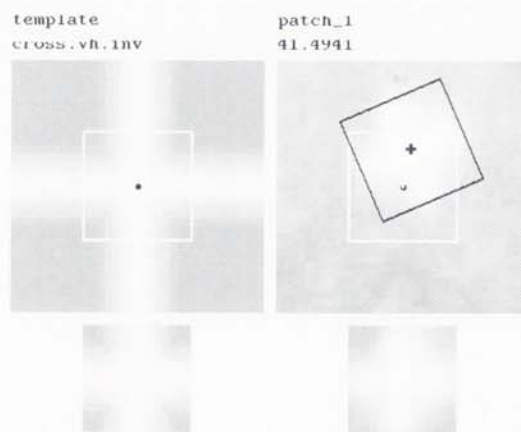


Figure 2 – Template matching of signalized points (15 μ m image data)

For matching fiducial marks and signalised points, artificial templates were created. The fiducial marks were well defined and the matching could be performed without problems. In Figure 1 the large images show the matching between template and patch indicating the initial position as a point and the final solution as a cross, while the lower small images depict visually the matching result.

The signalised points were not so straightforward to match in the 30 mm image patches as their images show a great variety in shape and contrast. On the average, the targets occupied a square of 5–7 pixels (30 μ m) resp. 10–14 pixels (15 μ m).

The quality of the 30 μ m digital image material did not allow template matching with an affine transformation. Thus, to obtain an acceptable result, the signalised points were matched with two translation parameters using a patch size of 7 x 7 pixels. In the high resolution patches all targets could be matched with the same template using a conformal transformation and an average patch size of 15 x 15 pixels. Figure 2 shows the template matching of one target. In total, 257 targets (minimum 3 and maximum 16 points per image) were matched. In the center of the block the same signalised points could be measured in up to six different images, while at the perimeter of the block the points have only two rays.

In the matching procedure of the tie points one natural point was used as the template point to be located in the other ROIs. Well defined points were mostly selected in the patches as natural tie points, in general, points in flat areas, and the matching could be done without problems. For reliability reasons two tie points were matched in each 512 x 512 patch. In total, 460 tie points in the 30 μ m images and 442 in the 15 μ m images were matched for the whole image data set. The image matching of four tie points in two strips is illustrated in Figure 3.

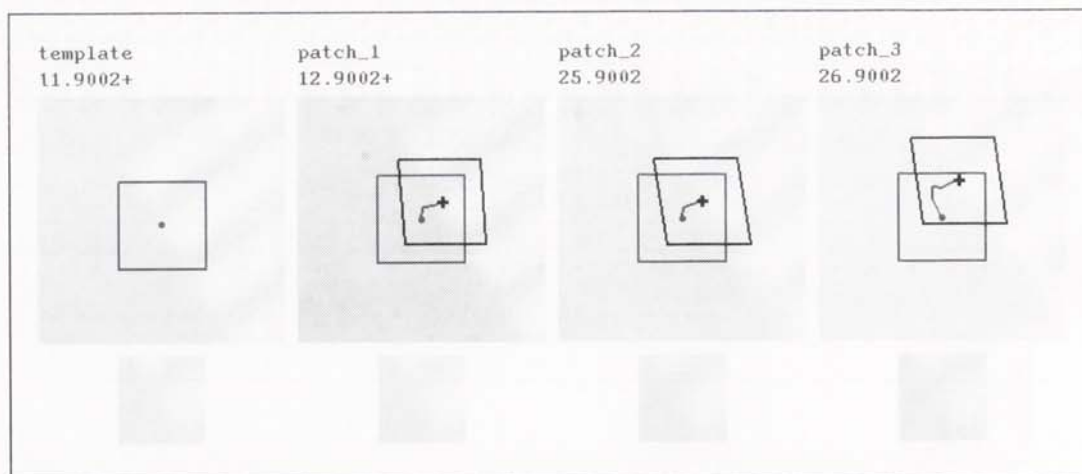


Figure 3 – Image Matching of four tie points (30 μ m image data)

4 Bundle block adjustment

Before the adjustment the pixel coordinates were transformed into image coordinates by an affine transformation and also a priori corrected for radial lens distortion, refraction, and earth curvature. The adjustment of these reduced image coordinates was performed with the software package BUN, which is a collection of more than 40 programs, separated in four parts, namely preprocessing of data, bundle adjustment with self calibration, analysis of results, and plot facilities. The mathematical background of the bundle adjustment in this program is described in Grün (1976). The bundle adjustment program, the main part of BUN, allows the automatic computation of initial values including checks for gross errors and their automatic elimination at that stage. For the compensation of systematic errors in aerial photos the 12 Additional Parameters (AP) of Ebner (1976) or the 44 APs of Grün (1978) can be used optionally in the adjustment. For the digital OEEPE test image data both additional parameter sets were used.

5 Conclusions, further works, criticism

In the investigations for the OEEPE test project a standard deviation of image coordinates of 0.25 pixel was obtained for the low and high resolution digital image data. The aerotriangulation of each digital data set was performed in less than 50 hours. Detailed descriptions of these investigations are given in Kersten/Stallmann (1994). At the current state the used procedure can be optimised as summarised in the following, to increase the degree of automation in aerial triangulation and to improve the efficiency in comparison to aerotriangulation using analytical plotters:

- Optimization of the interface between different software modules
- Use of tiled images and image pyramids
- Automation of interior and relative orientation
- Introduction of on-line triangulation by sequential estimation
- Introduction of blunder detection by data snooping

Finally, some critical aspects on the overall procedure of the OEEPE test are summarised:

- The digital test image data were delivered including some radiometric errors as described in Kersten/Stallmann (1994), which could be attributed to insufficient scanner calibration.
- The targets of the signalised points are not very suitable for measurements by template matching. Signalisation with disks might give better results.
- The control point configuration was not optimal for a reliable and geometrically stable bundle adjustment. Additional height control in the block center would stabilize the block geometry.
- The given a priori standard deviation of the control points was not very accurate compared with the photo scale of this data. This can seriously disturb a clear and conclusive analysis of the empirical results.

6 References

- Ebner, H.*, 1976. Self Calibrating Block Adjustment. Int. Archives of Photogrammetry and Remote Sensing, Vol. 21, Part 3, Invited Paper, Commission III, ISP Congress, Helsinki.
- Grün, A.*, 1976. Die simultane Kompensation systematischer Fehler mit dem Münchner Bündelprogramm MBOP. International Archives of Photogrammetry and Remote Sensing, Vol. 21, Part 3, Presented Paper, Commission III/1, ISP Congress, Helsinki.
- Grün, A.*, 1978. Experiences with Self-Calibrating Bundle Adjustment. Presented Paper, ASP Convention, Washington D.C., Febr./March.
- Grün, A., Baltsavias, E.P.*, 1988. Geometrically Constrained Multiphoto Matching. Photogrammetric Engineering and Remote Sensing, 54(5), pp. 633-641.
- Grün, A., Beyer, H.*, 1990. DIPS II – Turning a Standard Computer Workstation into a Digital Photogrammetric Station. Int. Archives of Photogrammetry and Remote Sensing, Vol. 28, Part. 2, pp. 247-255 and ZPF – Zeitschrift für Photogrammetrie und Fernerkundung, No. 1/91, pp. 2-10.
- Kersten, Th., Stallmann, D.*, 1994. Aerotriangulation with Digital OEEPE Test Image Data – Contribution of the IGP (ETH Zurich) to the OEEPE Test. Internal report for the OEEPE Workshop on Digital Methods in Aerial Triangulation, Helsinki-Espoo, Finland, May 8-10.

THE HISTORY OF THE
CITY OF BOSTON
FROM 1630 TO 1880
BY
JOHN B. HENNINGSEN
OF THE
BOSTON PUBLIC LIBRARY
PUBLISHED BY THE
BOSTON PUBLIC LIBRARY
1880

OEEPE Test on Digital Aerial Triangulation – Results from the Finnish Geodetic Institute

Jussi Lammi

Finnish Geodetic Institute

Department of Cartography and Geoinformatics

Geodeetinrinne 2, FIN-02430 Masala, Finland

1 Introduction

A digital photogrammetric workstation for user-guided image measuring in digital aerial triangulation has been designed and realized at the Finnish Geodetic Institute (FGI). The implementation of the workstation was done during the European Organization for Experimental Photogrammetry (OEEPE) test Aerotriangulation using digitized images. In this report, we shortly describe the technical and functional foundation of the workstation at the FGI. The different image measuring methods are discussed to clarify the differences between the test sets measured. Finally, we summarize the results from our triangulations. A more detailed description of both the workstation and the results can be found in *Lammi (1994)*.

2 Aerial Triangulation with the OEEPE Test Material

2.1 Digital Photogrammetric Workstation

The digital photogrammetric workstation at the FGI has been written under the UNIX operating system using object-oriented programming (C++), X-environment and OSF/MOTIF guidelines. The system is built on a Silicon Graphics Indy workstation (MIPS R4000 risc-processor). Our configuration has 48 MB of RAM and a small internal hard disk (512 MB). Several external hard disks can be connected to the workstation using a SCSI link. The monitor is a 20-inch display (Silicon Graphics GDM-20D11/Sony) with an Indy 1280.1024 24-bit full-color graphics card.

The workstation software is designed for interactive, user-guided measuring. Several windows can be opened on the display simultaneously. Overview images are used for general localizing and fast moving. Sub-images are automatically rotated into the block main direction in 90-degree steps. Here, the block main direction means an orientation that is chosen for all images of the block, for instance, the flight direction of the first strip. The user can ask the system to automatically display sub-images that contain the point wanted. Approximate orientation parameters of images are used in the automatic opening of windows containing the known XYZ point.

2.2 Image Measuring

The measuring is done either visually or semi-automatically. In the visual pointing mode, the sub-pixel accuracy is achieved with the help of zoom images and sub-pixel graphics. In sub-pixel graphics, real number are used in drawing commands instead of integer numbers. The cross-shaped pointing tool can be rotated (and resized) to any orientation, although the slightly tilted cross is the best one in a theoretical sense.

The semi-automatic fiducial mark measuring begins with a visual procedure whereby the position and identity of fiducials are determined from one of the images. Visually measured coordinates show the place from which the model patches are extracted. These patches are used as templates in the search for fiducials in other images. A normalized cross-correlation coefficient is calculated between the target and the search image. The highest correlation coefficient points to the match. Final measuring is done by calculating the fiducial's weighted center of gravity from the correlated point. The measuring process expects all images to be scanned in the same orientation, i.e. the fiducial numbers correspond to the same corners over the whole block.

The semi-automatic measuring of control and tie points is also based on the normalized cross-correlation. First, the homologous point is approximately measured on all the images containing it. Then, the user selects one image patch as a reference and measures the target visually on this image. The other image patches are correlated to the selected reference. In all correlations, the target image is extracted from the original image by resampling techniques. Sub-pixel accuracy in correlation is achieved by moving the target patch over the search image in steps of less than one pixel. After every step the search patch is resampled from the original image. The highest correlation coefficient indicates the match.

2.3 Observation Sets

The image coordinates of the fiducial marks and the given control, tie and check points were measured visually in both resolutions. The pure visual measurements produced two test sets, *visual_15* and *visual_30*. The same points were also measured by semi-automatic tools utilizing the normalized cross-correlation, referred as *ncc_15* and *ncc_30*. In addition, more tie points (140 points) were measured semi-automatically from the test images. These points were added to the correlation test sets already measured. Observation sets containing the extra tie points were named *ncc_tie_15* and *ncc_tie_30*. In all the correlation sets described above the signalized points were measured such that only one image was used as a reference in correlation. We also measured the signalized points in all combinations, i.e. every signal was measured once visually and used as a reference where the other images were correlated. Multiple measurements were added to all correlation sets; here, these new sets are referred to as *ncc_m_15*, *ncc_m_30*, *ncc_tie_m_15* and *ncc_tie_m_30*.

2.4 Block Adjustment

The observation sets were adjusted using the ESPA program (Sarjakoski, 1988). All the given ground control (14 points) was utilized in the calculations, and Ebner's set of additional-parameters (Ebner, 1976) was used in all adjustments. The correlation test sets with multiple observations of the same signalized point were adjusted as such; each observation set of a point had its own point identity number in the adjustment. Final ground coordinates of the multi-observed points were determined by calculating the average of corresponding points from the results of the block adjustment.

3 Conclusions

A digital photogrammetric workstation implemented at the Finnish Geodetic Institute was used to measure the OEEPE test material (28 images in 4 strips at 1 : 4000 scale). Results of our triangulations were promising. The standard error of unit weight from the bundle block adjustment with observations on 15 μ m images ranged from 2.9 μ m to 4.2 μ m, depending on the measuring technique and the number of observations. In the 30 μ m images, the standard error of unit weight ranged from 3.4 μ m to 5.3 μ m. The adjustment results for the measurements of 30 μ m images indicate that good results can be achieved with low-resolution images, too. The root-mean-square error comparisons between the XYZ coordinates of the calculated and known ground points were (ΔX , ΔY , ΔZ)_{RMS} = 0.021 m, 0.020 m, 0.030 m at their best. The use of correlation techniques improved the height accuracy of the measurements. It also increased the automation level and made the measuring faster and more convenient to use. The test indicates that the quality of tie points may sometimes be a more important factor than the number of tie points. Our results and practical experience together indicate that digital aerial triangulation is an accurate and operationally feasible technique.

References

- Ebner, H., 1976. Self calibrating block adjustment. In: International Archives of Photogrammetry and Remote Sensing, Helsinki, Finland, Vol. XXI, Part 3.
- Lammi, J., 1994. User-guided measuring in digital aerial triangulation. In: International Archives of Photogrammetry and Remote Sensing, München, Germany, Vol. XXX, Part 3/1, pp. 467–474.
- Sarjakoski, T., 1988. Automation in photogrammetric block adjustment systems – on the role of heuristic information and methods. Acta Polytechnica Scandinavica, Ci88, Helsinki.



The aerotriangulation report

Jussi Heikkinen

Helsinki University of Technology

Institute of Photogrammetry and Remote Sensing

Otakaari 1 02150 Espoo Finland

This report concerns the OEEPE-project "Aerotriangulation Using Digitized Images". The project was started in the beginning of October 1993. Our situation concerning resources was little bit modest. We didn't have any specific software in the field of digital photogrammetry and the capacity of our computers was quite poor concerning the storage size of data.

Preparatory works

For the reason explained above, we investigated possible existing software packages for the task. We didn't have any special commercial software for digital photogrammetry. The only thinkable alternative was a software package designed for remote sensing applications. The weakness of this was that it didn't provide any possibilities to perform image matching. Our decision was to develop a C-program connected with motif-interface to take care of image measurements.

Another problem with use of digital images was our poor resources to store huge digital images. As a solution, we designed an algorithm, which read approximate co-ordinates from file delivered by pilot centre. Based on these co-ordinates image patches of size 240*240 pixels were extracted from the whole image read earlier from tapes to harddisk. The procedure was consecutive, in other words each image was processed one at a time. These image patches were stored into TIFF-format image files, where all image patches concerning each point were included in a single file. The same way all fiducial marks concerning each image were stored into TIFF-file. At the same stage offset values of each image patch from the beginning of a whole image was stored into a different file. These offset values were used to transform image patch co-ordinates into image co-ordinates.

Measurements of image co-ordinates

As mentioned, no point selection was done. The selection of control and check points was purely based on the preliminary work of the pilot centre. For the given task and for

visualizing the point distribution over the image, reduced resolution images were generated. From this reduced image rough co-ordinates of selected points could be extracted. Actually two image patches were fetched afterwards using this possibility. The reason for reselecting new points in one case was that in the approximate image co-ordinate file there were the image co-ordinates only from one image of a control point, even though it was detectible also in an other image.

For the fiducial mark measurements we generated synthetic images of two fiducial marks, (two different fiducial types) and performed an image matching. As the output of matching we got image patch co-ordinates presenting the possible centre of the fiducial mark. According to this co-ordinate pair we interpolated new graylevel values for pixels and extracted the centre part of a fiducial mark image. Finally we averaged those images and improved the model of the fiducial marks. In this template the centre of the fiducial mark was precisely in the middle of the template. The templates were averaged from 112 patches (4*number of images). The size of template was 67 pixels in 30pm and 135 pixels 15pm images. The final results we got by matching the correct averaged template (we had two templates, one for the corner fiducial marks and one for the side fiducial marks) with the image patch of fiducial marks.

The actual measurements of the triangulation points and the control points were made using a program designed in our institute. The methods we used in our program were manual pointing with the cursor of the mouse and image matching. For the manual measurements we designed few possible cursors. Some of them were transparent. The best cursor according to operators was the smallest one which didn't cover the image too much. Zooming effect for pointing purpose was done by using bilinear interpolation.

The image matching was performed by using LSQ-method type matching. The image matching was accomplished by moving the target image on the search image according to the image gradients. The operator pointed the image point from one image. A subtemplate centred at this point was extracted and handled as target image. The program gave an opportunity to choose the size of the target image depending on operators request. The initial co-ordinates came from the correlation process of subimage on other images. Problems occurred when the image points were detected from images in adjacent image rows. In those cases the adjacent image rows had been flown in opposite directions and images were rotated by 180 degrees. This kind of situations we hadn't expected at the time the program was developed, so image matching failed in those cases unless the target image was symmetric (see the example at the end of report).

The image measurements were made by students of photogrammetry as an exercise, so the measurements were quite heterogenous. This was realized when the final check before adjustment was made. Fortunately the checking of possible gross errors was easy as the program fetched all the image patches on the screen where the corresponding point was present and superimposed the measurements on each image patch.

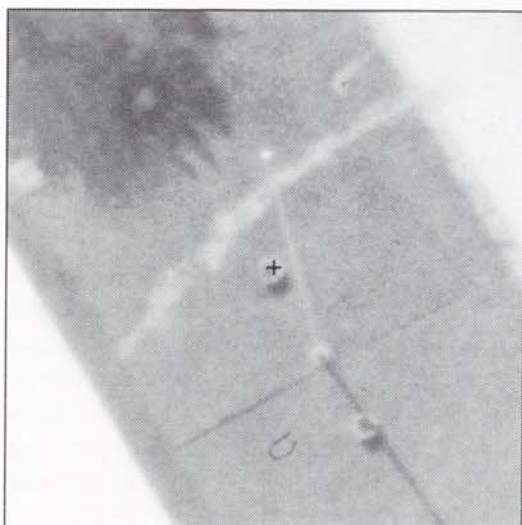


Figure a – The observation on image 11 from the first image row.

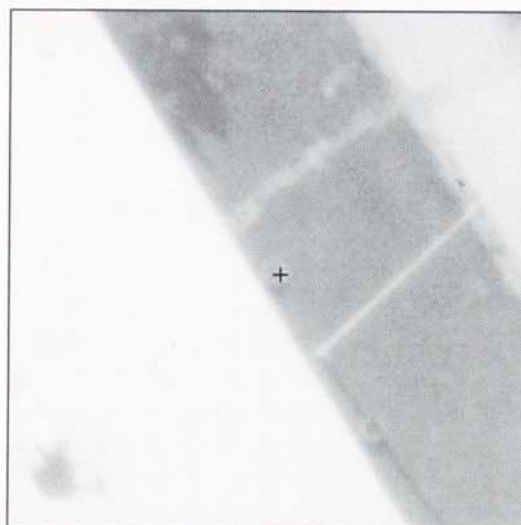


Figure b – The observation on image 12 from the first image row.

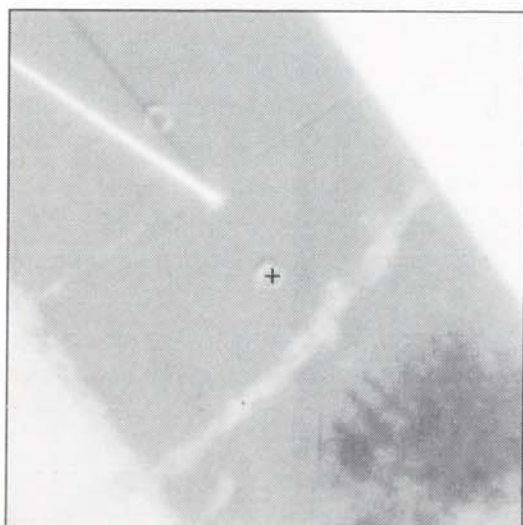


Figure c – The observation on image 25 from the second image row.

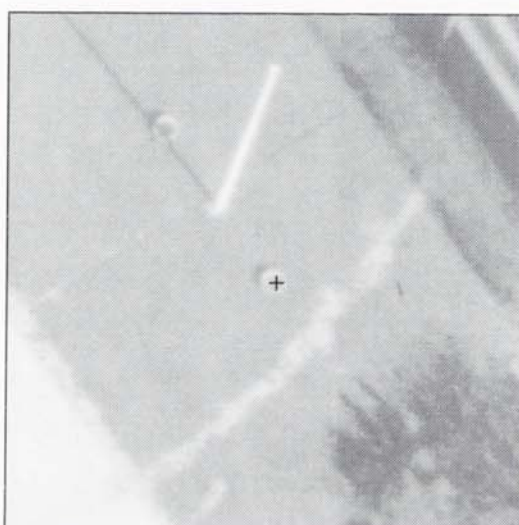


Figure d – The observation on image 26 from the second image row.

Block adjustment

Before block adjustment we made radial distortion corrections according to the calibration certificate. We estimated three first parameters of correction equation by LSQ-estimation. The six affine parameters were also estimated by using a LSQ-method. The results of parameter estimation are depicted in files in floppy disk (Coord15.out and Coord30.out).

The final block adjustment we made with a simple program developed in our institute. The adjustment program took care of refraction corrections and corrections due to earth curvature. The problem we had was that we didn't have any possibilities to involve additional parameters in the adjustment process. Because of that we made only four adjustments with varying control point set and image observations. We hope that the pilot centre has a possibility to make absent adjustments by using the observation files provided (ESPA15.obs ESPA30.obs).

The results of adjustments are quite promising. The standard error of unit weights are 9.0 pm and 9.2 pm with 30 pm data and 6.5 pm and 6.7 pm with 15 pm data, where the first value depicts the adjustment with dense control point set. The largest residuals were little less than 30 pm with 30 pm data and about 19 pm with 15 pm data in image observations. The weights we used in adjustment corresponded to about 10 pm accuracy in image observations in 30 pm data and corresponding value with 15 pm data was 5 pm. For the ground points estimated weights corresponded to the measurement accuracy of 10 cm in plane co-ordinates and 20 cm in height co-ordinates.

Time consumption

The time consumed is very difficult to estimate, because we didn't have any existing production scheme before we started this project. The development of the software was the most time consuming part. For the measurements we gave students a period of one month to perform the task. No precise estimate for time consumption per point can be given.

The preparatory work took quite a lot of time cause of troubles with hardware. The image patch extraction itself took only some 15 min per image with 30 pm data. For the 15 pm data the time was doubled.

The adjustment and gross error detection took couple weeks of time to carry out. Preliminary adjustment gave some gross error candidates which we checked out before the final adjustment.

Aerotriangulation using digitized images

Edouard Beauvillain

MATIS/DT

Institut Géographique National

94160 St-Mandé FRANCE

I Measuring system & software description

Two different sets of measurements were made during the OEEPE experiment.

1 *The 15 μ m experience :*

We used a Vax station (microvax 3100, VS4000) with a special personal system of point measurement (see 3). The pointing was made manually with the cursor on one of the photo visualised on the terminal display (monoscopic system). The point measurements were made with a cursor on the left photo and the homologous point is found by automatic correlation on the other photo at 1/8 of a pixel of resolution.

1 *The 30 μ m experience :*

The measurements were made on the Matra Traster T10 (linked to the global network via a SUN station). It is equipped with a stereoscopic vision and has the possibility of a sub-pixel pointing (up to 1/16 of a pixel) it is named the "sub pixel graphic cursor". The visualisation system is very similar to classic stereo photogrammetric system.

II Description of management of the image data

Using the Vax system was not a problem for the 15 μ m photo (excepted that handling data is quite long and time consuming). During the point measurements were made, it was necessary to store one photo on the local disc while the other photo was stored and accessible on an optic disc. Thus, the data transfers were difficult to handle (more than 30 minutes to store an image). Hence, the total time for all the measures on the 15 μ m photos was very long.

For the Traster measures, the disc capacity was not sufficient for the 15 μ m images. So, we had to make the measurements on the 30 μ m data. The time necessary to store an image was quite shorter but there were more data transfers to do: from the exabyte tape a SUN tape, then to the SUN station and to the T10 station (total time for one image: one hour).

For both systems, it was necessary to create a global management configuration for the images, the points, the measures, the block, the different parameters of the block adjustment,... and also for each image, we did create quick look that gave more flexibility for image management.

III Description of the measurements

For both systems used, the fiducial marks measures were made manually by monoscopic visualisation. The measurement accuracy is thus better than the pixel size, but no evaluation was made about its exact accuracy.

The point measurement on the vax system (15 μ m images) is done by mono visualisation, but the homologous point is determined by automatic correlation at 1/8 of a pixel on the right image. The point measurement accuracy can be estimated to half a pixel size. However, for some points, it was really difficult to determine its exact location (fuzzy detail, target that have been moved between the two photo captures, obstacle hiding the point ...) so some of the points had to be cancelled but the global accuracy is still hard to estimate.

Surprisingly, the measurement accuracy on the 30 μ m photo is quite similar (or even better) than for the 15 μ m ones. This is due firstly to the stereoscopic capability used for the point measurement and secondly to the fact that as the resolution is smaller, fuzzy points were not measured at all because it was not possible to distinguish them. Another fact is that for the previous method, the homologous point was determined by correlation on a "large" white cross (in number of pixels at that resolution) and at the 30 μ m resolution the target has fewer pixels.

V Short description of the block adjustment

The aerotriangulation software used (for both sets of data measurements) is named TOPAERO. It is the actual production soft from the IGN unit. It is a software for bundle adjustment, its main steps are:

- approximate orientation which enables to detect coarse faults
- adjustment by a least square method
- graphic visualisation of the results (it is then possible to see directly the worse point measures and the points that have to be remeasured).

This soft gives us the possibility to activate/unactivate a point (or a measure), to split a point or to activate/unactivate ground relations.

Additional details can be found in the report I send to you in late february.

VII Nature of the system

The TOPAERO soft is a production software used in the aerotriangulation unit.

The Traster T10 we used is under development. Our laboratory had to test it through different experiences for photogrammetric purposes.

The Vax system used is the system we use for our researches. Thus, we are developing programs on it, for example a process of automatic correlation including photo orientation, DTM production etc... These research developments may be implemented in the IGN production facilities.

THE HISTORY OF THE
CITY OF BOSTON
FROM 1630 TO 1800
BY
JOHN H. COLEMAN
IN TWO VOLUMES.
VOL. I.
BOSTON: PUBLISHED BY
J. B. LEECH, 1857.

Aerotriangulation using Digitized Images at KTH

Håkan Wiman

Department of Geodesy and Photogrammetry

KTH, S-100 44 Stockholm, Sweden

Introduction

KTH participated in the OEEPE project "Aerotriangulation using Digitized Images". The 30 mm image set was measured twice, manually and semiautomatically. The 15 mm image set was measured only semiautomatically. For the manual measurements, ERDAS commercial software was used. The semiautomatic measurements are made by cross correlation matching of image patches, either relative to masks (fiducial marks, signalized points) or relative to each other (tie points). All programs for the semiautomatic measurements were made at the department, most of them during the project. GENTRI [Larsson, 1983] was used for the block adjustments.

Manual measurements

ERDAS software, installed on a Sun SparcStation 2, was used for the manual measurements. The 64 Mbyte images were transferred from tape to HD one by one. Due to disk limitations, only two images could be stored simultaneously. The conversion from raw image files to the ERDAS LAN format caused the 128 first columns to be displaced to the last. This was of course corrected for. Other preparations before the manual measurements include writing camera data, control point coordinates, and selection of approximate areas where tie points are desired. The selection of tie points was made using PostScript printouts of very poor resolution. Therefore, only areas where tie points are needed were indicated. The decisions on actual points to measure were made in the first image the area occurred in. Only a limited number of natural tie points were selected; the signalized points doubled as tie points. A natural tie point defined in one image may not be visible in another. If the first image has been erased from the HD, you do not gladly read it into HD from tape again. In these cases yet a tie point has generally been introduced and both the original and the new have been measured in the following images. A print out of higher resolution, e.g. 1K by 1K or 2K by 2K pixels, would be better, so that the visibility of the tie points could be confirmed before deleting the images. The measurements were made at four times magnification using bilinear interpolation. All visible signalized points were measured. The parameters for the affine transformation from pixel to image coordinates were calculated inside ERDAS, but the transformation of the points as well as the corrections for earth curvature, radial distortion and refraction were made using own software. For the block adjustment, GENTRI was used.

We have only used ERDAS as a measuring device. As such it is comprehensive and easy to use. For the measurements of fiducial marks, two options should have been available (and may so be in Imagine); (i) the possibility to remeasure points one-by-one (ii) a file of residuals and standard deviations from the affine transformation. ERDAS supplies programs for block triangulation, but they were not tested by us.

Semiautomatic Measurements

The semiautomatic measurements were performed on both the 15 mm and the 30 mm image sets. All software was developed at the department on a Sun SparcStation10. The available disk space allowed only one full resolution 15 mm image to be read to HD at a time. The work flow is summarized in Table 1. Using approximate coordinates of the points to be measured, images patches were extracted from the full resolution images. The approximate coordinates were here the manual measurements in the 30 mm image set, so they were quite accurate. Therefore, the patch size was only 31 by 31 pixels. An alternative, which was tested on one image, is to make an overview image of 2K by 2K pixels. The operator points at the approximate position of the points, and patches of approximately 256 by 256 pixels are extracted. The overview images of the block can

Table 1 – Summary of the workflow for semiautomatic measurements including indication of operator interaction.

Action	Operator interaction
Preparation of Data Files	Yes
Read Images from Tape	No
Extract Overview Images	No
Select Tie Points	Yes
Measure Approximate coordinates in Overview Images: fiducial marks signalized points tie points	Yes
Read Images from Tape Again	No
Extract Patches around each Approximate Coordinate	No
Matching of fiducial marks to one mask signalized points to eight masks tie points to each other	No
Affine Transformation to Image Coordinates	No
Correction for Systematic errors and Earth Curvature	No
Block Adjustment	No
Summary of Results	Yes

easily be stored on a HD. The selection of the tie points is eased. One can quickly verify that a chosen tie point is visible in all images.

Masks of fiducial marks or signals were then matched with the patches, using the cross correlation coefficient. For tie points, one of the patches was decided master and the others were matched with it. All masks have a size of 13 by 13 pixels, except the fiducial marks in the 30mm image set which was 7 by 7 pixels. The masks were made ad hoc by examining the grey levels of a few fiducial marks and signalized points. The mask for the fiducial marks is the center white dot with a smooth transition to black. Correlations were high, 0.92–0.97. To take the different orientations of the signals (crosses) into account, the rotations were quantized into four angles (0, 22.5, 45, and 67.5 degrees). Each of these masks were made with a light background and a dark background, so that each patch of a signalized point was matched to eight masks. In spite of this elaborate jigsaw to cover most of the possibilities, correlation was generally low, especially for the 15mm image set. The tolerance for accepting a correct match was set as low as 0.55. However, even at this poor correlation, the indicated position was quite good, judged by visual inspection of some matching results. If a completely erroneous point would have been selected, we trust that the adjustment program detects it as a gross error. A novel approach for matching signalized points was introduced by *Gülch* [1994]. He performs a region based segmentation on the patches, places a snake inside a segment likely to be a part of the cross, lets the snake move around to detect the legs of the cross, and determines the center of gravity of the found contour. This approach was only tested on a few signalized points. *Gülch* also compares his method to manual measurements and matching by cross correlation and least squares. The matching of tie points was performed by arbitrarily choosing one of the patches and cut out the center 13 by 13 pixels from it. This "mask" was matched to the other tie point patches of the point. The very least one could do to improve this poor matching strategy, is to choose the most suitable of the patches as mask.

All matching was performed with subpixel accuracy by fitting a biquadratic polynomial

$$P(r, c) = \begin{pmatrix} 1 & r & r^2 \end{pmatrix} \begin{pmatrix} a_{00} & a_{01} & a_{02} \\ a_{10} & a_{11} & a_{12} \\ a_{20} & a_{21} & a_{22} \end{pmatrix} \begin{pmatrix} 1 \\ c \\ c^2 \end{pmatrix}$$

to the largest cross correlation coefficient and its 8-connected neighbors. The maximum of this polynomial is considered the best subpixel match.

Our system is not fully operational. It is far from user friendly. A more lengthy description of our system and approach can be found in [Wiman et al, 1994].

References

Gülch, E.: Using Feature Extraction to Prepare the Automated Measurements of Control Points in Digital Aerial Triangulation, IAPRS, Vol. 30, Part 3/1, Munich, 1994.

Larsson, R.: Simultaneous Photogrammetric and Geodetic Adjustment – Algorithms and Data Structures, Doctoral thesis, Dept. of Photogrammetry, KTH, Stockholm, 1983.

Wiman, H.: Aerial Triangulation using Digitized Images – The Contribution of KTH to the

Burman, H.: Project of OEEPE, Internal report, Dept. of Geodesy and Photogrammetry, KTH, Stockholm, 1994.

Report from the OEEPE-Test "Aerotriangulation using Digitized Images"

Øystein Andersen, Leif Erik Blankenberg, Ivar Maalen-Johansen

Agricultural University of Norway

Department of Surveying

1 Equipment

Our measurements were carried out on the ERDAS photogrammetric module OrthoMAX, under ERDAS IMAGINE, version 8.0.2. We worked under the module Block, which is the triangulation module. The computer was a SUN SparcStation 10, with 124 MB RAM and 1.6 GB harddisc.

2 Management of the image data

We used about 3 weeks for measuring both image sets, including some learning of the system and quite a lot of troubleshooting after the measurements.

The SUN machine was set up with timesharing, so our estimates of the time consumption may be set too high.

Time consumption:	15microns	30microns
Reading one image from tape:	15 min.	6 min.
Processing one image to ERDAS-format:	13 min.	5 min.
Building reduced resolution data sets:	10 min.	4 min.

Reading from tape, and formatting the data, took most of the time. Interior orientation took about 5 min. per image.

There was not made any radiometric pre-processing of the images before the measurements. Radial distortion was corrected during measurements, according to calibration certificate. Corrections for refraction and earth curvature could not be done.

3 Measurements

We did not use any automatic means for measurements. Up to 3 images can be displayed and measured at the same time. The measurements were done by pointing to the points with the cursor on the screen. This goes for fiducial marks, control points, check points and tie points.

The measurements were made in monoscopic mode. When measuring points that exists in more than one image, also the neighbouring images were shown on the screen to ensure proper identification of homologous points. The points were localized with the help of hardcopy prints of the image data.

The tie points were mostly targetted, existing points; but some natural tie points were added where necessary. The points 100–115, 200–215, 300–314, 400–418 are points which were added to make sure we had enough tie-points. These points are natural details.

The measurement of the images took approximately half an hour per image.

OrthoMAX have a triangulation module with computer-assisted correlation as an option. We did not use this, because it only worked with moderate image zooming (2x). We mostly found it necessary to use 8x magnification during the measurements.

The transformation from pixel coordinates to image coordinates in fiducial coordinate system, was a 6-parameter transformation.

4 Image patches

We used the whole images for this project, not any image patches.

5 Block adjustment software

The block adjustments were calculated with the PC program NLHBUNT. This is a bundle block adjustment program developed at our department. The adjustments were calculated as requested.

The a priori value of the σ_0 was set to 4.0 μm for the 15 μm images and 5.0 μm for the 30 μm images. The σ_x , σ_y and σ_z of the given coordinates were all set to 2.0 cm.

Additional parameters, or self calibration parameters, are used in this test. The set contains 12 "physical" parameters, which models corrections to the principal distance, principal point, radial lens distortion and film distortion up to 2. degree. These parameters give these extensions to the observation equations for the image points:

$$dx = \frac{x}{c} b_1 + b_2 + b_4x + b_5r^2x + b_6r^4x + b_7x + b_8y + b_9xy + b_{10}y^2 \quad (1)$$

$$dy = \frac{y}{c} b_1 + b_3 + b_4y + b_5r^2y + b_6r^4y + b_{11}xy + b_{12}x^2 \quad (2)$$

The parameters are treated as free unknowns in the adjustment.

For all the blocks with additional parameters in the adjustment, the same two parameters were found significant; radial distortion (b5) and trapezium shape (b11).

During the post-processing of the results, point 5825 was suspected to be mis-identified. Still, the point is included in the results.

We have not recorded time spent on adjustment, since this is just standard block adjustment.

6 Exceptions from the common instructions

We had problems identifying some of the check-points (which were without any description). Therefore some of these points are not measured.

7 Operational status of the system

The system is a fully commercial system from ERDAS, Inc.

8 Limitations and problems in the current state

Since we were not so very skilled in OrthoMAX when starting up, we chose a wrong datum for our block, not knowing that datums and projections were impossible to correct later. This led to a lot of problems when we later tried to run the bundle block adjustment module of OrthoMAX.

We also met another problem: The system was not able to give us image-coordinates or pixel coordinates in any form that is readable. All measurements are hidden in a binary file. ERDAS would not give us information about this file, so we had to write down by hand from the screen every pixel coordinate. We did the same with the interior orientation elements.

It has to be mentioned that ERDAS released a new version of OrthoMAX after this project was finished, hopefully much better than this first version.

9 Future development of the system

This is a Erdas, Inc. matter.

10 References to more detailed description of the system.

For further information about the Orthomax system, the Erdas IMAGINE OrthoMax, User's Manual, Version 8.0.2, Dec. 1993, should be read.

THE UNIVERSITY OF CHICAGO
LIBRARY

100 EAST HARTWELL STREET
CHICAGO, ILL. 60607

DATE OF ACQUISITION
1968

BY
LIBRARY

FROM
LIBRARY

REMARKS
LIBRARY

LIBRARY

LIBRARY

LIBRARY

LIBRARY

Aerotriangulation using digitized images. NLS participation.

J. Talts

National Land Survey of Sweden

Summary

The approach taken by the NLS for this experiment is to use an image processing system as a mono comparator. There is no automation in the measurements and the only refinement is that the measurements can be made with subpixel precision.

Pixel coordinates were corrected for systematic errors and the block adjustment was made with the program PATB-RS from Impho in Stuttgart.

The accuracy obtained is very good and comparable with that obtained with an analytical instrument.

Overview of the process and used equipment

We have downloaded the images in one computer and transported the data on a LAN to a VAX computer. Attached to this computer we have our image processing system which is a Teragon system. The Teragon system is a special purpose image processor which by now is ten years old.

In the image processor the pixel coordinates have been measured. There is a routine in the system which works so that you can give the pixel coordinates of a point. The displayed wiewport is then centered over that point. As the locations of the points were given approximately, the measurements could be made easily.

Another routine is used for measurements of pixel coordinates which works so that when you point at a point a subpicture is created. This image is magnified five or ten times. The measurement is made in this enlarged image.

A special program was written for the transformation of the measured coordinates on given fiducals and for the correction for radial distortion, earth curvature and refraction. At the same time the program was used to adapt the coordinates for the block adjustment program.

The block adjustment was made with the program PATB-RS from Impho in Stuttgart.

Time consumption

It was a time consuming procedure to read the image files from the Exabyte tape and transfer the data to the VAX-computer. The reading of one file on the tape took 10 minutes and the transfer took 18 minutes. These operations can however be made in the background and in parallel. In this experiment, however, there was not enough disk space available.

The time to measure one image was as an average 30 minutes. Five minutes were spent on the eight fiducial marks and 25 minutes on the control and tie points.

Some observations

It is interesting to see that even when the pixel resolution only was 30 micrometer it is possible to measure with an accuracy of about 5 micrometer. It is also interesting to observe that a transition seems to be possible from dedicated and expensive photogrammetric equipment to a general purpose workstation for the measurements of image coordinates.

Data management seems to be an important topic. Data must and can be managed in an efficient way.

The fiducial marks can be measured in a more automated way, but very much cannot be gained by this. As judged from these images it seems difficult to automate the measurements of control and connection points.

Report on aerotriangulation using digitized images and the ERDAS measuring system

Ingolf Hådem

University of Trondheim

Norway

This report presents some items concerning the contribution of the Department of Surveying and Mapping at the University of Trondheim to the OEEPE project Aerotriangulation Using Digitized Images at the organizing centre at the Finnish Geodetic Institute.

1 Measuring system

The derivation of image coordinates from digitized images delivered by the Centre used GCP the software program in the commercially available ERDAS program package for remote sensing implemented on a SUN SPARC LX 1 work station with an 8 bits display monitor.

2 Data management

The image data was translated from the tape (delivered by the Centre) to the computer disc storage and reformatted to ERDAS specifications. This disk stored a maximum of 4 images simultaneously.

3 Measurement

Both the fiducial marks and the actual image points (signalized or natural) were visually (and monoscopally) measured in the digital image displayed on a monitor. A window (30 x 30 pixels) designed to search for the point to be measured was zoomed four times. This enabled a pointing resolution of a 1/4 pixel to be achieved by the following procedure: (a) a coarse pointing by moving the measuring mark to the vicinity of the image point position using a mouse, (b) a final pointing by moving the mark by means of the arrow keys. The operator had no a priori training in this procedure.

4 Selection of tie points

The 15 μm image set was measured first. Before the measurement, connection points representing features like house corners and road intersections were visually selected, described and marked on hard copies of the images. A reselection was in many cases necessary during the actual measurement because of identification difficulties (see below).

5 Block adjustment

The actual adjustment program, FOMAKON (Hådem, 1989), was run on a MICRO VAX 3100. Orientation and coordinate unknowns were simultaneously solved by the Gauss-Newton method. Good approximate initial values were obtained by a program for stepwise triangulation (Hådem, 1989) based on the formulas for strip triangulation (Schut, 1967) and exact linear similarity transformation in space (Schut, 1961). (The a priori approximate values given by the Centre were not used.) With these initial values the bundle adjustment required 2–3 iteration steps.

The bundle adjustment with additional parameters included affinity and lack of orthogonality as unknowns. The known coordinates, with a priori given standard deviation $s_{XYZ} = 0.02\text{m}$ were constrained with weight $= (s_0/s_{XYZ})^2$, where s_0 is the estimated sigma 0.

The gross error search used the well-known Baarda's method both in the introductory stepwise triangulation and in the final constrained bundle adjustment.

6 Exceptions from the common instructions

Due to many gross errors and identification problems it became necessary in some cases to use natural tie points instead of signalized points as prescribed in the common instructions. There were also cases where a point could not be used both in the 15 μm set and in the 30 μm set.

7 Operational status

The system may be characterized as an experimental one, enabling digital aerotriangulation to be executed by hardware and software which originally had other purposes. It allows image enhancement, visual pointing and recording of image coordinates as options in the ERDAS (originally adapted to analysing remote sensing imagery), and photo triangulation by a self-developed program called FOMAKON (originally adapted to close range photogrammetry).

8 Limitation and particular problems

The digital measurement resolution using ERDAS is limited to a 1/4 pixel.

There was a high frequency of (small) gross errors in the selection, identification and measurement of natural tie points.

Another problem was the slowness of some procedures, particularly the translation of data from tape to disk storage. The approximate waiting time for this translation was 20 minutes (the 15 μ m set) and 10 minutes (the 30 μ m set). Some time could have been saved if a CD-ROM storage device could have been used.

The time consumption of the measurement was:

The 15 μ m set: 70 minutes (including the selection of tie points and other preparatory work)

The 30 μ m set: 25 minutes on average per image of a mean number of 17 image points + 8 fiducial marks.

The numerical procedure for solving the unknowns in the bundle adjustment program FOMAKON did not take advantage of the particular structure of the coefficient matrix of the normal equations. Thus, to solve for the approximately 600 unknowns took approximately 25 minutes per iteration step.

9 Future development of the system

In the first place, more advanced (automatic) digital point measuring of both natural points and signalized points will be implemented. The more powerful SPARC station 5 will be introduced.

10 References

- Hådem, I.*, 1989: "FOMAKON, A Program Package for Industrial Photogrammetry". *Kart og Plan*, Vol 49, No 1, pp 25-34.
- Schut, G. H.*, 1961: "On Exact Linear Equations for the Computation of the Rotational Elements in Absolute Orientation." *Photogrammetria*, Vol XVII, pp 34-37.
- Schut, G. H.*, 1967: "An Introduction to Analytical Strip Triangulation", NRC-9396, National Research Council of Canada, Ottawa.



OEEPE Test on Aerotriangulation using digitized images

Christian Heipke

Chair for Photogrammetry and Remote Sensing

Technical University Munich

1 Overview of work

This report covers the activities carried out by members of the Chair for Photogrammetry and Remote Sensing, Technical University Munich for the OEEPE Test "Aerotriangulation using digitized images" prepared and managed by the Finish Geodetic Institute on behalf of the Commission A of OEEPE.

The images were observed solely manually. Image processing in order to enhance the images etc. was not used. One operator (a 3rd year student) carried out all measurements. Only the 15 micron images were used. Since a digital stereo device was not available, the image coordinates were measured in mono. For the measurement of the control, check, and tie points parts of two overlapping images were displayed side by side on the monitor at all times in order to reduce errors in point transfer.

Two measurement cycles were carried out. In the first cycle the original images were used. In other words, one screen pixel was identical to one pixel of 15 μms . The image coordinates were thus measured with a resolution of one pixel. This cycle is termed "1fach" in this report. In the second cycle the original images were zoomed by a factor of 3 and interpolated using a bilinear interpolation. In this cycle the nominal measurement resolution was one third of a pixel. This second cycle was expected to yield more accurate results and is termed "3fach" in this report.

Point measurement was carried out according to the suggested positions given in the file `appr_obs.pix`, which was provided by the Finish Geodetic Institute. In the tie point areas more than one point was occasionally measured. Thus, an even and dense enough distribution of the points was guaranteed.

Following the point measurement the obtained pixel coordinates were transformed into the image coordinate system by an affine transformation using the fiducials as identical points. Subsequently, a standard bundle adjustment was computed yielding object coordinates for the points measured in the images, and orientation parameters of all images, both including their theoretical standard deviations. Altogether 8 runs were carried out. The best result in terms of σ_0 (standard deviation of the measured image coordinates) was 5.64 μms .

2 Detailed description of different work phases

2.1 Hard- and software environment

The project was carried out using a standard workstation (SUN 4) and a graphical monitor with approximately 1000^2 screen pixels. The image coordinates were measured using the standard SUN mouse as pointing device. The SUN was equipped with an exabyte device and enough free SCSI disk space to hold 3 of the digitized images.

For the coordinate measurement the program package IMD for image visualisation and measurement, which was developed by VTT, Helsinki, was used. In the installed version this program package allows for the simultaneous display of multiple images on the screen, for roaming, for zooming with different interpolation modes (however, roaming and zooming are not performed online), and for storing the measured image coordinates with subpixel resolution.

For the affine transformation self-written software was employed.

The bundle adjustment was carried out using the program package CLIC developed at the Chair for Photogrammetry and Remote Sensing, Technical University Munich within the last 12 years. CLIC provides for all possibilities necessary in this test.

2.2 Image coordinate measurement

The image coordinates were measured in image pairs in order to reduce errors in point transfer (see table 1). All images were used one after the other. Whenever an image was used the whole image was used. At no time windows of the images were cut out and physically stored on disk, because such a procedure would result in much more files and thus the file organisation would have had to be significantly more sophisticated.

Table 1 – Overview of measured image pairs

No. of strip	No. of images forming a pair						
1	11/12	12/13	13/14	14/15	15/16	16/17	
2	20/21	21/22	22/23	23/24	24/25	25/26	
3	37/38	38/39	39/40	40/41	41/42	42/43	
4	46/47	47/48	48/49	49/50	50/51	51/52	
1/2	17/20	16/21	15/22	14/23	13/24	12/25	11/26
2/3	26/43	25/42	24/41	23/40	22/39	21/38	20/37
3/4	37/52	38/51	39/50	40/49	41/48	42/47	43/46

The following sequence of operations was carried out for each pair (as an example images 13 and 14 are used in this description):

- read the whole image #14 from exabyte onto the magnetic disk (image #13 was still on the disk, because it was used in the image pair #12/#13 which was measured immediately before #13/#14).
- display a reduced version of image #14 of 1000^2 pixels for general inspection.
- measure the pixel coordinates of all 8 fiducials of image #14 using the original images with a measurement resolution of one pixel (cycle 1fach). For this task a 1000^2 pixel window of image #14 with the relevant fiducial approximately in the centre of the monitor was displayed. The mouse was pointed at the fiducial centre, the actual measurement was carried out by a mouse click.

(the pixel coordinates for the fiducials of image #13 had already been measured).

- repeat the measurement with a zoom factor of 3 and bilinear interpolation for the image data (cycle 3fach).
- display two windows with 1000 rows x 500 columns side by side on the monitor. Load part of image #13 in the left window, and part of image #14 in the right window.
- Roam both images to the approximate position of each control, check, and tie point by using the coordinates provided in the file `appr_obs.pix` as a guide.
- measure the pixel coordinates of each control, check, and tie point visible in the image pair using the original images with a measurement resolution of one pixel (cycle 1fach). The mouse was pointed at the point to be measured in both images, the actual measurements were carried out by two mouse clicks, one in each image.
- after all points for cycle 1fach had been measured, repeat the measurement with a zoom factor of 3 and bilinear interpolation for the image data (cycle 3fach).
- repeat the whole process with the next image pair.

Only points visible in both images were captured. Therefore, some points used in `appr_obs.pix` were not measured. These are control points we only found in one image (eg control point 6033, only visible in image #16) and points we found in one image, not in the next one, and again in the third one (eg check point 5925, which we found in image #12 and 14, but not in image #13).

In the described way the image pairs were observed as indicated in table 1 within each image strip and across the strips. The result of this step were pixel coordinates of all fiducials per image and all control, check, and tie points per image pair, both in cycle 1fach and cycle 3fach.

2.3 Transformation of pixel into image coordinates

After the pixel coordinate measurement, the pixel coordinates and the image coordinates of all 8 fiducials were available for each image. The latter were taken from the

Table 2 – Overview of bundle adjustment runs

Run #	cycle	No. of GCP	additional parameters
1	1fach	all	none
2	1fach	all	2 for radial distortion
3	3fach	all	none
4	3fach	all	2 for radial distortion
5	1fach	sparse	none
6	1fach	sparse	2 for radial distortion
7	3fach	sparse	none
8	3fach	sparse	2 for radial distortion

provided camera calibration certificate. Thus, for each image the parameters of an affine transformation could be computed. They were used to transform the pixel coordinates of the check, control, and tie points into the image coordinate system.

All computations were carried out independently for the cycles 1fach and 3fach.

2.4 Bundle adjustment

Using the computed image coordinates as input various bundle adjustment runs (see table 2) were computed yielding the object coordinates of all measured points and the orientation parameters of all images, both together with the theoretical standard deviations.

In the used bundle adjustment program each point can only be present once per image. Due to the described measurement strategy, however, some points appeared several times in an image. For instance, control point 5934 was measured in the image pairs 11/12 and 11/26. Thus, two measurements for this point were available in #11. In every such case the coordinates of these measurements were averaged prior to computing the bundle adjustment.

Neglecting the effects of the averaging process just described, all observation were considered as equally accurate and uncorrelated. The object coordinates of the control points were introduced as observations with the given accuracy of 0.02 m in all three coordinates.

Initial values for the unknown orientation parameters had to be provided for our bundle adjustment program. The positions X and Y were taken from the overview map, Z was assumed to be identical and set to 700 m for all images (flying height of 600 m and terrain height of 100 m). The rotation angles omega and phi were set to 0, kappa was 200 gon in image strip 1 and 4, and 0 gon in image strip 2 and 3.

In 4 adjustment runs two additional parameters for modelling the radial distortion of the camera were introduced. The following standard formula was used to compute the parameters A1 and A2 from the information in the camera calibration certificate:

$$DR = A1 R (R^2 - R_0^2) + A2 R (R^4 - R_0^4)$$

R distance from the point of best symmetry (assumed to be identical with the principal point)

DR mean distortion as given in the calibration certificate

R₀ distance with DR = 0, R₀ = 0.1165 m was used according to the mean radial distortion curve

A1, A2 parameters to be determined

The parameters of radial distortion were computed to

$$A1 = -3.3945 \cdot 10^{-3} \text{ m}^{-2}$$

$$A2 = 1.8766 \cdot 10^{-2} \text{ m}^{-4}$$

In the adjustment runs as indicated in table 2 these parameters were introduced and held constant during the adjustment.

Earth curvature and refraction cannot be modelled in the used bundle adjustment program and therefore had to be neglected.

Two different control point configurations were used as requested. In the first configuration all measured control points were used. Since point 6033 was not measured (see above) only the remaining 13 control points could be used. All 13 were introduced as control points in X, Y, and Z. The second configuration was a sparse one. Again, 6033 was missing. Therefore, only the three points 160, 3821, and 6801 were used as control points in X, Y, and Z together with the points 4024, 4846, 5010, and 5943 for additional height control.

In preliminary adjustment runs using all checkpoints and no additional parameters two points in cycle 1fach (1000013 in image 11 and 1000016 in image 24) and one point in cycle 3fach (1000028 in image 22) had residuals larger than 3 sigma₀ and were therefore identified as gross errors. They were excluded from the further computations.

3 Results

The results of the eight bundle adjustment runs are given in table 3.

The following can be seen from these results:

- the achieved accuracy is in the order of 5 to 6 µm for the standard deviations of the image coordinates. This is about one third of a pixel.
- the cycle 3fach is more accurate than the cycle 1fach in all cases by about 1.1 µm.
- the introduction of the parameters for radial distortion does not significantly influence the results.

Table 3 – Results of bundle adjustment

Run #	sigma_0 [μm]	RMS_X [m]	RMS_Y [m]	RMS_Z [m]
1	6.90	0.030	0.034	0.079
2	6.89	0.030	0.033	0.079
3	5.84	0.026	0.028	0.067
4	5.77	0.025	0.028	0.066
5	6.86	0.066	0.077	0.104
6	6.84	0.066	0.077	0.103
7	5.70	0.055	0.064	0.086
8	5.64	0.054	0.063	0.085

sigma_0 standard deviation of the image coordinates

RMS_X root mean square value of the theoretical standard deviations of the computed X-coordinates of the check and tie points

RMS_Y root mean square value of the theoretical standard deviations of the computed Y-coordinates of the check and tie points

RMS_Z root mean square value of the theoretical standard deviations of the computed Z-coordinates of the check and tie points

- the sparse control point configuration is rather weak as indicated by the larger values for RMS_X, RMS_Y and RMS_Z. Since only three points were used for X and Y, the results should not be overinterpreted.

Thus, the results are in the range of the expected accuracy. It is interesting that cycle 3fach while being more accurate than cycle 1fach in all runs only slightly improves the results. This is partly due to the fact that the image details turned unsharp due to the bilinear interpolation. It remains to be seen, whether more accurate results can be obtained using a more sophisticated zooming. Moreover, a zoom of 3 means that the viewing area is only one ninth of that without zoom. Therefore, it is more difficult to search for individual points as long as online roaming, zooming or at least an overview image are not available.

4 Comments

This test is very valuable, because it showed the potential and the problems encountered when trying to use digital imagery for a standard photogrammetric task in a “pre-operational” way.

We have followed a rather traditional way of carrying out the aerotriangulation, using only manual measurements, and only using two images at a time. Since the work was carried out using a standard workstation, mono rather than stereo measurements had to be taken, and the used pointing device (the SUN mouse) was not as sensitive and comfortable as the one at the analytical plotter. It could be shown that in this case the achieved accuracy for aerotriangulation is in the range of that known from analytical photogrammetry.

Of course, the digitized images offer an additional potential in terms of automation, simultaneous multi image measurement, and accuracy improvement. An investigation into these issues was planned within the project, but could not be carried out due to time constraints.

The major problem was that of data handling. We had decided early in the project to only use the 15 μ m images, because from experience gained in other projects, we felt that the accuracy required in aerotriangulation could only be achieved in this way. This meant a data set of approximately 250 MB per image. This data volume, but even more so the time needed to transfer an image from backup medium (exabyte in this case) to disk, from disk to monitor etc. did limit our activities to a large extent, especially, since we worked in a multi-user environment. Therefore, we are not in a position to make any comments on the time spent for the different project phases. However, it seems to us, that these data can only be used economically by streamlining the whole process of aerotriangulation as much as possible, and by using image compression. In addition to this, special software is needed to speed up all tasks relating to the digital imagery. In some cases, even special hardware devices such as real-time disks might be required.

At the end I would like to thank all individuals who put work and effort into preparing and managing this OEEPE test, my colleague Olaf Hellwich, who supervised the project together with me, and Markus Hampel, who actually carried out the coordinate measurements and all the tiny little bits and pieces necessary to complete such a project.

THE HISTORY OF THE
CITY OF BOSTON
FROM 1630 TO 1880
BY
JOHN H. COVINGTON
BOSTON
PUBLISHED BY
J. B. LEECH, 15 NASSAU ST.
1880

Automatic Aerial Triangulation

Vassilios Tsingas

Institute for Photogrammetry

University of Stuttgart

1 Introduction

Digital aerial triangulation was a subject of investigations at the Institute for Photogrammetry of Stuttgart University during the past few years. In 1986 an example of semiautomatic point transfer by digital image correlation was given in [Ackermann/Schneider 1986]. The example demonstrated at that time already the high accuracy potential of digital aerial triangulation ($\sigma_0 \approx 4\mu\text{m}$). The question, how to obtain automatically approximate values and to select the tie-points, was not treated. In the meantime a new method on automatic digital aerial triangulation was developed [Tsingas 1992]. The essential part of the method is the automatic selection and transfer of tie-points, operating with multiple feature matching. The procedure is potentially fully automatic, but allows interactive guidance and interference, whenever necessary. The approximate values are also obtained automatically. In 1991 there has been a first test of automatic digital aerial triangulation using this method [Tsingas 1991]. 21 photographs of the scale of 1 : 7800 of the 20 year old test block Appenweier were scanned with $15\mu\text{m}$ pixel-size. 2236 tie-points were determined automatically. The block-adjustment gave an image coordinate precision of $7.9\mu\text{m}$. At that time existed no integrated software solution. The processing time was about 50 minutes per image on a VAX 3500 workstation. In the meantime additional developments and experiments have brought the method to an operational level. The Institute for Photogrammetry of Stuttgart University has participated in the OEEPE test, applying the above automatic method. For comparative purposes two additional cases of conventional block triangulations and bundle-adjustments were made (chapter 3).

2 Aerial Triangulation with automatic selection and transfer of tie-points

There are, at present, two strategy lines which can be pursued in digital aerial triangulation. The first strategy uses semi-automatic methods and is close to the conventional procedure of analytical photogrammetry. The human operator selects interactively one or several suitable tie-points in each of the overlap areas of an image. That image point is transferred by image matching into all other images in which it appears. That point-transfer is automatic but is guided (for sufficient approximation) and controlled interactively. A first experimental use of this strategy was given in [Ackermann/Schneider

1986]. The second strategy, which is pursued here, goes one essential step further and attempts a fully automated procedure for selecting, transferring (matching) and measuring tie-points. In this case not only the selection of tie-points is automatic but the approximations are obtained automatically too.

2.1 Multiple Feature Matching

By photogrammetric blocks in the aerial photogrammetry the problem of various and multiple overlap is appearing. Therefore a method of multiple feature image matching was developed. The method provides pixel coordinates of automatically selected and matched multiple tie-points assessed to subpixel precision. The method operates with many more tie-points than are conventionally used in aerial triangulation. Such strong ties imply high redundancy with all its advantages concerning easy and safe blunder detection and high accuracy of the exterior orientation parameters. Other advantages are low processing time, robustness and that it needs only coarse initial approximations.

In our case, features are image points which are extracted with the Förstner interest operator. The extraction implies pixel coordinate assessment to subpixel precision and represents eventually the measurement of the image coordinates of the respective image points. Therefore the precision of the point extraction defines the precision of the matching. After the second step the preliminary list of candidate pairs of corresponding points contain wrong or double valued matchings. These point pairs are therefore tested in the third step, against the mathematical model of affine relations between the sets of point pairs of all image pairs. In the case of n homologous image patches are $n(n-1)/2$ pair-combinations but only $(n-1)$ independent affine transformations. The affine relations are, in case of aerial photographs, local approximations to the perspective relationships. The remaining ambiguous matchings must be eliminated in the last step. Whilst in case of two homologous images this task is quite simple, we need a universal method to solve this task by multiple overlap. Image points and candidate point pairs can be associated to the nodes and the links of an undirected weighted n -partite graph (by n overlap), respectively. The inverse of the similarity measure of a pair is the cost of the respective link. Assuming that all point pairs exist between n homologous points, a multiple point matching is associated to a n -clique. A n -clique is the maximal complete subgraph that can exist in a n -partite graph. Therefore the best multiple point matching is defined by the maximal complete subgraph with the minimal costs of links in a n -partite graph. When we decrease the parameter n , we can find multiple matchings of lower order until pairwise matchings ($n=2$). That means, that homologous points can be found also in areas with partial overlap.

With this formalisation of the matching problem each standard algorithm of binary programming can be used to solve the problem. Complete subgraphs (clique) and binary programming are combinatorial problems and its computational complexity is NP-complete. With each additional variable (link in the matching graph) the number of possible solutions is doubled, which resulted in an exponential increase of the computational efforts. Therefore it was essential to develop an optimizing search algorithm. Empirical experience has shown that in this case the computational efforts increase exponential to the number of image pairs and not to the points pairs.



Figure 1 – Initial, automatically defined, image patches

2.2 *Strategie and Operational aspects*

The above elementary method operate with overlapping image patches. In order to automate the point transfer we need a strategy for the automatic operation of this method through the vertical structure of the image pyramid and through the horizontal structure of the photogrammetric block. A major problem in image matching is the provision of sufficiently close approximations. In order to solve that problem automatically the system goes step by step through an image pyramid. Three levels are sufficient, separated by a scale factor of about 4 or 5. Another, most coarse level of the image pyramid is used for the automatic identification of the forward and side overlap.

In case of conventional aerial triangulation the initial image patches are normally located near the 9 standard position within an image at which the tie-points are ideally positioned (Fig. 1), but also irregular overlaps can be accommodated. Once the initial homologous image patches have been identified the actual process of the image point selection and multiple matching of tie-points will start on the next lower level of the



DIGITAL AERIAL TRIANGULATION – OEEPE TEST BLOCK FORSSA				
	Analytical	Digital – Automatic		
Pixel size	–	15 μ m	30 μ m	
Pyramid strategy	–	safe 	minimal 	
Overlap areas	–	780	234	
Interactiv support (approx. values)	–	6%	6%	
Points per patch	–	10 best	20 best	all
Image points (per image)	492 (17)	7623 (272)	3686 (131)	6641 (237)
Terrain points	151	3401	1526	2991
Outliers in adj.	–	6%	0.7%	1.6%
processing time per image	(6 min)	5.3 min	1.7 min	
σ_o [μ m] ([pixel])	3.5 (–)	6.2 (0.41)	10.6 (0.35)	11.7 (0.39)

Figure 2 – Results of conventional and automatic aerial triangulation

image pyramid. This process is subsequently repeated through the remaining two levels of the image pyramid. Any selected point serves as an approximate center for defining the respective image patch on the next lower level on which again the method is applied. With regard to the number of selected points per patch different strategies can be pursued. In the minimum case only one point is selected and transferred onto the next lower level of the image pyramid. Another safer strategy could be to transfer two or three points, resulting in four or nine local patches (within the initial patch) on the lowest level (Fig. 2, Pyramid strategy).

The test was run on a Silicon Graphics IRIS/Indigo workstation with a MIPS-R3000/33MHz processor and 32 MB RAM. The station was equipped with a 5 GB harddisk. It was sufficient capacity for storing the complete block of 28 digital images (include the image pyramid) with the 30 μ m pixel resolution. On the 15 μ m level of pixel-size the harddisk could store 12 images simultaneously. The software "Point-T" runs under the UNIX operating system and the X-Windows environment. It has a graphical user interface which allows to monitor the process and to visualize the results.

Interactive support of the automatic process was required in 6% of all image patches. The support was limited to interactive provision of the approximate values. The problem areas are related mostly to the small side overlap between the strips. Other problem areas can be forests or built-up areas with large perspective distortion, espe-

cially in large scale aerial images. The number of issued tie-points was quite large, amounting to 272 image tie-points per image (15 μm data). 6% of the delivered image points were discarded as small outliers in the final adjustment. This rate of errors seems quite acceptable, as the high redundancy permits safe and complete detection. With the 30 μm data the rate of outliers is reduced to 0.7% and 1.6% (Fig.2). The net processing time took 150 min or 5.3 min per image, referring to 7643 image tie-points and the safer patch strategy with 54 (6x9) patches per image. By applying the minimal patch strategy with 9 patches per image (30 μm data) the processing time reduced to 47 min or 1.7 min per image.

Looking at the accuracy results the major item of interest concerns the σ_o . It concerns in first instance the precision of the feature extraction and the feature matching. It describes, in other words, the image coordinate precision of the automatic digital procedure and can be compared with the conventional values obtained by traditional point marking and point transfer, resp., as well as, with the precision of signalized triangulation points. The σ_o of the digital aerial triangulation amounted to 6.2 μm (0.4 pixel) with the 15 μm data and 10.6 μm (0.35 pixel) with the 30 μm data. This result is close to the theoretical precision of feature extraction (0.3 pixel). The theoretical accuracy of the exterior orientation parameters was clearly better than the accuracy obtained with the conventional analytical block triangulation, because of the high redundancy.

3 Digital Conventional Aerial Triangulation with interactive observations

Two different interactive measurement of the signalized points were made using the original diapositives and the digitized images. The first measurement was carried out by Dipl.-Ing. W. Schneider with the Zeiss monocomparator PK1. The second measurement is related to digital aerial triangulation, based on interactive image point measurement of signalized points, on a mono computer screen. The measurements took place under visual observation on the computer screen with a pointing accuracy of 1/3 until 1/10 pixel. For the accuracy assessment of the automatic digital method all signalized points in the block had to be measured interactively, on both pixel levels, as they were required as control points and as check points. These points, complemented by a few additional quasi-signalized points, were practically the same points which had been measured and processed in the analytical aerial triangulation. Those signalized points, about 17 per image, were sufficient for a complete block adjustment, in fact they represent quite a conventional standard case of tie-points. Hence the block could also be calculated with the interactively measured image points as observations. The result give an independent example of block adjustment with interactive digital measurements, on a mono-screen, of signalized points. Also, the results can be directly compared with the analytical block, as they refer essentially to the same points. On the 15 μm level the image coordinate precision (σ_o) reaches 3.9 μm (0.26 pixel), to be compared with the 3.6 μm of the PK1 monocomparator measurements. On the 30 μm level the value amounts to 5.3 μm (0.18 pixel). Thus interactive digital (mono-)measurement of signalized points is capable of excellent accuracy which comes close to the corresponding results of analytical block triangulation.

4 Conclusion

It can be concluded in general that the digital aerial triangulation gave very good accuracy results, which qualify the method as a high precision aerial triangulation. Summarizing the empirical test it can be stated that the results are extremely promising in every respect. Automatic digital aerial triangulation will not only be more accurate than comparable conventional aerial triangulation. Once properly implemented it can also be expected to be very fast and less expensive. A high economic and accuracy performance is certainly anticipated. Feature development aims to increase the reliability of the system and to minimize the interactive support.

References

- Ackermann, F., Schneider, W. (1986): "High Precision Point Transfer by Digital Image Correlation", Int. Arch. of Photogrammetry, Vol. 26-III, Rovaniemi 1986.*
- Ackermann, F., Tsingas, V. (1994): "Automatic Digital Aerial Triangulation", Proceedings ASPRS Annual Convention Vol. I, p. 1-12, Reno 1994.*
- Tsingas, V. (1991): "Automatische Aerotriangulation", Proceedings 43rd Photogrammetric Week, Inst. for Photogrammetry, Stuttgart University, Stuttgart 1991, p. 253-268.*
- Tsingas, V. (1992): "Automatisierung der Punktübertragung in der Aerotriangulation durch mehrfache digitale Bildzuordnung", Deutsche Geodätische Kommission, Reihe C, Heft 392, München.*

Report of the Institute for Photogrammetry and Remote Sensing at the TU Vienna

Franz Rottensteiner and Reinhard Prinz

Technische Universität Wien

Institut für Photogrammetrie und Fernerkundung

Austria

1 Hard- and Software

The software used for the identification of the signals and the measurement of the natural points was developed at our institute and is still in an experimental state. The measurements were carried out on a Hewlett Packard 9000/700 workstation which had an additional 2.8 GB hard disc. Any X – terminal could serve as a display for the measuring process.

After measurement had been completed, the results were transferred to a 80486 PC via local network, and on this PC bundle block adjustment was performed using the program package ORIENT which has been developed at our institute and is commercially available.

2 Data Storage

As only a 2.8 GB disc was available for storing the image data, we decided to extract patches from the images immediately after they were read from the tape. The size of the patches was 150×150 pixels, and they were centered at the approximate positions as we got them from the pilot centre. The file with the approximations we obtained from the centre was the input for our patch extraction program. Thus, about 31 patches per image (8 patches containing fiducial marks, 8 for natural tie points and 15 for signalized points) were extracted. In order not to have too many image files, all the patches of one particular image were stored on one 'reduced' image file; the offsets of the individual patches were stored on an ASCII file.

3 Identification of Fiducial Marks and Signalized Points

A two dimensional hierarchical area based matching algorithm was used for the detection of the fiducial marks and the signal points. The templates were artificial images derived from vectorized descriptions. The accuracy of the approximations had to be good enough to ensure that only one signal was inside each search region.

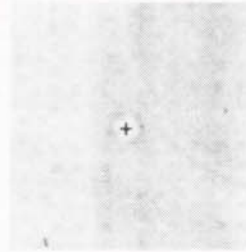


Figure 1 – left: template rotated by 55 gons (enlarged);
right: a black cross indicates the position of the point (resolution 1 pixel).

The position of the maximum of the cross correlation coefficient is searched for in a certain area with variable stepwidth. In order to achieve an accuracy better than 1 pixel, the cross correlation function is approximated by a polynomial of second order; the subpixel estimate of the position of the signal is found at the position of the maximum of the polynomial.

As the above algorithm is not invariant to rotations of the signals, the search has to be repeated with templates of different orientation; the best fit is accepted. If a point has been detected in one image, the rotation of the template is stored and used as an approximation for the rotation of that signal in the other images. Figure 1 (next page) shows the position of point 5854 in image 11 and the template which was rotated by 55 gons.

Finally, the maximum correlation coefficient is tested against a threshold. Only if this threshold is hurt, the user has to interact: the position of the signal as calculated by the program will be shown on the screen, and he can either accept the result or not.

The accuracy of the method was empirically estimated to be about 1/4 pixel for 30 μm images. In the course of this project it turned out that the relative accuracy was much better for the 30 μm images than for the ones scanned with 15 μm although the signals were hardly visible in the 30 μm images. We think that this is due to the fact that scale differences of the signals are neglected by our approach, but have already some influence on the matching accuracy in the 15 μm case. Problems also occurred when the signals were partly occluded (e.g. point 6801). In this case, specific templates had to be used.

4 Measurement of Natural Tie Points

A semi - automatical algorithm was used for the measurement of natural tie points. First, distinct features are selected in homologous image patches applying the Foerstner interest operator. The homologous patches with the extracted features are then displayed on screen simultaneously, and the user can interactively decide which features represent homologous points; of course, more than one tie point can be

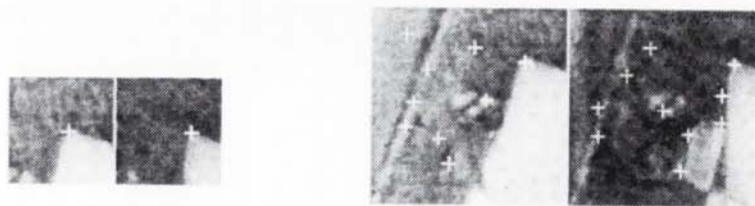


Figure 2 – right: two homologous image patches. The white crosses indicate features found by the Foerstner operator;
left: homologous image points selected by the user; final position

measured in one patch. The subpixel location of the tie points is derived either by intersection of gray level edges or by intersection of lines of steepest descent within a small window. Thus, no exact pointing has to be done. The accuracy of that method was estimated to be worse by a factor 2 compared to the algorithm applied for signals. Figure 2 shows two homologous image patches with the centres of the windows selected by the Foerstner operator marked as crosses.

5 Bundle Block Adjustment

For this purpose, the interactive bundle block adjustment system ORIENT was used. ORIENT is a program designed for adjustment of hybrid observations. Additional parameters (e.g. distortion values) can not only be introduced as observations, but they can also be determined in the adjustment. ORIENT also offers the possibility to perform gross error detection either by robust estimation or by data snooping.

A 6 parameter transformation was applied for picture coordinate correction. The number of measured points and the a priori r.m.s of the observations can be seen in table 1 (next page).

The ratio $\sigma_{\text{SIG}} : \sigma_{\text{NAT}} = 1 : 2$ was confirmed by estimation of variance components.

In all the cases, robust estimation and data snooping were applied for interactive detection of gross errors. Thus, about 35–40 observations were excluded from adjustment.

Table 1 – number of measured points and r.m.s. errors of their coordinates (a priori)

Resolution	Signals	Natural points	σ_{CON} [mm]	σ_{SIG} [μm]	σ_{NAT} [μm]
15 μm	309	248	20	5	10
30 μm	281	305	20	8	16

Additional parameters were introduced to model affinity and radial distortion.

Affinity:

$$dy_0 = a_1 \cdot x + a_2 \cdot y$$

Radial Distortion:

$$dx_0 = a_3 \cdot x \cdot (r^2 - r_0^2) + a_4 \cdot x \cdot (r^4 - r_0^4)$$

$$dy_0 = a_3 \cdot y \cdot (r^2 - r_0^2) + a_4 \cdot y \cdot (r^4 - r_0^4)$$

$$\text{with } r^2 = x^2 + y^2$$

The parameters for radial distortion a_3 and a_4 could also be determined from the distortion curve included in the calibration protocol. These values were introduced as observations. Parameter a_4 turned out to be not significant. Additionally, it was highly correlated with a_3 . That is why it was no longer determined in the adjustment.

6 Limitations and problems of the current state:

- Patch extraction is not operational if no approximations are known
- The accuracy potential of our subpixel estimation is limited
- The visual check of the positions of the signal only gives a very coarse impression whether the result is correct or not
- There is no possibility for automatical point transfer

7 Future Development of the System

In the near future, least squares matching will be implemented to achieve better results mainly for signalized points. We will also try to solve the problem of digital point transfer by applying some feature based algorithms. Currently, we are working on a visualization toolbox which will also be used by our system. To conclude, there exists the possibility that digital image processing tools for point determination might be implemented into ORIENT.

8 References

Kager, H.: Orient: A Universal Photogrammetric Adjustment System. in: Gruen, Kahmen (eds.): Optical 3-D Measurement Techniques, Wichmann Verlag, Karlsruhe 1989, pp. 447-455.

Rottensteiner, F.: Area Based Matching of Fiducial Marks in Scanned Images. in: Pölzleitner, Wenger (eds.): Image Analysis and Synthesis, R. Oldenburg Verlag, Wien, München, 1993

The OEEPE Aerotriangulation Test Using Digitized Images Performed with DVP-TRI

J.-P. Agnard, P.-A. Gagnon and M. Boulianne

Department of Geodetic Sciences and Remote Sensing
Laval University, Ste-Foy, Quebec, Canada, G1K 7P4

Abstract

The results of the OEEPE aerotriangulation test using digitized images performed with DVP-TRI are given. The DVP-TRI module is presented and the methodology followed explained. The results obtained with the independent-model program SPACE-M of J.A.R. Blais and the bundle program BUNBLK of G.H. Schut are compared. Improvements planned for DVP-TRI are presented.

1 Introduction

The potential of aerotriangulation using softcopy photogrammetry has been investigated at Laval University since 1990. It started with conventionally prepared diapositives (mechanically drilled tie points), the results being presented at the 1991 ACSM/ASPRS/AUTO-CARTO Annual Convention of Baltimore [Agnard and Gagnon, 1991]. Experiments with digital preparation (digitally marked tie points) followed, with results presented in a doctoral dissertation submitted to the University of Tokyo in 1992 [Agnard, 1992]. After that, the program has been successfully tested in production conditions with a few small projects.

Given this background, it was felt that it would be interesting to participate in the OEEPE test. This meant bringing a small modification to the original DVP-TRI which had been initially designed for independent-model triangulation, the method currently used in Canada as implemented, for instance, in SPACE-M, the well known system for block adjustment. The modification meant creating photograph coordinate files, necessary for a bundle adjustment, in addition to the existing model coordinate files.

2 DVP-TRI

DVP-TRI is an aerotriangulation module developed at Laval University from the now well known DVP (Digital Video Plotter) distributed by LEICA.

At first, developed to get rid of all mechanical process in software photogrammetry, the module allows, however, the triangulation of blocks conventionally prepared with mechanically drilled tie points. But its originality results in the fact that it utilizes digital pugging for tie points.

The half-pixel coordinates of these points are stored into special files in such a way that the same photo coordinates are given to the same tie point when measured in the second model where it appears in the strip. Sub-images are stored when a tie point measured in one model is to be used as a tie point for two different strips. This avoids the necessity of loading the same image twice: first for formation of the models and second for the transfer of tie points from strip to strip. It also utilizes digital Dove prisms to help the removal of residual y-parallax.

The results are automatically arranged in PAT-M format for the SPACE-M adjustment. Small modifications would be necessary to make the output directly compatible with other block adjustment systems.

3 Methodology

No corrections have been applied to the photograph coordinates. The scanner-correction option of DVP-TRI has not been used: the scanner was considered distortion free. As for lens distortion, earth curvature and atmospheric refraction, their combined resulting effect tend to be negligible, considering the pixel size.

At the time of our first measurements (beginning of August), it was not known that the scanner coordinates of the points would also have to be sent to the pilot center (letter of August 23). Fortunately, DVP-TRI provides for the automatic storage of the „in“ and itout“ interior orientation parameters (MODEL.INT), as well as for the storage of the scanner coordinates of the fiducial marks. Because of this, it was possible to compute, outside the program, the original scanner coordinates corresponding to the photograph coordinates used in the bundle adjustment. The bundle program used is the program BUNBLK, version 2.2, created by G. H. Schut [Schut, 1987].

3.1 *The choice of tie points*

After the interior orientation on the fiducial marks with an artificial zoom-In of 2X, the choice of tie points is made on small details, preferably with a round shape (there are thousands of them on each photograph) having a few pixels in diameter. The artificial zoom-in, the same as the one used in the interior orientation, is used to center each measuring mark on the same detail of each image, displayed on each half screen of the monitor. If the small details are made of an odd or an even number of pixels, the result of the artificial zoom-in function is the same, they are transformed in details having an odd number of half-pixels, so they can be centered with a half-pixel accuracy. The x-parallax is then removed under stereoscopic vision and, to facilitate the removing of the y-parallax, a digital Dove prisms function has been introduced to transform instantaneously the remaining y-parallax into + or - x-parallax.

Before making the measurements with a half-pixel accuracy in x and y , the operator decides whether this tie point has to be marked on the left or on the right image. After the tie point number has been typed and entered, its number, with left and right photo coordinates, are stored for the relative orientation, and its number and pixel coordinates (in half-pixels), corresponding to the image where the tie point has been marked, are stored in a special file, as well as those of all the other tie points to be put on the same image. At the same time, is displayed, on the side where the tie point has been digitally marked, a color circle, 'ust to indicate the area where the tie point has been chosen.

3.2 *Transferred tie points*

If the tie point is to be transferred on the image of an other strip, the operator, after centering the two marks on the tie point in the middle of each half-screen of the monitor with the centering function, types a „t“ (for transfer) in front of the tie point number. In addition to all that has already been explained when the operator types a tie point number, a sub-image representing the half-screen where the tie point has been marked is recorded with the same format that the one of the images and its number and new sub-pixel coordinates (in half-pixels) are stored in a special file. This represents a 200 Kbytes file for each sub-Image or tie point to be transferred on an adjacent strip. This function has been provided to avoid the reinstallation of the images, each image being installed in this case only once, at the very moment of the measurements. This is particularly interesting when the image files are large and the hard disk is small. This can save hours of tape reading.

When all the tie points have been thus marked and measured, the relative orientation is computed. The existing control points and check points are then measured and all the model coordinates then transformed so that the left and right perspective centers coordinates have the following values:

$$\begin{aligned}x &= 300.00 \text{ mm}, y = 500.00 \text{ mm and } z = 500.00 \text{ mm} \\ \text{and } x &= 500.00 \text{ mm}, y = 500.00 \text{ mm and } z = 500.00 \text{ mm}\end{aligned}$$

When measuring in a model already having existing tie points (second and following models of the first strip or all models of a following strip), the software automatically brings to the screen one after the other, the tie points present in the left image then goes to the tie points in the right image. The operator then zooms-in the tie point, and the measuring mark, on the image where the marked tie point is, is frozen at the half-pixel location already determined in the previous model.

Before measuring the first model of the second strip, a false model in made with the sub-image of the first tie point to be transferred and the image where this tie point has to be transferred. No interior orientation is needed, the operator bringing on the right half-screen of the monitor the conjugate window of the sub-image of the tie point with the help of the paper positive being in reference on the digitizing tablette. Inside the zoom-in function, the ground appears with the y -parallax in place of the x -parallax and, by activating the Dove prisms function, this y -parallax is transformed instantaneously in $+$ and $-x$ -parallax, allowing in any case a good transfer of the tie point from one strip

to the other. For non-parallel strips, as can be the case for electricity or road projects where only corridors are photographed, the right portion of the ground appearing inside of the 2X zoom-in can be rotated by a resampling of pixels at any angle. When the first tie point has been transferred on the first image of the second strip, the software allows the operator to substitute the sub-Image of the second tie point to be transferred on the same image to the sub-image of the first one, the same operation being made until the last tie point is transferred. Then, the same kind of transfer is made on the second image of the second strip. The first model of the second strip can, after this preparation, be oriented and measured.

4 Special Features

For the OEEPE test, photo coordinates of all the measured points were recorded at the same time, because of the requirement to use a bundle adjustment.

The program has been written to prepare also automatically the SPACEM.IN file in PAT-M format for the block adjustment program SPACE-M.

Once the adjustment is obtained, the model coordinates from DVP-TRI and their ground coordinates from the adjustment are used to create automatically the XXX.ABS files needed by the DVP main program to apply the absolute orientation to models. This means that the models are ready for plotting with one and only one measure on all the points: the interior, relative and absolute orientations are performed from the measurements executed at the aerotriangulation phase. This procedure ensures efficiency as well as consistency.

The mean measuring time, for the 30 ptm pixel models, was 2 hours and 10 minutes per model. This amount has been reduced to 56 minutes, for the 15 gm pixel models that we measured after the 30 ptm pixel models test. The time includes: the interior orientation, the choice and measurements of tie points as well as their transfer to other images, the relative orientation computation and the preparation of the SPACEM.IN file.

5 Future Improvements

We plan to improve the software by implementing at least three new functions that, we found, could have been useful for this job. The first one is a zoom-out function, to facilitate the location of conjugate windows. This is particularly helpful for 15 Aim pixel models where only a very small part of each image appears on the screen.

The second one is the possibility of displaying on the screen previously zoomed-in areas, with their measuring marks, so that it would be possible to see the exact position of the floating mark on the details or targets already measured before accepting a new measurement on these points. This would facilitate interpretation at the very moment of the measurement, specially for points being transferred from a different strip. The zoomed-in areas recorded being still referenced to their original files, it will then be

possible, in the case where a tie point already measured is not visible on a subsequent model, to replace inside of its previous zoomed-in areas the tie point by a new one that would be visible on all the images. The relative orientations concerned by these changes could be then recomputed automatically and the SPACEM-IN file automatically modified consequently.

The addition of a second screen option is also planned. This will be very useful in order to construct automatically the aerial triangulation index, simultaneously with the digital pugging and measurements of the tie and pass points. With this new development, already existing with the commercial version of DVP, the triangulation index, from its passive role, passes to an active one. Indeed, it may be used as a macro command to bring, for example, the sub-images used to transfer the pass points from a given strip to the adjacent one. The second screen can also show in real-time the results of a preliminary adjustment program, as soon as the measurements in a new model are completed, showing to the operator in real time the quality of his work.

6 Conclusion

Working for the OEEPE aerotriangulation test has been a very interesting. Sending blind results is always something like putting one's head on the bloc(k) ... The OEEPE aerotriangulation test demonstrates, once again, that softcopy photogrammetry works and produces goods results. It demonstrates also the quality and efficiency of DVP-TRI.

7 References

- Agnard, J.-P. and P.-A. Gagnon*, 1991. PC-Based Digital Block Adjustment, ACSM/ASPRS/AUTO-CARTO 10 Annual Convention, Baltimore, Vol.5, P. 7-10.
- Agnard, J.-P.*, 1992. Development of a Digital Video Stereoplotter on Personal Computer, Doctoral Dissertation, University of Tokyo. Japan, 143 p.
- Schut, G. H.*, 1987. Adjustment of Bundles, Publication of the National Research Council of Canada, NRC-16832 and NRC-17401.

THE HISTORY OF THE
CITY OF BOSTON
FROM THE FIRST SETTLEMENT
TO THE PRESENT TIME
IN TWO VOLUMES
BY NATHANIEL BENTLEY
OF THE BOSTON BAR
VOL. I.
BOSTON: PUBLISHED BY
J. B. ALLEN, 1822.

LIST OF THE OEEPE PUBLICATIONS

State – March 1995

A. Official publications

- 1 *Trombetti, C.*: „Activité de la Commission A de l'OEEPE de 1960 à 1964" – *Cunietti, M.*: „Activité de la Commission B de l'OEEPE pendant la période septembre 1960 – janvier 1964" – *Förstner, R.*: „Rapport sur les travaux et les résultats de la Commission C de l'OEEPE (1960–1964)" – *Neumaier, K.*: „Rapport de la Commission E pour Lisbonne" – *Weele, A. J. v. d.*: „Report of Commission F." – Frankfurt a. M. 1964, 50 pages with 7 tables and 9 annexes.
- 2 *Neumaier, K.*: „Essais d'interprétation de »Bedford« et de »Waterbury«. Rapport commun établi par les Centres de la Commission E de l'OEEPE ayant participé aux tests" – „The Interpretation Tests of »Bedford« and »Waterbury«. Common Report Established by all Participating Centres of Commission E of OEEPE" – „Essais de restitution »Bloc Suisse«. Rapport commun établi par les Centres de la Commission E de l'OEEPE ayant participé aux tests" – „Test »Schweizer Block«. Joint Report of all Centres of Commission E of OEEPE." – Frankfurt a. M. 1966, 60 pages with 44 annexes.
- 3 *Cunietti, M.*: „Emploi des blocs de bandes pour la cartographie à grande échelle – Résultats des recherches expérimentales organisées par la Commission B de l'O.E.E.P.E. au cours de la période 1959–1966" – „Use of Strips Connected to Blocks for Large Scale Mapping – Results of Experimental Research Organized by Commission B of the O.E.E.P.E. from 1959 through 1966." – Frankfurt a. M. 1968, 157 pages with 50 figures and 24 tables.
- 4 *Förstner, R.*: „Sur la précision de mesures photogrammétriques de coordonnées en terrain montagneux. Rapport sur les résultats de l'essai de Reichenbach de la Commission C de l'OEEPE" – „The Accuracy of Photogrammetric Co-ordinate Measurements in Mountainous Terrain. Report on the Results of the Reichenbach Test Commission C of the OEEPE." – Frankfurt a. M. 1968, Part I: 145 pages with 9 figures; Part II: 23 pages with 65 tables.
- 5 *Trombetti, C.*: „Les recherches expérimentales exécutées sur de longues bandes par la Commission A de l'OEEPE." – Frankfurt a. M. 1972, 41 pages with 1 figure, 2 tables, 96 annexes and 19 plates.
- 6 *Neumaier, K.*: „Essai d'interprétation. Rapports des Centres de la Commission E de l'OEEPE." – Frankfurt a. M. 1972, 38 pages with 12 tables and 5 annexes.
- 7 *Wiser, P.*: „Etude expérimentale de l'aérotiangulation semi-analytique. Rapport sur l'essai »Gramastetten«." – Frankfurt a. M. 1972, 36 pages with 6 figures and 8 tables.

- 8 „Proceedings of the OEEPE Symposium on Experimental Research on Accuracy of Aerial Triangulation (Results of Oberschwaben Tests)“

Ackermann, F.: „On Statistical Investigation into the Accuracy of Aerial Triangulation. The Test Project Oberschwaben“ – „Recherches statistiques sur la précision de l'aérottriangulation. Le champ d'essai Oberschwaben“ – *Belzner, H.:* „The Planning. Establishing and Flying of the Test Field Oberschwaben“ – *Stark, E.:* Testblock Oberschwaben, Programme I. Results of Strip Adjustments“ – *Ackermann, F.:* „Testblock Oberschwaben, Program I. Results of Block Adjustment by Independent Models“ – *Ebner, H.:* Comparison of Different Methods of Block Adjustment“ – *Wiser, P.:* „Propositions pour le traitement des erreurs non-accidentelles“ – *Camps, F.:* „Résultats obtenus dans le cadre du projet Oberschwaben 2A“ – *Cunietti, M.; Vanossi, A.:* „Etude statistique expérimentale des erreurs d'enchaînement des photogrammes“ – *Kupfer, G.:* „Image Geometry as Obtained from Rheidt Test Area Photography“ – *Förstner, R.:* „The Signal-Field of Baustetten. A Short Report“ – *Visser, J.; Leberl, F.; Kure, J.:* „OEEPE Oberschwaben Réseau Investigations“ – *Bauer, H.:* „Compensation of Systematic Errors by Analytical Block Adjustment with Common Image Deformation Parameters.“ – Frankfurt a. M. 1973, 350 pages with 119 figures, 68 tables and 1 annex.

- 9 *Beck, W.:* „The Production of Topographic Maps at 1 : 10,000 by Photogrammetric Methods. – With statistical evaluations, reproductions, style sheet and sample fragments by Landesvermessungsamt Baden-Württemberg Stuttgart.“ – Frankfurt a. M. 1976, 89 pages with 10 figures, 20 tables and 20 annexes.

- 10 „Résultats complémentaires de l'essai d'«Oberriet» of the Commission C de l'OEEPE – Further Results of the Photogrammetric Tests of «Oberriet» of the Commission C of the OEEPE“

Hárry, H.: „Mesure de points de terrain non signalisés dans le champ d'essai d'«Oberriet» – Measurements of Non-Signalized Points in the Test Field «Oberriet» (Abstract)“ – *Stickler, A.; Waldhäusl, P.:* „Restitution graphique des points et des lignes non signalisés et leur comparaison avec des résultats de mesures sur le terrain dans le champ d'essai d'«Oberriet» – Graphical Plotting of Non-Signalized Points and Lines, and Comparison with Terrestrial Surveys in the Test Field «Oberriet»“ – *Förstner, R.:* „Résultats complémentaires des transformations de coordonnées de l'essai d'«Oberriet» de la Commission C de l'OEEPE – Further Results from Co-ordinate Transformations of the Test «Oberriet» of Commission C of the OEEPE“ – *Schürer, K.:* „Comparaison des distances d'«Oberriet» – Comparison of Distances of «Oberriet» (Abstract).“ – Frankfurt a. M. 1975, 158 pages with 22 figures and 26 tables.

- 11 „25 années de l'OEEPE“

Verlaine, R.: „25 années d'activité de l'OEEPE“ – „25 Years of OEEPE (Summary)“ – *Baarda, W.:* „Mathematical Models.“ – Frankfurt a. M. 1979, 104 pages with 22 figures.

- 12 *Spieß, E.:* „Revision of 1 : 25,000 Topographic Maps by Photogrammetric Methods.“ – Frankfurt a. M. 1985, 228 pages with 102 figures and 30 tables.

- 13 Timmerman, J.; Roos, P. A.; Schürer, K.; Förstner, R.: On the Accuracy of Photogrammetric Measurements of Buildings – Report on the Results of the Test "Dordrecht", Carried out by Commission C of the OEEPE. – Frankfurt a. M. 1982, 144 pages with 14 figures and 36 tables.
- 14 Thompson C. N.: Test of Digitising Methods. – Frankfurt a. M. 1984, 120 pages with 38 figures and 18 tables.
- 15 Jaakkola, M.; Brindöpke, W.; Kölbl, O.; Noukka, P.: Optimal Emulsions for Large-Scale Mapping – Test of "Steinwedel" – Commission C of the OEEPE 1981–84. – Frankfurt a. M. 1985, 102 pages with 53 figures.
- 16 Waldhäusl, P.: Results of the Vienna Test of OEEPE Commission C. – Kölbl, O.: Photogrammetric Versus Terrestrial Town Survey. – Frankfurt a. M. 1986, 57 pages with 16 figures, 10 tables and 7 annexes.
- 17 Commission E of the OEEPE: Influences of Reproduction Techniques on the Identification of Topographic Details on Orthophotomaps. – Frankfurt a. M. 1986, 138 pages with 51 figures, 25 tables and 6 appendices.
- 18 Förstner, W.: Final Report on the Joint Test on Gross Error Detection of OEEPE and ISP WG III/1. – Frankfurt a. M. 1986, 97 pages with 27 tables and 20 figures.
- 19 Dorman, I. J.; Ducher, G.: Spacelab Metric Camera Experiment – Test of Image Accuracy. – Frankfurt a. M. 1987, 112 pages with 13 figures, 25 tables and 7 appendices.
- 20 Eichhorn, G.: Summary of Replies to Questionnaire on Land Information Systems – Commission V – Land Information Systems. – Frankfurt a. M. 1988, 129 pages with 49 tables and 1 annex.
- 21 Kölbl, O.: Proceedings of the Workshop on Cadastral Renovation – Ecole polytechnique fédérale, Lausanne, 9–11 September, 1987. – Frankfurt a. M. 1988, 337 pages with figures, tables and appendices.
- 22 Rollin, J.; Dorman, I. J.: Map Compilation and Revision in Developing Areas – Test of Large Format Camera Imagery. – Frankfurt a. M. 1988, 35 pages with 3 figures, 9 tables and 3 appendices.
- 23 Drummond, J. (ed.): Automatic Digitizing – A Report Submitted by a Working Group of Commission D (Photogrammetry and Cartography). – Frankfurt a. M. 1990, 224 pages with 85 figures, 6 tables and 6 appendices.
- 24 Ahokas, E.; Jaakkola, J.; Sotkas, P.: Interpretability of SPOT data for General Mapping. – Frankfurt a. M. 1990, 120 pages with 11 figures, 7 tables and 10 appendices.
- 25 Ducher, G.: Test on Orthophoto and Stereo-Orthophoto Accuracy. – Frankfurt a. M. 1991, 227 pages with 16 figures and 44 tables.
- 26 Dorman, I. J. (ed.): Test of Triangulation of SPOT Data – Frankfurt a. M. 1991, 206 pages with 67 figures, 52 tables and 3 appendices.

- 27 *Newby, P. R. T.; Thompson, C. N. (ed.):* Proceedings of the ISPRS and OEEPE Joint Workshop on Updating Digital Data by Photogrammetric Methods. – Frankfurt a. M. 1992, 278 pages with 79 figures, 10 tables and 2 appendices.
- 28 *Koen, L. A.; Kölbl, O. (ed.):* Proceedings of the OEEPE-Workshop on Data Quality in Land Information Systems, Apeldoorn, Netherlands, 4–6 September 1991. – Frankfurt a. M. 1992, 243 pages with 62 figures, 14 tables and 2 appendices.
- 29 *Burman, H.; Torlegård, K.:* Empirical Results of GPS – Supported Block Triangulation. – Frankfurt a. M. 1994, 86 pages with 5 figures, 3 tables and 8 appendices.
- 30 *Gray, S. (ed.):* Updating of Complex Topographic Databases. – Frankfurt a. M. 1995, 133 pages with 2 figures and 12 appendices.

B. Special publications

– Special Publications O.E.E.P.E. – Number I

Solaini, L.; Trombetti, C.: Relation sur les travaux préliminaires de la Commission A (Triangulation aérienne aux petites et aux moyennes échelles) de l'Organisation Européenne d'Etudes Photogrammétriques Expérimentales (O.E.E.P.E.). 1^{ère} Partie: Programme et organisation du travail. – *Solaini, L.; Belfiore, P.*: Travaux préliminaires de la Commission B de l'Organisation Européenne d'Etudes Photogrammétriques Expérimentales (O.E.E.P.E.) (Triangulations aériennes aux grandes échelles). – *Solaini, L.; Trombetti, C.; Belfiore, P.*: Rapport sur les travaux expérimentaux de triangulation aérienne exécutés par l'Organisation Européenne d'Etudes Photogrammétriques Expérimentales (Commission A et B). – *Lehmann, G.*: Compte rendu des travaux de la Commission C de l'O.E.E.P.E. effectués jusqu'à présent. – *Gotthardt, E.*: O.E.E.P.E. Commission C. Compte-rendu de la restitution à la Technischen Hochschule, Stuttgart, des vols d'essai du groupe I du terrain d'Oberriet. – *Brucklacher, W.*: Compte-rendu du centre «Zeiss-Aerotopograph» sur les restitutions pour la Commission C de l'O.E.E.P.E. (Restitution de la bande de vol, groupe I, vol. No. 5). – *Förstner, R.*: O.E.E.P.E. Commission C. Rapport sur la restitution effectuée dans l'Institut für Angewandte Geodäsie, Francfort sur le Main. Terrain d'essai d'Oberriet les vols No. 1 et 3 (groupe I). – I.T.C., Delft: Commission C, O.E.E.P.E. Déroulement chronologique des observations. – *Photogrammetria XII (1955–1956) 3*, Amsterdam 1956, pp. 79–199 with 12 figures and 11 tables.

– Publications spéciales de L'O.E.E.P.E. – Numéro II

Solaini, L.; Trombetti, C.: Relations sur les travaux préliminaires de la Commission A (Triangulation aérienne aux petites et aux moyennes échelles) de l'Organisation Européenne d'Etudes Photogrammétriques Expérimentales (O.E.E.P.E.). 2^e partie. Prises de vues et points de contrôle. – *Gotthardt, E.*: Rapport sur les premiers résultats de l'essai d'«Oberriet» de la Commission C de l'O.E.E.P.E. – *Photogrammetria XV (1958–1959) 3*, Amsterdam 1959, pp. 77–148 with 15 figures and 12 tables.

- *Trombetti, C.*: Travaux de prises de vues et préparation sur le terrain effectuées dans le 1958 sur le nouveau polygone italien pour la Commission A de l'OEEPE. – Florence 1959, 16 pages with 109 tables.
- *Trombetti, C.; Fondelli, M.*: Aérotriangulation analogique solaire. – Firenze 1961, 111 pages, with 14 figures and 43 tables.

– Publications spéciales de l'O.E.E.P.E. – Numéro III

Solaini, L.; Trombetti, C.: Rapport sur les résultats des travaux d'enchaînement et de compensation exécutés pour la Commission A de l'O.E.E.P.E. jusqu'au mois de Janvier 1960. Tome 1: Tableaux et texte. Tome 2: Atlas. – *Photogrammetria XVII (1960–1961) 4*, Amsterdam 1961, pp. 119–326 with 69 figures and 18 tables.

- „OEEPE – Sonderveröffentlichung Nr. 1“

Gigas, E.: „Beitrag zur Geschichte der Europäischen Organisation für photogrammetrische experimentelle Untersuchungen“ – *N. N.:* „Vereinbarung über die Gründung einer Europäischen Organisation für photogrammetrische experimentelle Untersuchungen“ – „Zusatzprotokoll“ – *Gigas, E.:* „Der Sechserausschuß“ – *Brucklacher, W.:* „Kurzbericht über die Arbeiten in der Kommission A der OEEPE“ – *Cunietti, M.:* „Kurzbericht des Präsidenten der Kommission B über die gegenwärtigen Versuche und Untersuchungen“ – *Förstner, R.:* „Kurzbericht über die Arbeiten in der Kommission B der OEEPE“ – „Kurzbericht über die Arbeiten in der Kommission C der OEEPE“ – *Belzner, H.:* „Kurzbericht über die Arbeiten in der Kommission E der OEEPE“ – *Schwidefsky, K.:* „Kurzbericht über die Arbeiten in der Kommission F der OEEPE“ – *Meier, H.-K.:* „Kurzbericht über die Tätigkeit der Untergruppe „Numerische Verfahren“ in der Kommission F der OEEPE“ – *Belzner, H.:* „Versuchsfelder für internationale Versuchs- und Forschungsarbeiten.“ – *Nachr. Kt.- u. Vermess.-wes., R. V, Nr. 2, Frankfurt a. M. 1962, 41 pages with 3 tables and 7 annexes.*

- *Rinner, K.:* Analytisch-photogrammetrische Triangulation eines Teststreifens der OEEPE. – *Österr. Z. Vermess.-wes., OEEPE-Sonderveröff. Nr. 1, Wien 1992, 31 pages.*

- *Neumaier, K.; Kasper, H.:* Untersuchungen zur Aerotriangulation von Überweitwinkelaufnahmen. – *Österr. Z. Vermess.-wes., OEEPE-Sonderveröff. Nr. 2, Wien 1965, 4 pages with 4 annexes.*

- „OEEPE – Sonderveröffentlichung Nr. 2“

Gotthardt, E.: „Erfahrungen mit analytischer Einpassung von Bildstreifen.“ – *Nachr. Kt.- u. Vermess.-wes., R. V, Nr. 12, Frankfurt a. M. 1965, 14 pages with 2 figures and 7 tables.*

- „OEEPE – Sonderveröffentlichung Nr. 3“

Neumaier, K.: „Versuch »Bedford« und »Waterbury«. Gemeinsamer Bericht aller Zentren der Kommission E der OEEPE“ – „Versuch »Schweizer Block«. Gemeinsamer Bericht aller Zentren der Kommission E der OEEPE.“ – *Nachr. Kt.- u. Vermess.-wes., R.V, Nr. 13, Frankfurt a. M. 1966, 30 pages with 44 annexes.*

- *Stickler, A.; Waldhäusl, P.:* Interpretation der vorläufigen Ergebnisse der Versuche der Kommission C der OEEPE aus der Sicht des Zentrums Wien. – *Österr. Z. Vermess.-wes., OEEPE-Sonderveröff. (Publ. Spéc.) Nr. 3, Wien 1967, 4 pages with 2 figures and 9 tables.*

- „OEEPE – Sonderveröffentlichung Nr. 4“

Schürer, K.: „Die Höhenmeßgenauigkeit einfacher photogrammetrischer Kartiergeräte. Bemerkungen zum Versuch »Schweizer Block« der Kommission E der OEEPE.“ – *Nachr. Kt.- u. Vermess.-wes., Sonderhefte, Frankfurt a. M., 1968, 25 pages with 7 figures and 3 tables.*

- „OEEPE – Sonderveröffentlichung Nr. 5“

Förstner, R.: „Über die Genauigkeit der photogrammetrischen Koordinatenmessung in bergigem Gelände. Bericht über die Ergebnisse des Versuchs Reichenbach der Kommission C der OEEPE.“ – Nachr. Kt.- u. Vermess.-wes., Sonderhefte, Frankfurt a. M. 1969, Part I: 74 pages with 9 figures; Part II: 65 tables.

- „OEEPE – Sonderveröffentlichung Nr. 6“

Knorr, H.: „Die Europäische Organisation für experimentelle photogrammetrische Untersuchungen – OEEPE – in den Jahren 1962 bis 1970.“ – Nachr. Kt.- u. Vermess.-wes., Sonderhefte, Frankfurt a. M. 1971, 44 pages with 1 figure and 3 tables.

- „OEEPE – Sonderveröffentlichung Nr. D-7“

Förstner, R.: „Das Versuchsfeld Reichenbach der OEEPE.“ – Nachr. Kt.- u. Vermess.-wes., Sonderhefte, Frankfurt a. M. 1972, 191 pages with 49 figures and 38 tables.

- „OEEPE – Sonderveröffentlichung Nr. D-8“

Neumaier, K.: „Interpretationsversuch. Berichte der Zentren der Kommission E der OEEPE.“ – Nachr. Kt.- u. Vermess.-wes., Sonderhefte, Frankfurt a. M. 1972, 33 pages with 12 tables and 5 annexes.

- „OEEPE – Sonderveröffentlichung Nr. D-9“

Beck, W.: „Herstellung topographischer Karten 1 : 10 000 auf photogrammetrischem Weg. Mit statistischen Auswertungen, Reproduktionen, Musterblatt und Kartenmustern des Landesvermessungsamts Baden-Württemberg, Stuttgart.“ – Nachr. Kt.- u. Vermess.-wes., Sonderhefte, Frankfurt a. M. 1976, 65 pages with 10 figures, 20 tables and 20 annexes.

- „OEEPE – Sonderveröffentlichung Nr. D-10“

Weitere Ergebnisse des Meßversuchs „Oberriet“ der Kommission C der OEEPE. *Härry, H.:* „Messungen an nicht signalisierten Geländepunkten im Versuchsfeld «Oberriet»“ – *Stickler, A.;* *Waldhäusl, P.:* „Graphische Auswertung nicht signalisierter Punkte und Linien und deren Vergleich mit Feldmessungsergebnissen im Versuchsfeld «Oberriet»“ – *Förstner, R.:* „Weitere Ergebnisse aus Koordinatentransformationen des Versuchs «Oberriet» der Kommission C der OEEPE“ – *Schürer, K.:* „Streckenvergleich «Oberriet».“ – Nachr. Kt.- u. Vermess.-wes., Sonderhefte, Frankfurt a. M. 1975, 116 pages with 22 figures and 26 tables.

- „OEEPE – Sonderveröffentlichung Nr. D-11“
Schulz, B.-S.: „Vorschlag einer Methode zur analytischen Behandlung von Reseauaufnahmen.“ – Nachr. Kt.- u. Vermess.-wes., Sonderhefte, Frankfurt a. M. 1976, 34 pages with 16 tables.

- „OEEPE – Sonderveröffentlichung Nr. D-12“
Verlaine, R.: „25 Jahre OEEPE.“ – Nachr. Kt.- u. Vermess.-wes., Sonderhefte, Frankfurt a. M. 1980, 53 pages.

- „OEEPE – Sonderveröffentlichung Nr. D-13“
Haug, G.: „Bestimmung und Korrektur systematischer Bild- und Modelldeformationen in der Aerotriangulation am Beispiel des Testfeldes „Oberschwaben.“ – Nachr. Kt.- u. Vermess.-wes., Sonderhefte, Frankfurt a. M. 1980, 136 pages with 25 figures and 51 tables.

- „OEEPE – Sonderveröffentlichung Nr. D-14“
Spiess, E.: „Fortführung der Topographischen Karte 1 : 25 000 mittels Photogrammetrie“ (not published, see English version in OEEPE official publication No. 12)

- „OEEPE – Sonderveröffentlichung Nr. D-15“
Timmerman, J.; Roos, P. A.; Schürer, K.; Förstner, R.: „Über die Genauigkeit der photogrammetrischen Gebäudevermessung. Bericht über die Ergebnisse des Versuchs Dordrecht der Kommission C der OEEPE.“ – Nachr. Kt.- u. Vermess.-wes., Sonderhefte, Frankfurt a. M. 1983, 131 pages with 14 figures and 36 tables.

- „OEEPE – Sonderveröffentlichung Nr. D-16“
Kommission E der OEEPE: „Einflüsse der Reproduktionstechnik auf die Erkennbarkeit von Details in Orthophotokarten.“ – Nachr. Kt.- u. Vermess.-wes., Sonderhefte, Frankfurt a. M. 1986, 130 pages with 51 figures, 25 tables and 6 annexes.

- „OEEPE – Sonderveröffentlichung Nr. D-17“
Schürer, K.: „Über die Genauigkeit der Koordinaten signalisierter Punkte bei großen Bildmaßstäben. Ergebnisse des Versuchs „Wien“ der Kommission C der OEEPE.“ – Nachr. Kt.- u. Vermess.-wes., Sonderhefte, Frankfurt a. M. 1987, 84 pages with 3 figures, 10 tables and 42 annexes.

C. Congress reports and publications in scientific reviews

- *Stickler, A.*: Interpretation of the Results of the O.E.E.P.E. Commission C. – Photogrammetria XVI (1959–1960) 1, pp. 8–12, 3 figures, 1 annexe (en langue allemande: pp. 12–16).
- *Solaini, L.; Trombetti, C.*: Results of Bridging and Adjustment Works of the Commission A of the O.E.E.P.E. from 1956 to 1959. – Photogrammetria XVI (1959–1960) 4 (Spec. Congr.-No. C), pp. 340–345, 2 tables.
- *N. N.*: Report on the Work Carried out by Commission B of the O.E.E.P.E. During the Period of September 1956–August 1960. – Photogrammetria XVI (1959–1960) 4 (Spec. Congr.-No. C), pp. 346–351, 2 tables.
- *Förstner, R.*: Bericht über die Tätigkeit und Ergebnisse der Kommission C der O.E.E.P.E. (1956–1960). – Photogrammetria XVI (1959–1960) 4 (Spec. Congr.-No. C), pp. 352–357, 1 table.
- *Bachmann, W. K.*: Essais sur la précision de la mesure des parallaxes verticales dans les appareils de restitution du 1^{er} ordre. – Photogrammetria XVI (1959–1960) 4 (Spec. Congr.-No. C), pp. 358–360).
- *Wiser, P.*: Sur la reproductibilité des erreurs du cheminement aérien. – Bull. Soc. Belge Photogramm., No. 60, Juin 1960, pp. 3–11, 2 figures, 2 tables.
- *Cunietti, M.*: L'erreur de mesure des parallaxes transversales dans les appareils de restitution. – Bull. Trimestr. Soc. Belge Photogramm., No. 66, Décembre 1961, pp. 3–50, 12 figures, 22 tables.
- „OEEPE – Arbeitsberichte 1960/64 der Kommissionen A, B, C, E, F“
Trombetti, C.: „Activité de la Commission A de l'OEEPE de 1960 à 1964“ – *Cunietti, M.*: „Activité de la Commission B de l'OEEPE pendant la période septembre 1960–janvier 1964“ – *Förstner, R.*: „Rapport sur les travaux et les résultats de la Commission C de l'OEEPE (1960–1964)“ – *Neumaier, K.*: „Rapport de la Commission E pour Lisbonne“ – *Weele, A. J. van der.*: „Report of Commission F.“ – Nachr. Kt.- u. Vermess.-wes., R. V. Nr. 11, Frankfurt a. M. 1964, 50 pages with 7 tables and 9 annexes.
- *Cunietti, M.; Inghilleri, G.; Puliti, M.; Togliatti, G.*: Participation aux recherches sur les blocs de bandes pour la cartographie à grande échelle organisées par la Commission B de l'OEEPE. Milano, Centre CASF du Politecnico. – Boll. Geod. e Sc. affini (XXVI) 1, Firenze 1967, 104 pages.
- *Gotthardt E.*: Die Tätigkeit der Kommission B der OEEPE. – Bildmess. u. Luftbildwes. 36 (1968) 1, pp. 35–37.
- *Cunietti, M.*: Résultats des recherches expérimentales organisées par la Commission B de l'OEEPE au cours de la période 1959–1966. Résumé du Rapport final. – Présenté à l'XI^e Congrès International de Photogrammétrie, Lausanne 1968, Comm. III (en langues française et anglaise), 9 pages.

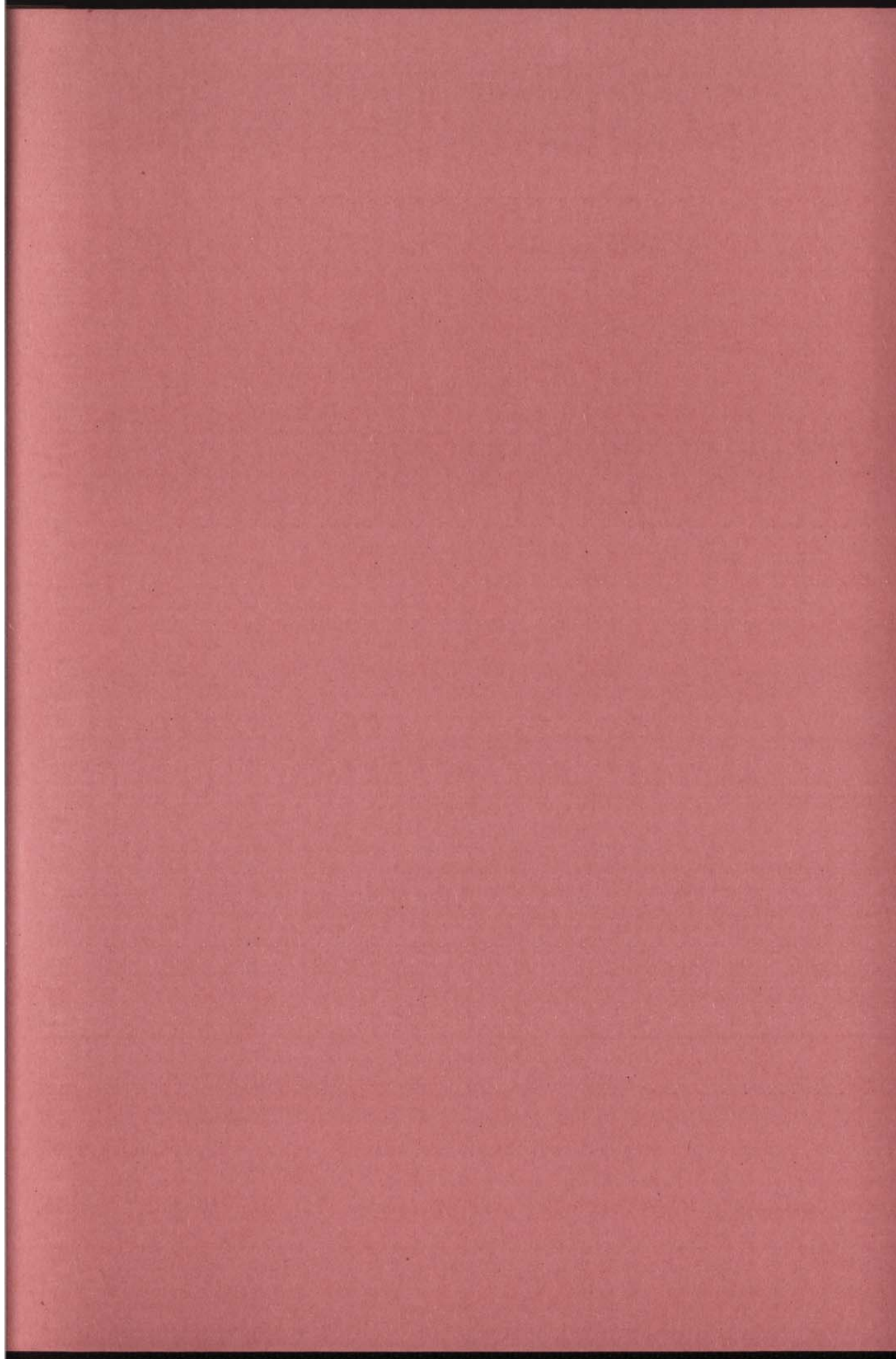
- Förstner, R.: Résumé du Rapport sur les résultats de l'essai de Reichenbach de la Commission C de l'OEEPE. – Présenté à l'XI^e Congrès International de Photogrammétrie, Lausanne 1968, Comm. IV (en langues française, anglaise et allemande), 28 pages, 2 figures, 2 tables.
- Timmerman, J.: Proef „OEEPE-Dordrecht“. – ngt 74, 4. Jg., Nr. 6, Juni 1974, S. 143–154 (Kurzfassung: Versuch „OEEPE-Dordrecht“. Genauigkeit photogrammetrischer Gebäudevermessung. Vorgelegt auf dem Symposium der Kommission IV der I.G.P., Paris, 24.–26. September 1974).
- Timmerman, J.: Report on the Commission C. "OEEPE-Dordrecht" Experiment. – Presented Paper for Comm. IV, XIIIth Congress of ISP, Helsinki 1976.
- Beck, W.: Rapport de la Commission D de l'OEEPE sur l'établissement de cartes topographiques au 1/10 000 selon le procédé photogramétrique. – Presented Paper for Comm. IV, XIIIth Congress of ISP, Helsinki 1976.
- Verlaine, R.: La naissance et le développement de l'OEEPE – Festschrift – Dr. h. c. Hans Härry, 80 Jahre – Schweizerische Gesellschaft für Photogrammetrie und Wild Heerbrugg AG, Bern 1976.
- Förstner, R.: Internationale Versuche (Essais contrôlés) – Festschrift – Dr. h. c. Hans Härry, 80 Jahre – Schweizerische Gesellschaft für Photogrammetrie und Wild Heerbrugg AG, Bern 1976.
- Bay, E.; Cunietti, M.; Vanossi, A.: Détermination Expérimentale des Erreurs Systématiques des Faisceaux Perspectives. – Société Belge de Photogrammétrie, Bulletin trimestriel, Brüssel 1977, pp 21–49.
- Timmerman, J.: Fotogrammetrische stadskartering de OEEPE-proef Dordrecht. – Geodesia 19, Amsterdam 1977, pp. 291–298.
- Waldhäusl, P.: The Vienna Experiment of the OEEPE/C. Proceedings – Standards and Specifications for Integrated Surveying and Mapping Systems. – Schriftenreihe HSBw, Heft 2, München 1978.
- Bachmann, W. K.: Recherches sur la stabilité des appareils de restitution photogramétriques analogiques. – Vermessung, Photogrammetrie, Kulturtechnik, Zürich 1978, pp. 265–268.
- Parsic, Z.: Untersuchungen über den Einfluß signalisierter und künstlicher Verknüpfungspunkte auf die Genauigkeit der Blocktriangulation. – Vermessung, Photogrammetrie, Kulturtechnik, Zürich 1978, pp. 269–278.
- Waldhäusl, P.: Der Versuch Wien der OEEPE/C. – Geowissenschaftliche Mitteilungen der Studienrichtung Vermessungswesen der TU Wien; Heft 13, Wien 1978, pp. 101–124.
- Waldhäusl, P.: Ergebnisse des Versuches Wien der OEEPE/C. – Presented Paper for Comm. IV, XIVth Congress of ISP, Hamburg 1980.
- Timmerman, J.; Förstner, R.: Kurzbericht über die Ergebnisse des Versuchs Dordrecht der Kommission C der OEEPE. – Presented Paper for Comm. IV, XIVth Congress of ISP, Hamburg 1980.

- *Bernhard, J.; Schmidt-Falkenberg, H.*: OEEPE – Die Arbeiten der Kommission E „Interpretation“. – Presented Paper for Comm. IV, XIVth Congress of ISP, Hamburg 1980.
- *Bachmann, W. K.*: Elimination des valeurs erronées dans un ensemble de mesures contrôlées. – Papers written in honor of the 70th birthday of Professor *Luigi Solaini* – *Ricerca di Geodesia Topografia e Fotogrammetria*, Milano 1979, pp. 27–39.
- *Visser, J.*: The European Organisation for Experimental Photogrammetric Research (OEEPE) – The Thompson Symposium 1982. – The Photogrammetric Record, London 1982, pp. 654–668.
- *Spiess, E.*: Revision of Topographic Maps: Photogrammetric and Cartographic Methods of the Fribourg Test. – The Photogrammetric Record, London 1983, pp. 29–42.
- *Jerie, H. G. and Holland, E. W.*: Cost model project for photogrammetric processes: a progress report. – ITC Journal, Enschede 1983, pp. 154–159.
- *Ackermann, F. E.* (Editor): Seminar – Mathematical Models of Geodetic/Photogrammetric Point Determination with Regard to Outliers and Systematic Errors – Working Group III/1 of ISP – Commission A of OEEPE. – Deutsche Geodätische Kommission bei der Bayerischen Akademie der Wissenschaften, Reihe A, Heft Nr. 98, München 1983.
- *Brindöpke, W., Jaakkola, M., Noukka, P., Kölbl, O.*: Optimal Emulsions for Large Scale Mapping – OEEPE–Commission C. – Presented Paper for Comm. I, XVth Congress of ISPRS, Rio de Janeiro 1984.
- *Ackermann, F.*: Report on the Activities of Working Group III/1 During 1980–84. – Comm. III, XVth Congress of ISPRS, Rio de Janeiro 1984.
- *Förstner, W.*: Results of Test 2 on Gross Error Detection of ISP WG III/1 and OEEPE. – Comm. III, XVth Congress of ISPRS, Rio de Janeiro 1984.
- *Gros, G.*: Modèles Numériques Altimétriques – Lignes Caractéristiques – OEEPE Commission B. – Comm. III, XVth Congress of ISPRS, Rio de Janeiro 1984.
- *Ducher, G.*: Preparation d'un Essai sur les Ortho- et Stereo-Orthophotos. – Comm. IV, XVth Congress of ISPRS, Rio de Janeiro 1984.
- *van Zuylén, L.*: The influence of reproduction methods on the identification of details in orthophoto maps. – ITC Journal, Enschede 1984, pp. 219–226.
- *Visser, J.*: OEEPE- News – The European Organization for Experimental Photogrammetric Research. – ITC Journal, Enschede 1984, pp. 330–332.
- *Brindöpke, W., Jaakkola, M., Noukka, P., Kölbl, O.*: Optimale Emulsionen für großmaßstäbige Auswertungen. – Bildmess. u. Luftbildw. 53 (1985) 1, pp. 23–35.
- *Thompson, C. N.*: Some New Horizons for OEEPE. Presented Paper to the Symposium of Commission IV, ISPRS in Edinburgh, 8.–12. September 1986, pp. 299–306.

- *Dowman, I.:* The Restitution of Metric Photography Taken From Space – Comm. II, XVIth Congress of ISPRS, Kyoto 1988.
- *Kilpelä, E.:* Statistical Data on Aerial Triangulation – Comm. III, XVIth Congress of ISPRS, Kyoto 1988.
- *de Haan, A.:* An Analysis of the Precision of a DEM Obtained from SPOT Data – Comm. IV, XVIIth Congress of ISPRS, Washington 1992.
- *Ducher, G.:* OEEPE Test on Orthophoto and Stereo-Orthophoto Accuracy – Comm. IV, XVIIth Congress of ISPRS, Washington 1992.
- *Veillet, I.:* Accuracy of SPOT Triangulation With Very Few or no Ground Control Point – Comm. IV., XVIIth Congress of ISPRS, Washington 1992.

The official publications and the special publications issued in Frankfurt am Main are for sale at the

Institut für Angewandte Geodäsie
– Außenstelle Berlin –
Stauffenbergstraße 13, D-10785 Berlin



Organisation Européenne d'Etudes Photogrammétriques Expérimentales
Publications officielles

Content

page

<i>J. Jaakola, T. Sarjakoski</i> : Experimental Test on Digital Aerial Trinangulation	13
---	----